

UNIVERSITÀ DEGLI STUDI DI VERONA

DEPARTMENT OF

NEUROSCIENCE BIOMEDICINE AND MOVEMENT SCIENCE

GRADUATE SCHOOL OF

APPLIED LIFE AND HEALTH SCIENCES

DOCTORAL PROGRAM IN

LIFE AND HEALTH SCIENCES

WITH THE FINANCIAL CONTRIBUTION OF

ATENEIO - UNIVERSITY OF VERONA

Cycle XXXIII, year 2020-2021

**MOLECULAR MECHANISMS REGULATING BIOLOGICAL
HETEROGENEITY IN CHRONIC LYMPHOCYTIC LEUKEMIA:
FROM THE VARIABLE SIGNALING RESPONSE TO CD20
ANTIBODIES AND KINASE INHIBITORS TO THE DIFFERENTIAL
EXPRESSION OF CATALASE**

S.S.D. BIO13

Coordinator: Prof. Giovanni Malerba

Tutor: Prof.ssa Maria Grazia Romanelli

Co-tutor: Prof.ssa Maria Teresa Scupoli

Doctoral Student: Dott.ssa Marilisa Galasso

This work is licensed under a Creative Commons Attribution-NonCommercial-NoDerivs 3.0 Unported License, Italy. To read a copy of the licence, visit the web page:

<http://creativecommons.org/licenses/by-nc-nd/3.0/it/>



Attribution — You must give appropriate credit, provide a link to the license, and indicate if changes were made. You may do so in any reasonable manner, but not in any way that suggests the licensor endorses you or your use.



NonCommercial — You may not use the material for commercial purposes.



NoDerivatives — If you remix, transform, or build upon the material, you may not distribute the modified material.

*MOLECULAR MECHANISMS REGULATING BIOLOGICAL HETEROGENEITY
IN CHRONIC LYMPHOCYTIC LEUKEMIA: FROM THE VARIABLE
SIGNALING RESPONSE TO CD20 ANTIBODIES AND KINASE INHIBITORS
TO THE DIFFERENTIAL EXPRESSION OF CATALASE.*

Marilisa Galasso
PhD thesis
Verona, Febbraio 2021

ABSTRACT

Chronic lymphocytic leukemia (CLL) is the most prevalent form of leukemia in Western countries with the highest incidence among adults. CLL remain an incurable disease characterized by an extremely variable clinical course and response to treatment. In the last decades, therapeutic CD20 monoclonal antibodies (mAbs) have represented one of the most important advances in the treatment of lymphoproliferative disorders, including CLL. CD20 mAbs are the most important promising therapeutic partners for inhibitors of BCR-associated kinase (BAKi), however their biological activity remains elusive. To this aim, the purpose of my PhD research was to expand the knowledge of the biological basis of CD20 antibodies treatment. In this study, we showed that in leukemic cells from CLL patients the CD20 therapeutic antibodies, namely rituximab, ofatumumab, and obinutuzumab, inhibit BCR signaling pathways. Moreover, we showed that the combination of CD20 mAbs and BAKi enhanced the activity of the single agents in inducing cell death in CLL. Moreover, there is a growing interest in CLL cells' metabolism and its role in the clinical course of the disease. In CLL, it has been recently identified a differential catalase (CAT) expression associated with divergent clinical behaviors and progression. A single nucleotide polymorphism (SNP) (rs1001179, CAT-262 C/T) in the catalase promoter has been demonstrated to alter catalase cellular expression. Moreover, epigenetic modifications, such as DNA methylation, contribute to the regulation of catalase expression in several biological contexts. However, the precise molecular mechanisms controlling catalase expression are still poorly understood. For this purpose, we aimed at investigating the mechanisms in regulating catalase expression in CLL patients. Therefore, we first confirmed that CLL patients express increased levels of catalase compared with healthy donors. Then, we investigated the involvement of genetic and epigenetic regulatory mechanisms in the differential catalase expression in CLL patients. Our data showed that the rs1001179 SNP, as well as methylation within the catalase promoter, play a role in the regulation of catalase gene expression in CLL cells. Taken together, these data indicate that a lower level of methylation in the catalase promoter may constitute a risk factor in CLL harboring the T allele.

In conclusion, the results of my PhD thesis for one side advances our understanding of mechanisms of action of CD20 mAbs as single agents or in combination with BAKi, thus informing on the potential of combined therapies in ongoing and future clinical trials in patients with CLL. On the other side, it provides new insights into the knowledge of genetic and epigenetic mechanisms regulating the catalase expression in CLL. Moreover, these data form the basis for future studies aimed at dissecting molecular mechanisms that regulate catalase expression, which could be of crucial relevance for the development of prognostic and therapeutic tools targeting redox pathways.

SUMMARY/RIASSUNTO

La leucemia linfocitaria cronica (LLC) è la forma di leucemia più diffusa nei paesi occidentali con la più alta incidenza tra gli adulti. La LLC rimane una malattia incurabile caratterizzata da un decorso clinico e una risposta al trattamento estremamente variabile. Negli ultimi decenni gli anticorpi monoclonali anti-CD20 (mAbs) hanno rappresentato uno dei progressi più importanti nel trattamento dei disturbi linfoproliferativi, tra cui la LLC. Gli anticorpi terapeutici anti-CD20 sono i più importanti e promettenti partner terapeutici per gli inibitori delle chinasi associate al recettore delle cellule B (BAKi), tuttavia la loro attività biologica rimane elusiva. A questo scopo, obiettivo dello studio è ampliare la conoscenza delle basi biologiche di risposta al trattamento con anticorpi anti-CD20. In questo studio abbiamo dimostrato che nelle cellule leucemiche dei pazienti affetti da LLC anticorpi terapeutici CD20, rituximab, ofatumumab e obinutuzumab, inibiscono la segnalazione del BCR. Abbiamo inoltre dimostrato che la combinazione di mAbs CD20 e BAKi determina un aumento della morte cellulare nella LLC. Secondo obiettivo dello studio è investigare il metabolismo delle cellule LLC e il suo ruolo nel decorso clinico della malattia. Nella LLC, è stata recentemente identificata un'espressione differenziale della catalasi (CAT) associata alla progressione e a comportamenti clinici divergenti. È stato dimostrato che un polimorfismo (SNP) (rs1001179, CAT-262 C/T) nel promotore della catalasi altera l'espressione cellulare di quest'ultima. Inoltre, le modifiche epigenetiche, come la metilazione del DNA, contribuiscono alla regolazione dell'espressione della catalasi in diversi contesti biologici. Tuttavia, gli effetti delle variazioni nella sequenza del promotore e dei livelli di metilazione che controllano l'espressione della catalasi sono ancora poco conosciuti. A questo scopo, abbiamo studiato i livelli di espressione della catalasi nei pazienti con LLC e in soggetti sani. Facendo seguito ad uno studio precedente, abbiamo confermato che i pazienti con LLC esprimono livelli di catalasi più elevati rispetto ai donatori sani. In seguito, abbiamo studiato il coinvolgimento dei polimorfismi e dei livelli di metilazione del promotore nell'espressione differenziale della catalasi in pazienti con LLC. I nostri dati hanno mostrato che il polimorfismo rs1001179 e la metilazione a livello del promotore si associano a diversità significative nella regolazione dell'espressione del gene della

catalasi nelle cellule di LLC. L'analisi di questi dati suggerisce che un livello più basso di metilazione nel promotore della catalasi possa costituire un fattore di rischio nei pazienti con LLC che presentano la variante allelica T.

In conclusione, i risultati della mia tesi di dottorato di ricerca per un lato contribuiscono all'avanzamento della comprensione dei meccanismi d'azione dei CD20 mAbs come agenti singoli o in combinazione con BAKi, a supporto dell'interpretazione degli effetti di potenziali terapie combinate in pazienti con LLC. Dall'altro lato, fornisce nuovi approfondimenti sul ruolo dei meccanismi genetici ed epigenetici che regolano l'espressione della catalasi nella LLC. Questi dati potranno costituire la base per studi futuri volti a definire i meccanismi molecolari che regolano l'espressione della catalasi e che potrebbero essere di importanza cruciale per lo sviluppo di strumenti prognostici e terapeutici mirati ai percorsi redox della cellula leucemica.

INDEX	
ABSTRACT	3
SUMMARY/RIASSUNTO	5
LIST OF TABLES	10
LIST OF FIGURES	10
ABBREVIATIONS	16
1. CHAPTER 1: General introduction	21
1.1. Introduction to the thesis	21
1.2. Chronic lymphocytic leukemia	21
1.3. The cellular origin of CLL	22
1.4. Recurrent genetic aberrations	23
1.4.1. Somatic mutations within the IGHV genes	25
1.5. B-cell receptor signaling	26
1.6. Therapy	29
1.6.1. Inhibitors targeting the BCR signaling: idelalisib and ibrutinib	29
1.6.2. CD20 monoclonal antibodies	30
1.6.3. Combined therapy	32
2. CHAPTER 2: Effects of CD20 antibodies and kinase inhibitors on BCR signaling and survival of CLL cells	33
2.1. Introduction	33
2.1.1. B-lymphocyte antigen CD20	33
2.1.2. CD20 monoclonal antibodies: mechanism of action	34
2.1.3. CD20 monoclonal antibodies: type I and type II	35
2.2. Aim of the study	37
2.3. Materials and methods	38
2.3.1. Sampling and sample preparation	38
2.3.2. Analysis of CD20 and IgM expression on CLL surface	38
2.3.3. Phosphospecific flow cytometry	40
2.3.4. Western blot analysis	41
2.3.5. Apoptosis	42
2.3.6. Analysis of drug interaction on CLL cell survival	43
2.3.7. Statistical analysis	43

2.4. Results	44
2.4.1. CD20 therapeutic antibodies inhibit BCR signaling	44
2.4.2. Combination of CD20 mAbs with BAKi enhances the BCR-inhibitory effects induced by single agents	51
2.4.3. CD20 therapeutic antibodies inhibit LYN phosphorylation	53
2.4.4. Combination of CD20 mAbs with ibrutinib enhances the cell death induced by single agents	54
2.5. Discussion	58
3.CHAPTER 3: Regulation of catalase expression in CLL cells	61
3.1. Introduction	61
3.1.1. Human catalase characteristics	61
3.1.2. Tissue and cellular distribution of catalase	62
3.1.3. Physiological role of catalase	62
3.2. Regulation of catalase expression	64
3.2.1. Genetic modifications	65
3.2.2. Epigenetic modifications	67
3.2.3. Transcriptional regulation	67
3.2.4. Post-transcriptional regulation	70
3.2.5. Post-translational regulation	71
3.3. Role of catalase in cancer	72
3.4. Aim of the study	75
3.5. Materials and Methods	77
3.5.1. Sampling and sample preparation	77
3.5.2. Quantitative RT-PCR (qRT-PCR)	78
3.5.3. Flow cytometry	78
3.5.4. Catalase activity assay	79
3.5.5. DNA extraction and genotyping by restriction fragment length polymorphism (RFLP)-PCR	80
3.5.6. Pyrosequencing analysis / CpG sites methylation analysis	80
3.5.7. Inhibition of DNA methyltransferase in CLL cells	80
3.5.8. Software and statistical analysis	81
3.6. Results	82
3.6.1. CLL cells express higher levels of catalase than normal B cells	82

3.6.2. Differential catalase expression in CLL associates with divergent clinical behaviors	83
3.6.3. The rs1001179 SNP is not a risk factor for CLL	85
3.6.4. The rs1001179 SNP influences catalase gene expression	86
3.6.5. Methylation influences catalase gene expression	90
3.6.6. Methylation and rs1001179 T allele influences catalase gene expression	96
3.7. Discussion	98
4. References	102

LIST OF TABLES

Table 1. Clinical and biological characteristics of CLL patients	39
Table 2. Antibodies used for CD20 and IgM expression analysis	39
Table 3. Antibodies used for phosphospecific flow cytometry.....	40
Table 4. Antibodies used for phospho-LYN detection	41
Table 5. Modulation of BCR signaling pathway induced by CD20 mAbs in mutated and unmutated CLL in unstimulated condition	48
Table 6. Modulation of BCR signaling pathway induced by CD20 mAbs in mutated and unmutated CLL in anti-IgM stimulated condition	48
Table 7. Spontaneous apoptosis induced by CD20 mAbs in mutated and unmutated CLL	56
Table 8. Clinical and biological characteristics of CLL patients	77
Table 9. Antibodies used for catalase detection.....	79
Table 10. Catalase activity in CLL and HD reported as mean±SD	85
Table 11. Distributions of CAT rs1001179 genotypes in CLL patients and HD.....	85
Table 12. DNA methylation percentage in CLL samples.....	91
Table 13. DNA methylation percentage in HD samples.....	91
Table 14. Coefficients and goodness-of-fit statistics for the linear regression model shown in Figure 37	97
Table 15. ANOVA table for the linear regression model shown in Figure 37	97

LIST OF FIGURES

Figure 1. The cellular origin of chronic lymphocytic leukemia (Fabbri and Dalla-Favera 2016).....	23
Figure 2. Prognostic relevance of genomic aberrations in chronic lymphocytic leukemia (CLL) (Zenz, Döhner, and Stilgenbauer 2007).....	25
Figure 3. B-cell receptor signaling (BCR). Antigen engagement by the BCR results in the formation of a micro-signalosome whereby BTK activates four families of non-receptor protein tyrosine kinases that transduce key signaling events including phospholipase γ , mitogen-activated protein kinase (MAPK) activation, nuclear factor kappa-light-chain-enhancer of activated B cells (NF- κ B) pathway components and activation of the serine/threonine kinase AKT (PKB). In addition, BTK mediated signaling events are regulated by various phosphatases that can be recruited to the cell membrane, following crosslinking of inhibitory receptors, e.g., Fc γ RIIB that is exclusively expressed on B cells and signals upon immune complex binding (Pal Singh, Dammeijer, and Hendriks 2018).	28
Figure 4. Structure of CD20 and epitope targets of ofatumumab, rituximab, and obinutuzumab (GA101) (Hill and Kalaycio 2015).	32
Figure 5. Interacting partners of CD20 on cell membrane. mAbs: monoclonal antibodies; BCR: B-cell receptor; HDACi: histone deacetylase inhibitors; DNMTi: DNA methyltransferase inhibitors; NICD: NOTCH1 intracellular domain; TGF β : transforming growth factor β (Pavlasova and Mraz 2020).	34
Figure 6. Graphical abstract. Effects of CD20 antibodies and kinase inhibitors on BCR signaling and survival of CLL cells. mAbs: monoclonal antibodies; BAKi: BCR-associated kinase inhibitors.....	36

Figure 7. Expression of CD20 and IgM on CLL cells. Flow cytometry histograms of CD20 (red) and IgM (blue) expression compared to autofluorescence (gray) measured in CLL samples (n = 10). 44

Figure 8. Functional characterization of BCR in CLL cells. BCR signaling profiles in basal condition or following stimulation with anti-IgM across CLL samples (n = 10). Data are expressed as median fluorescence intensity (MFI) divided by autofluorescence (relative median fluorescence intensity = RMFI) and represented as a pseudo-color map. 45

Figure 9. Responses of BCR signaling proteins to treatments with CD20 mAbs. Representative flow cytometry contour plots of phosphorylation levels of BCR proteins measured in CLL cells treated with CD20 mAbs or irrelevant IgG1 antibody as control in the unstimulated or anti-IgM stimulated conditions. Vertical line indicates autofluorescence upper limit. Median fluorescence intensity value is reported for each contour plot. BCR, B-cell receptor; CLL, chronic lymphocytic leukemia; RTX, rituximab; OFA, ofatumumab; OBZ, obinutuzumab. 46

Figure 10. Responses of BCR signaling proteins to treatment with CD20 mAbs. CLL cell samples were thawed and rested for 24 h before treatment with 20 µg/ml RTX, OFA, OBZ, or irrelevant isotype-matched control antibody (isotype) for 2 h, followed by stimulation with 20 µg/ml anti-IgM (anti-IgM-stimulated) for 10 min or left unstimulated. (A) BCR signaling protein phosphorylation responses in CLL cell samples (n = 10) after treatment with RTX, OFA or OBZ, in the unstimulated or anti- IgM-stimulated conditions, were calculated as the log₂-fold change between CD20- treated and isotype-treated and represented as a pseudo-color map. Comparisons were performed using the one-way ANOVA and each P value was corrected for multiple comparison using the Sidak test. (B) Comparison of phosphorylation responses of BCR proteins to CD20 mAbs in CLL cell samples (n = 10) in the unstimulated or anti-IgM-stimulated conditions. Protein phosphorylation was measured as the log₂-fold change between CD20-treated and isotype-treated signals. Dashed line indicates the log₂ value = 0, corresponding to ‘no change’ with respect to the control. Comparisons were performed using the one-way ANOVA and each P value was corrected for multiple comparison using the Tukey multiple comparison test. *, P ≤ 0.050; **, P ≤ 0.010; ***, P ≤ 0.001. BCR, B-cell receptor; CLL, chronic lymphocytic leukemia; RTX, rituximab; OFA, ofatumumab; OBZ, obinutuzumab. 47

Figure 11. Comparison of Western blot (WB) and flow cytometry (FCM) analyses of pBTK^{Y551} modulation induced by CD20 mAbs. Ramos cells were incubated with CD20 mAbs rituximab (RTX), ofatumumab (OFA), obinutuzumab (OBZ) or left unstimulated (vehicle) for 2 hours. Cells were then divided and lysed for Western blot analysis or fixed and permeabilized for flow cytometry analysis. WB signals of pBTK^{Y551} are normalized dividing by GAPDH signals and FCM data are expressed as median fluorescence intensity divided by autofluorescence (relative median fluorescence intensity = RMFI). Modulation of pBTK^{Y551} in response to CD20 mAbs are represented as pseudo-color map setting the vehicle control to 100%. A representative experiment of 3 is shown. 49

Figure 12. Responses of BCR signaling proteins to BAKi. CLL cell samples (n = 4) were thawed and rested for 24 h before treatment with 1 µM ibrutinib or idelalisib, and then stimulated with 20 µg/ml anti-IgM (anti-IgM-stimulated) for 10 min or left unstimulated (vehicle). Data are expressed as median fluorescence intensity (MFI) divided by autofluorescence (relative median fluorescence intensity = RMFI). Comparisons were performed using the two-way ANOVA and each P value was corrected for multiple

comparison using the Sidak test. *, $P \leq 0.050$; **, $P \leq 0.010$; ***, $P \leq 0.001$. BCR, B-cell receptor; CLL, chronic lymphocytic leukemia. 51

Figure 13. Responses of BCR signaling proteins to combination of CD20 mAbs and BAKi. CLL cell samples (n = 4) were thawed and rested for 24 h before treatment with 1 μM ibrutinib or idelalisib followed by stimulation with 20 $\mu\text{g}/\text{ml}$ of RTX, OFA, or OBZ for 2 h, and then stimulated with 20 $\mu\text{g}/\text{ml}$ anti-IgM (anti-IgM-stimulated) for 10 min or left unstimulated. Data are expressed as median fluorescence intensity divided by autofluorescence (relative median fluorescence intensity = RMFI), setting the vehicle control to 100%, and represented as a pseudo-color map (A) or as aggregate data expressed as mean \pm SEM (B). Comparisons were performed using the two-way ANOVA and each P value was corrected for multiple comparison using the Tukey test. *, $P \leq 0.050$; **, $P \leq 0.010$; ***, $P \leq 0.001$. BCR, B-cell receptor; CLL, chronic lymphocytic leukemia; RTX, rituximab; OFA, ofatumumab; OBZ, obinutuzumab; BAKi: BCR-associated kinase inhibitors..... 52

Figure 14. LYN phosphorylation response to treatments with CD20 mAbs. CLL cell samples were thawed and rested for 24 h before treatment with 20 $\mu\text{g}/\text{ml}$ of RTX, OFA, OBZ, or 0.1 μM dasatinib for 2 h, followed by stimulation with 20 $\mu\text{g}/\text{ml}$ anti-IgM (anti-IgM-stimulated) for 10 min or left unstimulated. LYN protein phosphorylation responses in CLL cell samples (n = 3) were calculated as log₂-fold change between CD20-treated and untreated signals and represented as pseudo-color maps. Comparisons were performed using the one-way ANOVA and each P value was corrected for multiple comparison using the Dunnett test. CLL, chronic lymphocytic leukemia; RTX, rituximab; OFA, ofatumumab; OBZ, obinutuzumab. 53

Figure 15. Annexin V/PI flow cytometry assay after CD20 mAb treatments. Representative flow cytometry analysis of leukemic cells from CLL patients stained with annexin V/PI. CLL cell sample was thawed and treated with 20 $\mu\text{g}/\text{ml}$ of RTX, OFA or OBZ for 2 hours, followed by stimulation with 20 $\mu\text{g}/\text{ml}$ anti-IgM for 24 hours or left unstimulated. CLL, chronic lymphocytic leukemia; RTX: rituximab; OFA: ofatumumab; OBZ: obinutuzumab..... 54

Figure 16. CLL cell survival after anti-IgM stimulation. CLL cell samples (n = 3) were thawed and stimulated with 20 $\mu\text{g}/\text{ml}$ anti-IgM or left unstimulated for 24 hours. Spontaneous apoptosis in CLL cell samples was measured as annexin V-negative/PI-negative. Comparison was calculated by Student T test. *: $P \leq 0.050$. CLL, chronic lymphocytic leukemia. 55

Figure 17. Effects of CD20 mAbs on CLL cell survival. CLL cell samples (n = 5) were thawed and treated with 20 $\mu\text{g}/\text{ml}$ of RTX, OFA or OBZ for 2 hours, followed by stimulation with 20 $\mu\text{g}/\text{ml}$ anti-IgM for 24 hours or left unstimulated. Percentage of live CLL cells was measured as annexin V-negative/PI-negative. Comparisons were performed using the one-way ANOVA and each P value was corrected for multiple comparisons using the Dunnett test. *, $P \leq 0.050$; **, $P \leq 0.010$; ***, $P \leq 0.001$. CLL, chronic lymphocytic leukemia; RTX: rituximab; OFA: ofatumumab; OBZ: obinutuzumab..... 55

Figure 18. Association of CD20 cell surface expression with cell apoptosis induced by CD20 mAbs. CD20 expression level are expressed as RMFI (median fluorescence intensity (MFI) divided by autofluorescence (relative median fluorescence intensity = RMFI), and was correlated to CD20 mAbs-mediated apoptosis, measured using annexin V/PI staining and flow cytometry at 24 hours (n = 6)..... 56

Figure 19. Effects of combination of CD20 mAbs and BAKi on CLL cell survival. CLL cell samples (n = 5) were thawed, pre-treated with 1 μ M ibrutinib or 1 μ M idelalisib for 30 min and then stimulated with 20 μ g/ml of RTX, OFA or OBZ for 24 h. (A) Effect on CLL cell survival of CD20 in combination with BAKi. Percentage of live CLL cells was measured as annexin V-negative/PI-negative. Data were reported as mean \pm SEM. Comparisons were performed using the two-way ANOVA and each P value was corrected for multiple comparison using the Tukey test. *P \leq 0.050; **P \leq 0.010; ***P \leq 0.001. (B) Combination index (CI) was calculated for five CLL samples for each drug combination. CI = 1 (red line) indicated additive effect; CI > 1 is considered less than additive. +, mean value. CLL, chronic lymphocytic leukemia; RTX, rituximab; OFA, ofatumumab; OBZ, obinutuzumab; BAKi: BCR-associated kinase inhibitors..... 57

Figure 20. Schematic representation of human catalase gene end the most relevant SNPs. UTR – untranslated region (Kodydková et al. 2014). 61

Figure 21. Various levels of catalase expression regulation. Regulation of catalase expression from genetic, transcriptional to RNA processing, and to the post-translational modification of protein. Abbreviations: specificity protein 1 (Sp1), nuclear factor Y (NFY), fork-head box protein O (FoxO) family, miR (miRNA), Single nucleotide polymorphisms (SNPs). Created with BioRender.com. Figure. 65

Figure 22. Schematic representation of human catalase promoter and the main DNA-binding transcription regulators. Abbreviations: specificity protein 1 (Sp1), nuclear factor Y (NF-Y), Wilms tumor 1 (WT1), early growth response (Egr), fork-head box protein M1 (FoxM1), octamer-binding transcription factor 1(Oct-1), peroxisome proliferator-activated receptor gamma (PPAR γ), activator protein 1 (AP-1) member JunB, and retinoic acid receptor alpha (RAR α). 68

Figure 23. Biological function of catalase. Catalase modulate H₂O₂ levels, an imbalance between the production of ROS and the capacity of antioxidant defense mechanisms favoring oxidants leads to cellular oxidative stress. Under physiological conditions catalase is involved in regulating various cellular physiological processes, including signal transduction, proliferation, differentiation, apoptosis, in which H₂O₂ acts as a second messenger. Otherwise, ROS activate protumorigenic signals; enhance cell survival, proliferation, migration and chemoresistance; and cause DNA damage and genetic instability. However, increased levels of ROS can also promote antitumorigenic signals, resulting in an increase of oxidative stress and induction of cancer cell death. Created with BioRender.com. 73

Figure 24. Graphical abstract. Regulation of catalase expression in CLL cells. CAT: catalase; SNP: single nucleotide polymorphism. 74

Figure 25. Catalase levels in B cells from HDs and leukemic cells from CLL patients. A) The relative catalase gene expression in CLL samples (n = 54) compared with healthy donors (n = 18). B) Catalase protein expression in CLL cells (n = 20) compared with HD B cells (n = 10). Data are expressed as relative median fluorescence intensity (RMFI) calculated as median fluorescence intensity (MFI) divided by fluorescence-minus-one (FMO). Data are expressed as mean \pm SEM. Comparisons were performed with Mann Whitney test. **: P < 0.01. CLL, chronic lymphocytic leukemia; HDs, healthy donors.. 82

Figure 26. Catalase data distribution in CLL patients. A) Frequency distribution of mRNA expression data set. B) Frequency distribution of protein catalase expression data set. C) Ordered mRNA expression data set. D) Ordered protein expression data set. Red dotted line indicates median value (for mRNA = 5.943; for protein = 7.425). D'Agostino

& Pearson normality test was used to evaluate the data distribution. CLL, chronic lymphocytic leukemia. 83

Figure 27. Association between catalase expression levels and time-to-first-treatment (TTFT) in CLL. A) Kaplan-Meier curves of TTFT for subgroups of CLL patients distinguished by low (n = 27) and high (n = 26) catalase mRNA levels B) Kaplan-Meier curves of TTFT for subgroups of CLL patients distinguished by low (n = 9) and high (n = 11) catalase protein levels. High and low enzyme expression values were referred to the median expression values. Difference between the two curves was calculated with log-rank test. 84

Figure 28. Multiple sequence alignment of a selected upstream promoter region among 15 catalase genes. Multiple sequence alignment was conducted using the online MUSCLE software (<https://www.ebi.ac.uk/Tools/msa/muscle/>). Jalview software was used to calculate the percent identity among sequences. Multiple sequence alignment was conducted considering the upstream promoter region of 15 catalase genes that include primates, no-primate mammals, rodents, and zebrafish. Color intensity, from a deeper blue (>85%) to a fainter one (<25%), represent the percentage identity. GenBank accession references: *Homo sapiens* (human), NC_000011.10; *Pongo abelii* (orangutan), NC_036914.1; *Pan troglodytes* (chimpanzee), NC_036890.1; *Pan paniscus* (pygmychimpanzee), NC_048250.1; *Gorilla gorilla* (gorilla), NC_044613.1; *Nomascus leucogenys* (white-cheeked gibbon), NC_044395.1; *Macaca mulatta* (rhesus macaque), NC_041767.1; *Callithrix jacchus* (common marmoset), NC_048393.1; *Otolemur garnettii* (greater galago), NW_003852396.1; *Rattus norvegicus* (brown rat), NC_005102.4; *Mus musculus* (house mouse), NC_000068.8; *Bos taurus* (cattle), NC_037342.1; *Sus scrofa* (wild boar), NC_010444.4; *Canis lupus familiaris* (dog), NC_006600.3; and *Danio rerio* (zebrafish), NC_007136.7. 87

Figure 29. Association between catalase gene expression and rs1001179 SNP. A) Representative genotypes for the rs1001179 SNP. From left to right the lanes show: Marker) DNA size marker (100 bp ladder), #01) TT genotype (191 bp), #02) CT genotype (191, 157 and 34 bp) and #03) CC genotype (157 and 34 bp). B) Comparison of catalase mRNA expression between CC and CT/TT genotypes for rs1001179 SNP in CLL (n=34). C) Comparison of catalase mRNA expression between CC and CT genotypes for rs1001179 SNP in HDs (n=10). Data are expressed as mean±SEM; Comparison was performed with Mann Whitney test, *: P < 0.05. 88

Figure 30. Association of protein catalase expression and rs1001179 SNP in CLL cells. Comparison of protein catalase expression between CC and CT/TT genotypes for rs1001179 SNP. Data are expressed as relative median fluorescence intensity (RMFI) calculated as median fluorescence intensity (MFI) divided by fluorescence-minus-one (FMO). Data are expressed as mean±SEM (n=16); Comparison was performed with Mann Whitney test. 89

Figure 31. Schematic representation of human catalase promoter and location of the analyzed CpG sites. Location of the main DNA-binding transcription regulators and the CpG islands in the promoter region of human catalase gene. Red bars represent the location of the 8 CpG sites, on the proximal region of human catalase promoter, analyzed for bisulfite pyrosequencing. The analyzed CpGs sites range from ATG -357 to -306. This region covers or is directly adjacent to rs1001179 SNP (-330 bp up stream of the ATG translation start). Abbreviations: specificity protein 1 (Sp1), nuclear factor Y (NFY), Wilms tumor 1 (WT1), early growth response (Egr), fork-head box protein M1 (FoxM1), octamer-Binding transcription factor 1 (Oct-1), peroxisome proliferator-

activated receptor gamma (PPAR γ), activator protein 1 (AP-1) member JunB, and retinoic acid receptor alpha (RAR α).	90
Figure 32. Example of pyrogram reporting the DNA methylation status on eight CpG site in the catalase promoter region. Blue boxes highlighted the eight CpG sites analyzed for cytosine methylation percentage degree; yellow boxes represent bisulfite conversion efficacy control.	92
Figure 33. Methylation levels of catalase promoter region in HDs and CLL patients. Methylation levels of the analyzed catalase promoter in CLL samples (n=21) compared with HDs (n=10). DNA methylation levels are measured as mean among the analyzed sites. Data are expressed as mean \pm SEM. Comparisons were performed with Student T tests. **: P < 0.01. CLL, chronic lymphocytic leukemia; HDs, healthy donors.	92
Figure 34. Correlation between DNA methylation levels in CpG#21 site and catalase gene expression in CLL samples. DNA methylation levels in CpG#21 site, in the catalase promoter region, was expressed in percentage and correlated to catalase gene expression (n = 21). The comparisons indicated the Spearman correlation coefficient.	93
Figure 35. Correlation between mean percentage methylation levels with catalase expression level in CLL samples. DNA methylation levels expressed as mean percentage methylation. A) DNA methylation percentage of sites CpG#22 to CpG#18 correlated to catalase gene expression (n = 21). B) DNA methylation percentage of sites CpG#21 to site CpG#18 correlated to catalase gene expression (n = 21). C) DNA methylation percentage of sites CpG#20 to site CpG#18 was correlated to catalase gene expression (n = 21). D) DNA methylation percentage of sites CpG#19 and CpG#18 was correlated to catalase gene expression (n = 21). The comparisons indicated the Spearman correlation coefficient.	94
Figure 36. Catalase expression levels after DNA methyltransferase inhibitor (DAC) treatment in MEC-1 CLL cell line. Comparison of catalase gene expression between MEC-1 cells treated with 2 μ M 5-aza-20-deoxycytidine (DAC) or left unstimulated (vehicle) for 96 hours. Value bars represent the mean \pm SEM of 5 independent experiments. Comparison was performed with Wilcoxon matched-pairs signed rank test, *: P < 0.05.	95
Figure 37. Effects of the interaction of genotype with mean methylation levels on catalase mRNA expression. The interaction has been investigated within the context of linear models. We found significant regression results when methylation from site CpG#22 to site CpG#18 was averaged and stratified for the two genotypes CC and CT/TT. The line shows the marginal effects (i.e. predicted values) for the significant interaction between genotype CT/TT and methylation on mRNA expression (detailed in Table 13 and Table 14). Shaded colored areas indicate the 95% confidence intervals for all interactions. Measurements stratified by genotypes are shown as points.	96

ABBREVIATIONS

ADCC: antibody-dependent cellular cytotoxicity
ADCP: Antibody-dependent cell-mediated phagocytosis
AKT: protein kinase B
ANOVA: ANalysis Of Variance
AP-1: activator protein 1 member JunB
Arg: c-Abl-related gene
ATM: ataxia telangiectasia mutated
BAKi: inhibitors of BCR-associated kinase
BCA: bicinchoninic acid
BCL2: B-cell lymphoma 2
BCR: B-cell receptor
BLNK: B cell linker protein
BSA: bovine serum albumin
BTK: Bruton tyrosine kinase
c-Abl: Abelson murine leukemia viral oncogene homolog 1
CAT: catalase
CBP: C-terminal src kinase-binding protein
CDC: complement-dependent cytotoxicity
CI: combination index
CI: confidence interval
cPARP: cleaved poly (ADP-Ribose) Polymerase
c-REL: REL Proto-Oncogene, NF-KB Subunit
CuO: cupric oxide
DAG: diacylglycerol
DBCAT: Database of CpG islands and analytical tools
DLBCL: diffuse large B-Cell lymphoma
DNMTi: DNA methyl-transferase inhibitors
ECL: enhanced chemiluminescence
Egr: early growth response
ERK1/2: extracellular signal-regulated kinases 1/2
FCM: flow cytometry

Fc γ RIIB: Fc Fragment of IgG Receptor IIb
FDA: food and drug administration
FMO: fluorescence-minus-one
FoxM1: fork-head box protein M1
FOXO: forkhead box protein O
FoxO3a: forkhead box protein O3a
GAPDH: glyceraldehyde 3- phosphate dehydrogenase
GATA1: GATA-Binding Protein 1 (Globin Transcription Factor 1)
GC: germinal center
GPX: glutathione peroxidases
H₂O₂: hydrogen peroxide
HCC: hepatocarcinoma
HDACi: histone deacetylase inhibitors
HO-1: heme-oxygenase-1
HRP: horseradish peroxidase
HSCs: Hematopoietic Stem Cells
IG: immunoglobulin
IgG/M: immunoglobulin G/M
IgH/L: immunoglobulin heavy / light
IGHV M/UM: immunoglobulin heavy chain variable region genes mutated / unmutated
IP3: inositol triphosphate
ITAM: immunoreceptor tyrosine-based activation motif
ITIM: immunoreceptor tyrosine-based inhibition motif
JNK: Jun N-terminal kinase
LMO2: LIM Domain Only 2
LYN: (LYN proto-oncogene, SRC Family Tyrosine Kinase)
mAbs: monoclonal antibodies
MAC: membrane attack complex
MAPK: mitogen-activated protein kinase
MBL: monoclonal B cell lymphocytosis
MFI: median fluorescence intensity

MHCII: major histocompatibility complex class II
MIG: membrane immunoglobulin
M-MLV RT: Moloney Murine Leukemia Virus Reverse Transcriptase
MS4A: membrane-spanning 4-domain A
NADPH: nicotinamide adenine dinucleotide phosphate hydrogen
NCCN: national comprehensive cancer network
NFY: nuclear factor Y
NF- κ B: nuclear factor kappa-light-chain-enhancer of activated B cells
NICD: NOTCH1 intracellular domain
NOTCH1: Notch Receptor 1
NOXes: NADPH oxidases
NPs: nanoparticles
OBZ: obinutuzumab
Oct-1: octamer-Binding transcription factor 1
OD: odds ratio
OFA: ofatumumab
OS: overall survival
P53: tumor protein P53
PAX6: Paired Box 6
PBMCs: peripheral blood mononuclear cells
PCR: Polymerase chain reaction
PDGFR: platelet-derived growth factor receptor
PGC-1 α : peroxisome proliferator-activated receptor- γ co-activator-1 α
PI: propidium iodide
PI3K: phosphoinositide 3-kinase
PIP2: 4,5-bis- phosphate
PIP3: 3,4,5-triphosphate
PKC β : protein kinase C Beta
PKC δ : protein kinase C delta
PLC γ : phospholipase C Gamma
PPAR γ : peroxisome proliferator-activated receptor gamma
PTK: protein tyrosine kinase

PTPs: protein tyrosine phosphatases
PTS: peroxisomal-targeting signal
qRT-PCR: quantitative RT-PCR
RAR α : retinoic acid receptor alpha
RB1: retinoblastoma 1
RFLP: Restriction Fragment Length Polymorphism
RIP1: receptor-interacting protein 1
RMFI: relative median fluorescence intensity
ROS: reactive oxygen species
RPE: retinal pigment epithelium
RPLP0: ribosomal protein large P0
RPMI: Roswell park memorial Institute
rS: relative survival
RTX: rituximab
s.a: single agents
SD: standard error
SDS-PAGE: Sodium Dodecyl Sulphate - PolyAcrylamide Gel Electrophoresis
SEM: standard error of the mean
SF3B1: splicing factor 3B subunit 1
SHM: somatic hypermutation
SHP-2: SRC Homology Phosphatase 2
Sirt1: silent mating type information regulator 2 homolog 1
SNPs: single nucleotide polymorphisms
Sp1: specificity protein 1
STAT3: signal transducer activator of transcription 3
STAT3: signal transducer and activator of transcription 3
STAT4: Signal Transducer And Activator Of Transcription 4
SYK: SRC Homology 2 (SH-2) like spleen tyrosine kinase
TBS: Tris Buffered Saline
TFII-1: Transcription Elongation Factor A2
TGF β : transforming growth factor β
TP53: tumor protein 53

TSS: transcription start site

TTFT: time-to-first-treatment

UTR: untranslated region

WB: Western blot

WT1: wilms tumor 1

XBP-1: X-box binding protein 1

ZAP70: zeta chain of T cell receptor associated protein kinase 70

1. CHAPTER 1: General introduction

1.1. Introduction to the thesis

This thesis aims at investigating for one side the biological basis of CD20 antibodies treatment and on the other side the cellular and molecular mechanisms that contribute to the different outcome in chronic lymphocytic leukemia patients. The thesis project is focused on two main objectives:

- a. Study of direct effects of the three CD20 therapeutic monoclonal antibodies (rituximab, ofatumumab and obinutuzumab) on the activation status of B-cell receptor (BCR) kinases and on cell survival, used alone or in combination with inhibitors of BCR-associated kinase (BAKi). The results have been published (Cavallini, Galasso et al. 2020) and are described in Chapter 2.
- b. Study of mechanisms that regulate differential catalase expression in patients with divergent clinical outcome. The results take part of an ongoing project that has as long-term goal developing an integrated prognostic model including standard prognostic parameters and redox metabolic pathways to identify high-risk patients for progressive disease and faster progression. The results are described in Chapter 3.

1.2. Chronic lymphocytic leukemia

Chronic lymphocytic leukemia (CLL) is the most prevalent type of leukemia in Western countries, with the highest incidence in Caucasians (Europe and North America), and an age-adjusted incidence of 4.1 per 100.000 persons per year in the USA and in Europe (Chronic Lymphocytic Leukemia — Cancer Stat Facts <https://seer.cancer.gov/statfacts/html/clyl.html>). It is widespread among elderly people, affecting more male than female (1.7: 1), with the median age at the diagnosis around 70 years (Hallek 2019). CLL is characterized by the expansion of a malignant population of immunologically dysfunctional mature B cells, typically CD5-positive, that accumulate in the bone marrow, lymphoid tissues, peripheral blood and spleen, persisting for more than 3 months (Rozman and Montserrat 1995;

Hallek, Shanafelt, and Eichhorst 2018). CLL is an incurable disease with extremely variable clinical course and response to treatment with some patients having indolent disease and others experiencing a more accelerated course, treatment resistance, and a dismal outcome (Fabbri and Dalla-Favera 2016; Hallek, Shanafelt, and Eichhorst 2018; Hallek 2019).

1.3. The cellular origin of CLL

The specific cellular origin and the precise mechanisms that determine the development of CLL are still poorly understood. CLL is derived from a mature B cell based on the presence of clonal rearrangements of immunoglobulin (IG) genes, the weak expression of B cell markers (surface membrane immunoglobulins (Ig), CD19 and CD20), expression of CD23 (also known as FcεRII) and of the CD200 and CD5 antigens (U. Klein et al. 2001; Brown 2008). However, several lines of evidence indicate that self-renewing HSCs (hematopoietic stem cells) take play in pathogenesis of CLL, suggesting that the primary tumorigenic event in CLL might involve multipotent, self-renewing HSCs. Indeed, HSCs from CLL patients transplanted into an immunodeficient mouse efficiently engraft and proliferate (Kikushige et al. 2011). On the other hand, in multipotent cell progenitors from CLL patients some CLL-related genetic lesions were detected, further suggesting that immature precursors may be implicated in the pathogenesis of the disease (Fabbri and Dalla-Favera 2016). Other molecular and/or environmental factors may contribute to further B cell modifications. Two subgroups of patients can be distinguished based on the presence or absence of mutations in the immunoglobulin heavy chain variable region (IGHV) genes. The IGHV- mutated (IGHV-M) CLLs are derived from antigen-experienced B cells that have transited through the germinal center (GC) of secondary lymphoid organs, the site of immunoglobulin somatic hypermutation. On the contrary, IGHV-unmutated (IGHV-UM) CLLs are derived from pre-GC (naive) B cells or GC-independent antigen-experienced B cells. Overall, CLL derived from GC-experienced B cells has been distinguished from CLL arisen from pre-GC naive B cells or GC-independent memory B cells. In both cases, additional genetic and epigenetic alterations, antigenic stimulation and microenvironmental factors can contribute to CLL pathogenesis. The monoclonal

B cell lymphocytosis (MBL) is the early or low stage of CLL, identified between 6 months and 7 years before the diagnosis of CLL (Landgren et al. 2009). MBL is defined as the presence of a clonal B-cell population in the peripheral blood with fewer than $5 \times 10^9/L$ B-cells (Strati and Shanafelt 2015; Darwiche et al. 2018) (**Figure 1**).

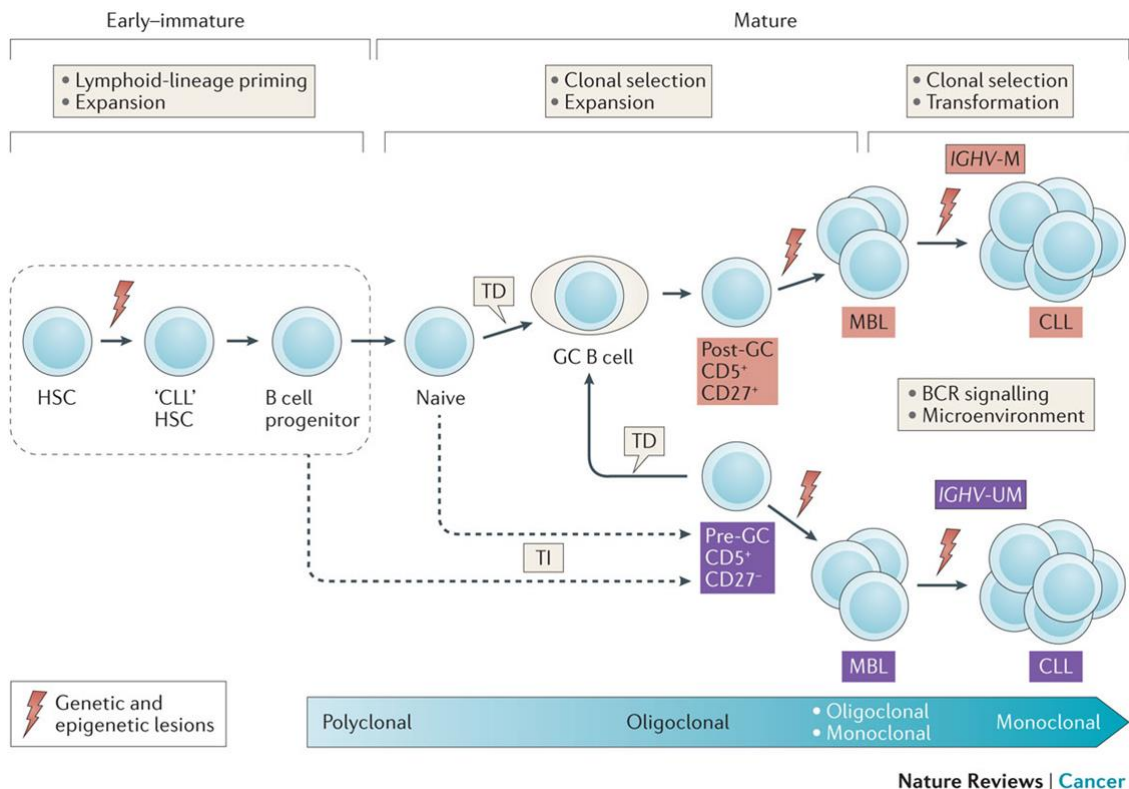


Figure 1. The cellular origin of chronic lymphocytic leukemia (Fabbri and Dalla-Favera 2016).

1.4. Recurrent genetic aberrations

The most frequent chromosomal abnormalities detected in CLL include deletion of 13q14 (~50-60%), trisomy 12 (~20%), deletions of chromosomal regions 11q (~20%), 17p (~10%), and 6q (~9%) (Kröber et al. 2002). The identification of specific genomic aberrations has contributed to the comprehension of the pathogenesis of the CLL disease involving two key regulatory factors of cell cycle, tumor protein 53 (TP53) and ataxia telangiectasia mutated protein (ATM) (17p13: TP53; 11q22–q23: ATM), while for other loci (e.g. 13q) the role of possible tumor

suppressors has not been fully clarified (Zenz, Döhner, and Stilgenbauer 2007). The deletion of 13q14 is more prevalent in IGHV-M than in IGHV-UM CLL and is generally associated with a favorable prognosis even if patients with a deletion extending to the loss of the retinoblastoma 1 (RB1) tumor suppressor gene (~20% of CLL cases) have a less favorable outcome (Dal Bo et al. 2011; Ouillette et al. 2011). This deletion affects the sequence of the miR-15a/16-1 genes, which negatively regulate the anti-apoptotic protein B-cell lymphoma 2 (BCL2) inducing its overexpression (Cimmino et al. 2005). The trisomy 12 is considered an intermediate-risk genetic lesion. Although the extra copy of chromosome 12 comprises approximately 20% of patients, the mechanisms by which it contributes to CLL pathophysiology remain unknown (Döhner et al. 2000; Edelmann et al. 2012). The 17p and 11q deletions typically cause the loss of tumor protein 53 (TP53) and ATM respectively (Döhner et al. 2000; Edelmann et al. 2012; Austen et al. 2007). These deletions are considered as adverse prognostic factors identifying subgroups of patients with rapid disease progression and short survival times in multivariate analysis (Zenz, Döhner, and Stilgenbauer 2007). In addition, specific chromosomal aberrations have been associated with CLL disease characteristics, such as marked lymphadenopathy (11q deletion) or resistance to treatment with conventional chemotherapy (17p deletion). Moreover, the progression of the disease and the overall survival (OS) times, defined by specific genomic aberrations, can significantly change between CLL subgroups (Zenz, Döhner, and Stilgenbauer 2007) (**Figure 2**). Furthermore, in ~10% of CLL patients' mutations in the coding region of the Notch Receptor 1 (NOTCH1) gene have been reported mainly in IGHV-UM subgroup. NOTCH1 mutations have been associated with unfavorable OS (5-year OS 50–70%), even in patients with IGHV-M (Fabbri et al. 2011). The gene encoding the splicing factor 3B subunit 1 (SF3B1) is an additional recurrent mutated gene in patients with CLL (Quesada et al. 2012). The frequency of these genetic alterations ranges from 10 to 17%, thus resulting more frequent in patients with del11q, del13q14 or trisomy 12 and it is related to a faster progression of disease and poor overall survival (Rossi et al. 2011). Therefore, the

crucial aspect in CLL is the lack of a genetic event shared by the overwhelming majority of patients (Fabbri and Dalla-Favera 2016).

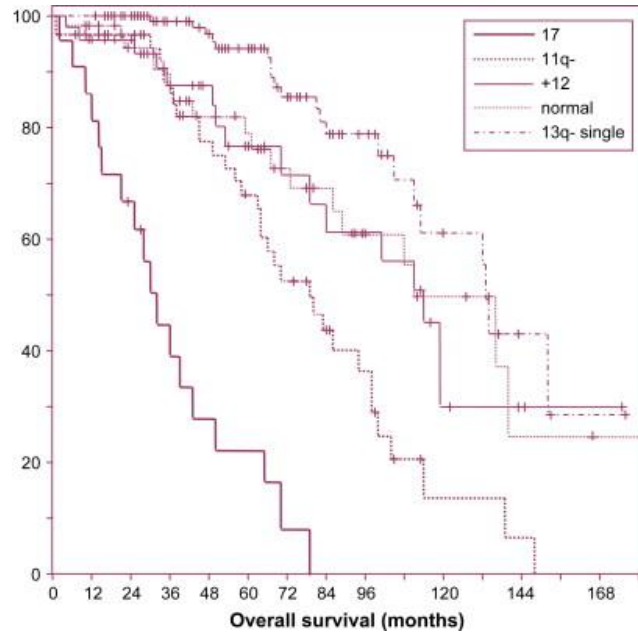


Figure 2. Prognostic relevance of genomic aberrations in chronic lymphocytic leukemia (CLL) (Zenz, Döhner, and Stilgenbauer 2007).

1.4.1. Somatic mutations within the IGHV genes

The primary antibody repertoire is generated by mechanisms involving the assembly of the exons that encode the antigen-binding variable regions of immunoglobulin heavy (IgH) and light (IgL) chains during the early development of B lymphocytes. After antigen-dependent activation, mature B cells can further alter their IgH and IgL variable region exons by the process of somatic hypermutation (SHM) within the germinal centers, which allows the selection of B cells in which SHMs resulted in the production of antibodies with increased antigen affinity (Hwang, Alt, and Yeap 2015). In CLL the presence or absence of somatic hypermutation in IGHV genes is a strong determinant of the patient's prognosis (Hamblin et al. 1999). Patients with mutated IGHV genes (M-CLL) (<98% homology to germline) are typically associated with an indolent course; they have a more favorable prognosis, longer time-to-first-treatment and survival than patients with unmutated IGHV genes (UM-CLL), who develop a more aggressive

and treatment-resistant disease (Hamblin et al. 1999). Furthermore, M-CLL cells show constitutive phosphorylation of signaling proteins and reduced activation of the signaling rebound after B-cell receptor (BCR) triggering by external antigens. On the other hand, cells carrying unmutated IGHV genes generally are more responsive to BCR stimulation (Muzio et al. 2008; Allsup et al. 2005; Damle et al. 1999; Cesano et al. 2013). Moreover, CLL cells are more inclined to apoptosis when cultured *in vitro*, because they lack prosurvival signals enhanced *in vivo* via BCR-dependent and -independent pathways. In particular, M-CLL B cells show a significantly higher rate of spontaneous apoptosis than UM-CLL B cells (Coscia et al. 2011; Steinbrecher et al. 2018).

1.5. B-cell receptor signaling

B-cell receptor (BCR) is an antigen-binding trans-membrane immunoglobulin (mIg) that forms a complex with two trans-membrane polypeptides, namely Ig α (CD79A) and Ig β (CD79B). Both, the CD79A and CD79B subunits, contain an immunoreceptor tyrosine-based activation motif (ITAM), which is composed of two conserved tyrosine residues. Antigen-induced BCR aggregation and its conformation changes lead to LYN-mediated phosphorylation of ITAMs, which initiate the BCR cascade activation (Monroe 2006). The phosphorylation of ITAMs residues creates docking sites for proteins that contain SRC Homology 2 (SH-2) like spleen tyrosine kinase (SYK), inducing its phosphorylation and activation (Seda and Mraz 2015; Monroe 2006). SYK in turn phosphorylates and activates phosphoinositide 3-kinase (PI3K), which consequently phosphorylates the protein kinase B (AKT). Activated PI3K phosphorylates phosphatidylinositol 4,5-bisphosphate (PIP2) in second messenger phosphatidylinositol 3,4,5-triphosphate (PIP3), which acts as a docking site to recruit other effector proteins. Activation of the BCR signal to a downstream signaling is achieved by recruiting the adaptor proteins B cell linker protein (BLNK) that recruit and activate Bruton tyrosine kinase (BTK) and other BCR kinases. BTK plays a central role in BCR signaling and is essential for the survival of leukemic cells in various B cell malignancies (Pal Singh, Dammeijer, and Hendriks 2018; Scupoli and Pizzolo 2012). BTK is activated through Y551 and Y223 phosphorylation (Marcotte et al. 2010; H. Park

et al. 1996). However, the inhibitory Fc-receptors (Fc γ RIIB) containing ITIM (immunoreceptor tyrosine-based inhibition motif) domains recruit phosphatases and reduce BTK activation. The activated BTK phosphorylates phospholipase C γ (PLC γ) which hydrolyses PIP₂ into inositol triphosphate (IP₃) and diacylglycerol (DAG). This second messenger mediates activation of protein kinase C β (PKC β), which activates several members of the mitogen-activated protein kinase (MAPK) family, including extracellular signal-regulated kinases 1 and 2 (ERK1/ERK2) and other MAPK targets, such as Jun N-terminal kinase (JNK), p38, and nuclear factor kappa-light-chain-enhancer of activated B cells (NF- κ B) pathway components (Hashimoto et al. 1998; Seda and Mraz 2015) (**Figure 3**). In M-CLL the balance of BCR signaling shifts towards a constitutive phosphorylation (Byrd et al. 2013; Muzio et al. 2008; Burger and Chiorazzi 2013).

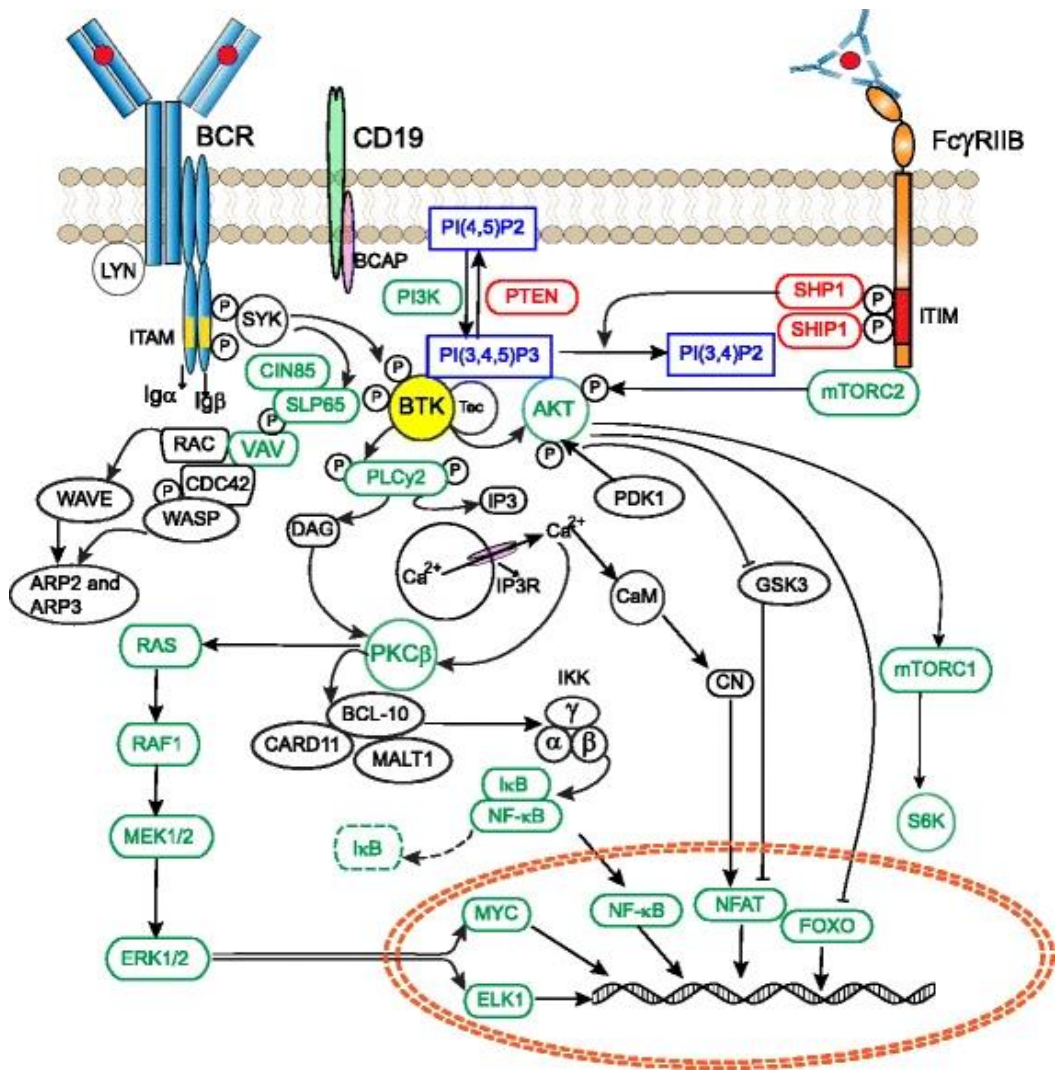


Figure 3. B-cell receptor signaling (BCR). Antigen engagement by the BCR results in the formation of a micro-signalosome whereby BTK activates four families of non-receptor protein tyrosine kinases that transduce key signaling events including phospholipase C γ , mitogen-activated protein kinase (MAPK) activation, nuclear factor kappa-light-chain-enhancer of activated B cells (NF- κ B) pathway components and activation of the serine/threonine kinase AKT (PKB). In addition, BTK mediated signaling events are regulated by various phosphatases that can be recruited to the cell membrane, following crosslinking of inhibitory receptors, e.g., Fc γ RIIB that is exclusively expressed on B cells and signals upon immune complex binding (Pal Singh, Dammeijer, and Hendriks 2018).

1.6. Therapy

During the last 5 years, the dissection of the genetic alterations underpinning CLL, together with the advent of novel drugs, has moved the treatment strategy from universal chemoimmunotherapy to a more individualized approach. At the diagnosis, the assessment of IGHV mutational status, molecular cytogenetics (using FISH) and mutational status of the TP53 gene can provide additional prognostic information (Hallek et al. 2018).

1.6.1. Inhibitors targeting the BCR signaling: idelalisib and ibrutinib

Different aspects, such as the immunoglobulin heavy chain variable gene mutational status and responsiveness to stimulation, have defined the BCR as important target and a prognostic marker in CLL. The B-cell receptor signaling in CLL cells is supported by different tyrosine kinases, such as BTK, spleen tyrosine kinase (SYK), SRC family kinases as well as PI3K (Stevenson et al. 2011). Targeting these B cell receptor associated kinases (BAKs), in particular BTK or PI3K, by specific inhibitors has revolutionized the treatment of CLL (Da Cunha-Bang and Niemann 2018).

In CLL the PI3K pathway is constitutively activated and dependent by PI3K δ (Hoellenriegel et al. 2011). The PI3K δ isoform importance in B-cell signaling have been demonstrated by genetic and pharmacologic approaches that specifically inactivate the δ isoform (Jou et al. 2002; Okkenhaug et al. 2002). Idelalisib is a potent and highly selective PI3K δ inhibitor that induces apoptosis in B-cell lines and primary cells from patients with different B-cell malignancies, including CLL (Sarah E.M. Herman et al. 2010). Idelalisib inhibits CLL cell chemotaxis, and down-regulates secretion of chemokines in stromal cocultures and after BCR triggering (Hoellenriegel et al. 2011). Moreover, idelalisib may acts by different mechanisms, directly decreasing cell survival as well as reducing interactions that retain CLL cells in bone marrow and lymph nodes (Lannutti et al. 2011) .

In CLL, Bruton's tyrosine kinase represent a therapeutic target based on its pivotal role in B-cell receptor signaling, B-cell maturation and survival (Young and Staudt

2013). In addition to its role in BCR signaling, BTK is involved in signaling regulation of B cell migration and adhesion, through chemokine receptors and adhesion molecules (de Gorter et al. 2007). Ibrutinib is a selective BTK inhibitor. The drug binds irreversibly the cysteine residue (C481) in the BTK kinase domain and inhibits BTK phosphorylation and its enzymatic activity inducing CLL cell apoptosis (Sarah E.M. Herman et al. 2011). It has also been reported that ibrutinib inhibits CLL cell survival and proliferation, as well as leukemia cell migration towards the tissue mediated by homing chemokines (Ponader et al. 2012). In CLL patients, ibrutinib induces lymphocytosis during the first weeks of treatment. This phenomenon is due to the redistribution of CLL cells from the tissue compartments into the peripheral blood where proliferation is strongly reduced due to the lack of favourable action of cell microenvironment, whereas pro-apoptotic effect is limited or none; ibrutinib induced lymphocytosis is asymptomatic and resolves in most patients during the first months of therapy (Primo et al. 2018).

1.6.2. CD20 monoclonal antibodies

First-line treatment of patients with active disease is based on chemoimmunotherapy using CD20 (Hallek 2019). The interest in CD20 as a therapeutic target is due to several properties related to its structure and expression. Clearly, the CD20 expression in mature B cell lymphoid malignancies makes CD20 an important therapeutic target. Rituximab, ofatumumab and obinutuzumab are the CD20 monoclonal antibodies approved by the US Food and Drug Administration (FDA) in CLL treatment.

Rituximab is a chimeric antibody murine/human mAb with a human κ constant region and murine light and heavy chain variable regions. It is a type I mAb, binding the large extracellular loop of CD20 (**Figure 4**) (Reff 1994). Rituximab was the first therapeutic mAb to be approved by the FDA for treatment of B-cell lymphoma. Since its approval, anti-CD20 therapy has determined a new epoch in the treatment of B cell malignancies (Pierpont, Limper, and Richards 2018). Rituximab is most often used along with chemotherapy or a targeted drug. The cytotoxic effects of this mAb on CD20-positive malignant B lymphocytes involve complement-dependent

cytotoxicity (CDC), antibody-dependent cellular cytotoxicity (ADCC) and induction of apoptosis. Furthermore, *in vitro* data indicate that rituximab increases sensitivity of cancer cells to the effects of conventional chemotherapy drugs (Plosker and Figgitt 2003).

Ofatumumab is a type I fully human CD20 antibody that binds both the large and the small protein loops (**Figure 4**). It was FDA approved for use in CLL in 2014. In comparison to rituximab, is more effective in complement-dependent cytotoxicity, probably due to the close proximity of the small- loop CD20 binding site for this mAb to the cell surface that, together with a lower dissociation rate, might support more effective antibody-driven deposition of complement on the cell surface (Pawluczko et al. 2009; Burger and O'Brien 2018). Ofatumumab has a toxicity profile similar to that of rituximab and is used as a monotherapy in CLL patients refractory to other treatments (Burger and O'Brien 2018).

Obinutuzumab (GA101) is a humanized glycol-engineered type II CD20 antibody that binds an epitope on the large loop of CD20 that partially overlaps with that of rituximab (**Figure 4**). FDA approved obinutuzumab for CLL treatment in 2013 (Evans, PharmD and Clemmons, PharmD, BCOP 2015). Glyco-engineering compared to non-glycol-engineered antibodies, such as rituximab, results in higher rates of direct death of non-malignant and malignant B cells as well as ADCC and in increased efficacy in inducing direct B cell apoptosis (Dalle et al. 2011). Obinutuzumab is used in combination with chlorambucil for previously untreated CLL (Evans, PharmD and Clemmons, PharmD, BCOP 2015; Du, Mills, and Mao-Draayer 2017).

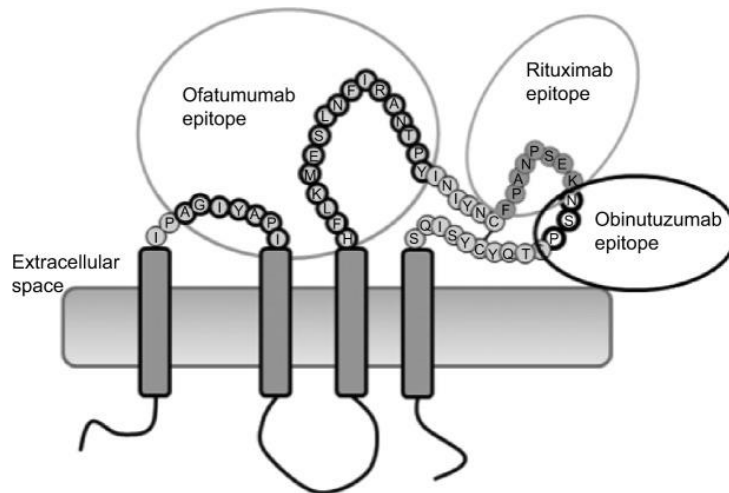


Figure 4. Structure of CD20 and epitope targets of ofatumumab, rituximab, and obinutuzumab (GA101) (Hill and Kalaycio 2015).

1.6.3. Combined therapy

Recently, based on clinical trial results, inhibitors of BCR-associated kinase (BAKi), with or without CD20 mAbs, are indicated as the preferred first-line treatment for most CLL patients, expecting to reduce the chemotherapies in the near future (Burger et al. 2014; Jaglowski et al. 2015; O'Brien et al. 2015; J. A. Jones et al. 2017; Moreno et al. 2019; Bojarczuk et al. 2014; Woyach et al. 2018). The advantage of the combined use of these agents rests on their different mechanisms of anti-leukemia activity. Moreover, BAKi may enhance the effect of CD20-targeting mAbs because they induce the release of CLL cells into the blood from tissue sites, thus potentially favoring the activity of CD20 mAbs (S. E.M. Herman et al. 2014). However, preclinical studies have shown that ibrutinib may antagonize CD20 cellular effector mechanisms (Bojarczuk et al. 2014; Skarzynski et al. 2016). Therefore, BAKi can promote both positive and negative interactions with CD20 mAbs, suggesting that the clinical outcome of combination therapy results from competing effects. Limited data are available on direct effects of CD20 mAbs on BCR signaling in CLL although interferences of CD20 mAbs on BCR signaling have been described in lymphoma cell lines (Bonavida 2006; Vega et al. 2009; Kheirallah et al. 2010; Pavlasova and Mraz 2020).

In chapter 2 is described the first PhD project developed to investigate the effects of CD20 antibodies and kinase inhibitors on BCR signaling and survival of CLL cells. The results have been published (Cavallini, Galasso et al. 2020).

2. CHAPTER 2: Effects of CD20 antibodies and kinase inhibitors on BCR signaling and survival of CLL cells

2.1. Introduction

2.1.1. B-lymphocyte antigen CD20

CD20 is a non-glycosylated protein that belongs to the membrane-spanning 4-domain A (MS4A) protein family. It is a lineage-specific antigen expressed on the surface of pre-B cells, mature and malignant B cells, except hematopoietic stem cell. The CD20 expression among B-cell malignancies is extremely variable with weak CD20 expression in CLL and the highest CD20 cell-surface expression on diffuse large B-cell lymphoma (DLBCL) and hairy cell leukemia cells. CD20 protein is characterized by four hydrophobic transmembrane domains with two extracellular domains, the large and small loops, and one intracellular domain (Pavlasova and Mraz 2020; Einfeld et al. 1988) (**Figure 4**). Three CD20 isoforms with molecular weight of 33, 34 or 35 kDa, result from phosphorylation at different sites. In resting B-cells CD20 phosphorylation is lower than proliferating malignant B cells (Tedder and Schlossman 1988). Additionally, it has been observed that CD20 phosphorylation increased after mitogen stimulation favoring the hypothesis on its activity as calcium channel in B-cell activation (Tedder and Schlossman 1988). CD20 is involved in B cell activation, differentiation, and calcium transport. Although CD20 biological function in B lymphocytes and its physiological ligand remain unclear, it is known that association with other cell-surface and cytoplasmic proteins such as major histocompatibility complex class II (MHCII), CD40, CD53, CD81, and CD82, mediates signal transduction. Moreover, CD20 protein tends to associate with BCR and the C-terminal SRC kinase-binding protein (CBP) that interacts with SRC kinases such as LYN (**Figure 5**) (Pavlasova and Mraz 2020). It has also been shown that CD20 colocalize into lipid rafts (Petrie and Deans 2002) and physically interact with BCR (Polyak et al. 2008). In lymphoma cell lines, treatment with rituximab mediates BCR downmodulation (Kheirallah et al. 2010) and in CLL cell lines the silencing of CD20 influences the phosphorylation of multiple BCR-associated kinases and proteins after BCR-engagement (Pavlasova

et al. 2018). This effect has important implications for combining BCR inhibitors with antibodies targeting CD20.

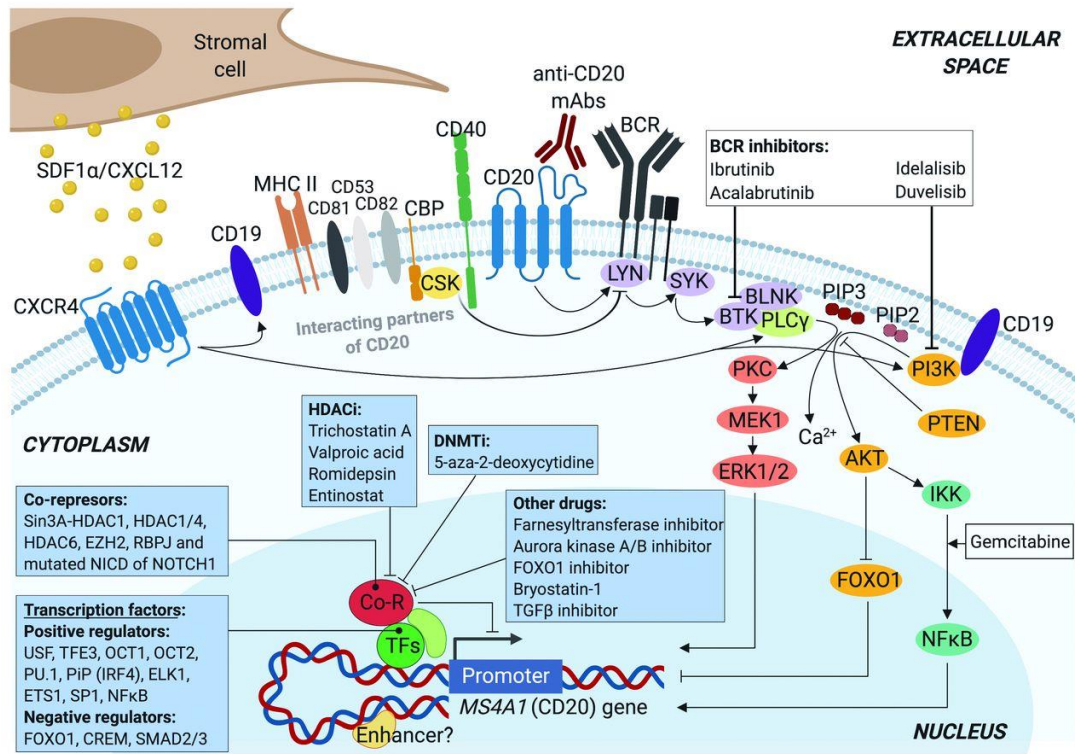


Figure 5. Interacting partners of CD20 on cell membrane. mAbs: monoclonal antibodies; BCR: B-cell receptor; HDACi: histone deacetylase inhibitors; DNMTi: DNA methyl-transferase inhibitors; NICD: NOTCH1 intracellular domain; TGFβ: transforming growth factor β (Pavlasova and Mraz 2020).

2.1.2. CD20 monoclonal antibodies: mechanism of action

Binding of CD20 by monoclonal antibodies can result in different effector mechanisms (Okroj, Österborg, and Blom 2013; M. J. E. Marshall, Stopforth, and Cragg 2017) including:

- ADCC, in which natural killer (NK) cells interact with CD20 antibodies via FcγRIIIA receptor, causing direct lytic attack on opsonized target cells;
- ADCP, in which phagocytic cells, such as macrophages, monocytes, and neutrophils interact with CD20 antibodies through FcγR-dependent mechanism, causing degradation and phagocytosis of opsonized target cells;

- CDC, in which binding of CD20 by CD20 mAbs causes the activation of the classical complement pathway, resulting in the formation of the membrane attack complex (MAC) and the consequent osmotic cell lysis;
- Induction of apoptosis. CD20 mAbs trigger intracellular signaling, resulting in induction of cell death (Lim et al. 2010).

2.1.3. CD20 monoclonal antibodies: type I and type II

The different CD20 mAbs can be functionally divided into two distinct subtypes, type I or type II, on the bases of the different functions they exert on B cells *in vitro*. Type I CD20 mAbs, which comprise the chimeric IgG1 (Immunoglobulin G1) mAb rituximab and the fully human xeno-mouse IgG1 mAb ofatumumab, are characterized by their ability to induce a translocation of CD20 into ‘lipid rafts’ within the plasma membrane upon binding and to activate a high CDC response. In contrast, type II mAbs, which include the glycol-engineered, humanized IgG1 mAb obinutuzumab, do not induce clustering of CD20 upon antibody binding and show low CDC activity while induce higher homotypic adhesion and direct cell death than type I mAbs (C. Klein et al. 2013; Oldham, Cleary, and Cragg 2014). Moreover, type I antibodies are able to bind CD20 tetramers in a manner that does not block binding of subsequent antibodies, whereas type II antibodies are thought to bind across the tetramer, blocking the binding of further mAbs (Oldham, Cleary, and Cragg 2014). The enhanced clustering of type I antibodies make them more susceptible to internalization and consequently lysosomal degradation and reduction in CD20 expression (Beers et al. 2010). On the other hand, type II antibodies induce a greater degree of directly induced cell death compared with type I (Chan et al. 2003).

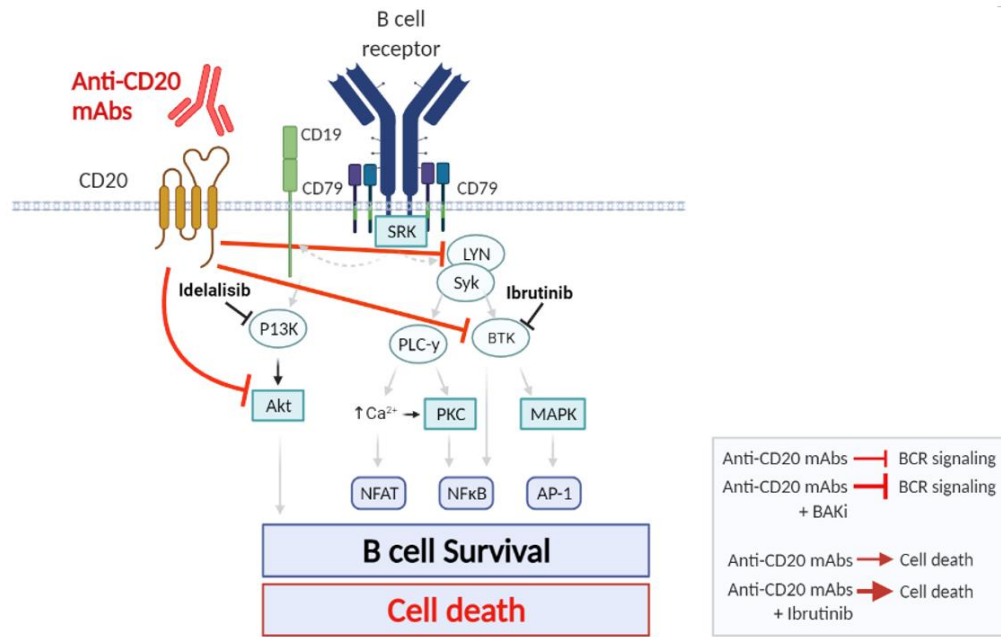


Figure 6. Graphical abstract. Effects of CD20 antibodies and kinase inhibitors on BCR signaling and survival of CLL cells. mAbs: monoclonal antibodies; BAKi: BCR-associated kinase inhibitors.

2.2. Aim of the study

First-line treatment of CLL patients with active disease is based on chemoimmunotherapy using CD20 monoclonal antibodies (mAbs) (Hallek 2019). Binding of CD20 by mAbs can result in different effector mechanisms including CDC, ADCC, ADCP and direct induction of apoptosis (Okroj, Österborg, and Blom 2013). In parallel to CD20-mAbs development, the knowledge about the importance of B-cell receptor signaling for survival and expansion of leukemic cell clones provides the basis for development of novel small-molecule inhibitors targeting BCR-associated kinases. Among the most important BAKi, BTK inhibitor ibrutinib and the PI3K δ inhibitor idelalisib, have emerged as breakthrough targeted therapy for patients with CLL (Packham et al. 2014; Cavallini et al. 2017; Q. Yang et al. 2015; Burger 2020). Inhibitors of BAK, with or without CD20 mAbs, have been established as the preferred first-line treatment for most CLL patients (Burger et al. 2014; Jaglowski et al. 2015; O'Brien et al. 2015; J. A. Jones et al. 2017; Moreno et al. 2019; Furman et al. 2014; Woyach et al. 2018; Shanafelt et al. 2018).

Elucidation of the possible influence of CD20 mAbs on BCR signaling and on the activity of BAKi is of pre-eminent importance for deciphering interactions of these agents and improving the clinical benefit of combination therapy.

The objectives of this study are:

- a) evaluate the effects of the CD20 mAbs rituximab, ofatumumab and obinutuzumab on the activation status of BCR kinases (**Figure 6**)
- b) evaluate the direct apoptotic effect of combination between CD20 mAbs and BAKi compared to the activity of the single agents (**Figure 6**)

2.3. Materials and methods

2.3.1. Sampling and sample preparation

Peripheral blood was collected from 10 untreated CLL patients at the Hematology Unit, Azienda Ospedaliera Universitaria Integrata (AOUI) in Verona (Italy), with the approval of the local Ethics Committee (Comitato Etico per la Sperimentazione, AOUI). Written informed consent was obtained from all patients in accordance with the Declaration of Helsinki. Clinical annotations at diagnosis are summarized in **Table 1**. Peripheral blood mononuclear cells (PBMCs) of CLL patients were isolated by Ficoll-hypaque gradient centrifugation (lymphoprep, nicomed, Oslo, Norway) and cryopreserved in liquid nitrogen. All the samples used in the study showed at least 85% viability after thawing, as assessed using 7-amino-actinomycin (7-AAD) dye (BD Biosciences, San Jose, CA) and flow cytometry analysis (FACSCanto; Becton Dickinson, Franklin Lakes, NJ). To avoid CD20 mAbs immuno-mediated cytotoxic effects in apoptosis analysis, CLL cells from samples with <90% B cells were isolated by negative selection using Human B-Cell Enrichment Kit (Stem Cell Technologies, Vancouver, Canada). After separation, cell purity was routinely above 98%, as assessed with CD19 staining and flow cytometry (FACSCanto; Becton Dickinson).

2.3.2. Analysis of CD20 and IgM expression on CLL surface

The presence of CD20 receptor and IgM on CLL cell surface was determined by staining 1×10^6 cells with cocktails of fluorochrome-conjugated antibodies for 10 minutes (**Table 2**). As a control, a tube was stained with only CD19, CD5 and 7AAD. 7AAD was added 10 minutes before acquisition, without washing. Approximately 1×10^4 -gated events were acquired on a BD LSRFortessa instrument (Becton Dickinson) and data were analyzed by FlowJo software (v10 TreeStar, Ashland, OR). Dead cells, debris, and doublets were excluded on the basis of forward-scatter, side-scatter, and 7AAD signals. CLL cells were identified on the basis of CD19/CD5 co-expression.

Table 1. Clinical and biological characteristics of CLL patients

Patient	Gender	Age at diagnosis [*] (years)	Follow up (years)	Requiring treatment	TTFT ^{††} (months)	Rai	Binet	CD38 [§]	ZAP70 [‡]	IGHV [†]	Cytogenetic	Cytogenetic risk ^{§§}
AIRC#0053	M	67	8	no	102	0	A	neg	neg	M	normal	neutral
AIRC#0184	M	82	3	no	35	1	B	neg	pos	M	del 13q	favorable
AIRC#0191	F	55	17	yes	2	0	A	pos	neg	UM	del 13q	favorable
CLL#000	F	48	9	yes	0	4	C	neg	neg	M	trisomy 12q + del 13q	neutral
CLL#001	M	42	9	yes	9	1	B	neg	neg	UM	del 11q + del 13q	unfavorable
CLL#005	M	63	14	yes	49	1	A	neg	pos	M	normal	neutral
CLL#006	F	81	2	yes	11	1	A	pos	neg	UM	normal	neutral
CLL#008	M	50	15	no	184	0	A	neg	neg	M	normal	neutral
CLL#013	F	55	6	yes	32	1	A	pos	neg	UM	normal	neutral
CLL#014	M	62	14	yes	78	0	A	pos	pos	UM	trisomy 12q	neutral

*diagnosed according to 2008 Guidelines for Diagnosis and Treatment of CLL (Hallek et al, 2008);

††TTFT: time-to-first-treatment;

§CD38 was determined using a 30% cut-off; neg: negative; pos: positive;

‡ZAP70 was determined using a 20% cut-off; neg: negative; pos: positive;

†IGHV sequencing utilized a 2% cut-off to discriminate mutated from unmutated IGHV; M: mutated; UM: unmutated;

§§Patients were stratified into major cytogenetic categories, based on national comprehensive cancer network (NCCN) CLL Guidelines (Hallek et al, 2008): favorable (del 13q as a sole aberration), neutral (normal karyotype, trisomy 12q), and unfavorable (11q and/or 17p deletion).

Table 2. Antibodies used for CD20 and IgM expression analysis

Antibody	Fluorochrome	Clone	Manufacturer
CD20	PE	2H7	BD Biosciences
IgM	APC	G20-127	BD Biosciences
7AAD	-	-	BD Biosciences
CD19	BV421	HIB19	BD Biosciences
CD5	BV510	L17F12	BD Biosciences

2.3.3. Phosphospecific flow cytometry

Phosphospecific flow cytometry was used to analyze the phosphorylation of SYK, ERK1/2, BTK, PLC γ 2, AKT, NF- κ B p65, and LYN. PBMCs were rested for 24 hours at 37°C in RPMI 1640 GlutaMAX medium supplemented with 10% fetal bovine serum at 37°C, treated with 20 μ g/ml CD20 mAbs (rituximab, RTX; ofatumumab, OFA; or obinutuzumab, OBZ) as single agent, irrelevant isotype-matched control antibody (isotype) or vehicle control for 2 hours at 37°C, and then stimulated with 20 μ g/mL goat F(ab')₂ anti-human immunoglobulin M (IgM; SouthernBiotech, Birmingham, AL) or vehicle for 10 minutes at 37°C. When indicated, before CD20 mAb treatment, cells were incubated with 1 μ M ibrutinib or 1 μ M idelalisib for 30 minutes. After modulation, cells were fixed and permeabilized with PerFix Expose kit (Beckman Coulter, Miami, FL). Permeabilized cells were washed, pelleted, and stained with cocktails of fluorochrome-conjugated antibodies (**Table 3**). Samples were prepared in duplicate, plating 1×10^5 cells per well in 96-well plates. Liquidator 96 (Mettler Toledo, Columbus, Ohio) was used to ensure reproducible results from well to-well and plate-to-plate.

Table 3. Antibodies used for phosphospecific flow cytometry

Antibody	Fluorochrome	Clone	Manufacturer
pERK1/2 (pT202/pY204)	AlexaFluor488	D13.14.4E	Cell Signalling Technology, Danvers, MA
pPLCγ2 (pY759)	AlexaFluor488	K86-689.37	BD Biosciences
pBTK (pY551)/Itk (pY511)	PE	24a/BTK(Y551)	BD Biosciences
pBTK (pY223)/Itk (pY180)	PE	N35-86	BD Biosciences
pAKT (pS473)	PE	D9E	Cell Signalling Technology
pSYK (pY352)/ZAP70 (pY319)	PECy7	17A/P-ZAP70	BD Biosciences
pNF-κB p65 (pS529)	PECy7	K 10-895.12.50	BD Biosciences
Cleaved PARP (cPARP)	AlexaFluor647	F21-852	BD Biosciences
CD3	APCCy7	UCHT1	BioLegend
CD19	BV510	SJ25C1	BD Biosciences
CD5	V450	L17F12	BD Biosciences

For LYN detection, cells were treated with 20 μ g/ml CD20 (RTX, OFA, or OBZ) as single agent or 0.1 μ M of dasatinib, Lyn inhibitor, for 2 hours at 37°C, and then

stimulated with 20 µg/mL goat F(ab')₂ anti-human IgM or vehicle for 10 minutes at 37°C. Permeabilized cells were washed, pelleted, FC receptors blocked with 10% heat-inactivated human serum + 0.5% BSA (both from Sigma-Aldrich, Milan, Italy) for 15 minutes and incubated with unconjugated pLYN (pY396; abcam, Cambridge, England) for 1 hour on ice. Cells were then washed and incubated with secondary antibody goat anti-rabbit IgG H&L-AlexaFluor488 (abcam) for 15 minutes on ice in the dark with subsequent washing and staining with CD5-BV605, CD19-BV786, anti-cleaved poly-ADP-ribose polymerase (cPARP)-Alexa Fluor700, and CD3-APCCy7 (for details see **Table 4**).

Table 4. Antibodies used for phospho-LYN detection

Antibody	Fluorochrome	Clone	Manufacturer
p-LYN (pY396)	-	Polyclonal	Abcam
Goat anti-rabbit	AlexaFluor488		Abcam
cPARP	AlexaFluor700	F21-852	BD Biosciences
CD3	APCCy7	UCHT1	BioLegend
CD19	BV786	SJ25C1	BD Biosciences
CD5	BV605	UCHT2	BD Biosciences

2.3.4. Western blot analysis

Ramos B cells (ECACC) were maintained in RPMI 1640 GlutaMAX medium supplemented with 10% fetal bovine serum, treated with 20 µg/ml CD20 mAbs (RTX, OFA, OBZ) or left unstimulated for 2 hours. Cells were then lysed and the concentration of the total proteins in cell lysates was determined by BCA Protein Assay (Thermo Fisher Scientific, Waltham, MA, USA). Equal amounts of cellular proteins (50 µg) were resolved in SDS-polyacrylamide gel electrophoresis (SDS-PAGE) and transferred to nitrocellulose membrane (Thermo Fisher Scientific, Waltham, Massachusetts, USA). The membranes were first blocked in TBS solution containing 5% nonfat-milk and 0.1% Tween-20 for 1h at room temperature, incubated overnight at 4°C with specific primary antibodies and 1h at room temperature with secondary antibodies. Glyceraldehyde 3- phosphate dehydrogenase (GAPDH) was used for the protein loading control. The bound

antibodies were visualized with appropriate HRP-linked secondary antibodies using ECL Western blotting Substrate (Madison, Wisconsin, USA). Signals were analyzed using the Alliance Q9 Advanced instrument (Uvitec, Cambridge UK), densitometry analysis of western blot protein bands was performed using the in-built software and normalized calculating the ratio between pBTK (pY551)/Itk (pY511) and glyceraldehyde 3-phosphate dehydrogenase (GAPDH) signals.

2.3.5. Apoptosis

Apoptosis was evaluated using the annexin V-FITC/propidium iodide (PI) detection kit (ThermoFisher Scientific, Waltham, MA, USA) and flow cytometry. After cryopreservation, PBMCs were thawed and rested for 1 hour at 37°C in RPMI 1640 GlutaMAX medium supplemented with 10% fetal bovine serum at 37°C, treated with 20 µg/ml CD20 mAbs (RTX, OFA, or OBZ) or vehicle for 2 hours at 37°C, and then stimulated with 20 µg/mL goat F(ab')₂ anti-human IgM (SouthernBiotech) or vehicle for 12 and 24 hours at 37°C. To assess the effect of combination of therapeutic agents on apoptosis, PBMCs were first treated with BAKi (1 µM ibrutinib or 1 µM idelalisib) for 30 minutes and then with 20 µg/ml CD20 mAbs for 24 hours at 37°C. Following treatment of PBMCs with CD20 mAbs and/or BAKi at the indicated time, 1.25x10⁵ cells were harvested and stained with anti-annexin V-FITC, CD5-BV605 (BD Biosciences), CD19-BV786 (BD Biosciences), CD3-APCCy7 (BioLegend, San Diego, CA) for 10 minutes in the dark. PI was added just before the acquisition on the sample on instrument. For annexinV/PI assay analysis, approximately 1x10⁴-gated events were acquired for each sample on a BD LSRFortessa flow cytometer (Becton Dickinson). Flow cytometry data were processed using FlowJo software (v10 TreeStar). For data analysis debris were excluded based on forward-scatter and side-scatter and residual T cells were excluded on the basis of CD3 signal. Viable cells were defined as annexin V-negative and PI-negative.

2.3.6. Analysis of drug interaction on CLL cell survival

Interaction between CD20 mAbs and BAKi at fixed concentrations (20 µg/ml CD20 mAbs and 1 µM BAKi) was assessed by combination index (*CI*), where $CI < 1$, $CI = 1$, and $CI > 1$ indicate synergistic, additive, or less than additive effect, respectively (Chou 2010). *CI* was calculated according to Krause et al. as the ratio of expected to observed combination apoptotic effect using the formula:

$$CI = \frac{1 - rS_{s.a.1} \times rS_{s.a.2}}{(1 - rS_{comb.})}$$

in which *rS* refers to the relative survival after treatment with the respective single agents (*s.a.*) or combination (Krause et al. 2016).

2.3.7. Statistical analysis

Outliers were identified by the ROUT method ($Q = 1\%$). For comparisons, one-way ANOVA or two-way ANOVA were used as appropriate, using the Tukey, Dunnett or Sydak multiple comparison test. Logit transformation was used for the analysis of percentage data of apoptosis. Correlation analyses were performed calculating Spearman correlation coefficient (Spearman *r*). $P \leq 0.050$ was considered statistically significant. Graphing and statistical analyses were performed using GraphPad Prism software (v.8.4.1, GraphPad Software Inc., La Jolla, CA, USA).

2.4. Results

2.4.1. CD20 therapeutic antibodies inhibit BCR signaling

To investigate the capacity of therapeutic CD20 mAbs to modulate BCR signaling, we analyzed, in 10 CLL cell samples, the phosphorylation levels of six proteins downstream of the BCR signaling (namely SYK, ERK1/2, BTK, PLC γ 2, AKT, NF- κ B p65) following treatment with rituximab (RTX), ofatumumab (OFA), or obinutuzumab (OBZ), three therapeutic CD20 mAbs approved for use in CLL. For BTK, we examined the two regulatory tyrosine residues involved in the catalytic activation, i.e. Y551 and Y223 (H. Park et al. 1996). Phosphorylation of the BCR signaling proteins was measured in the basal condition (i.e. unstimulated) or under BCR stimulation with anti-IgM (i.e. anti-IgM-stimulated) at the single-cell level using phosphospecific flow cytometry. Before treatments, we measured the expression levels of CD20 and IgM on the CLL cell membrane surface as shows **Figure 7**.

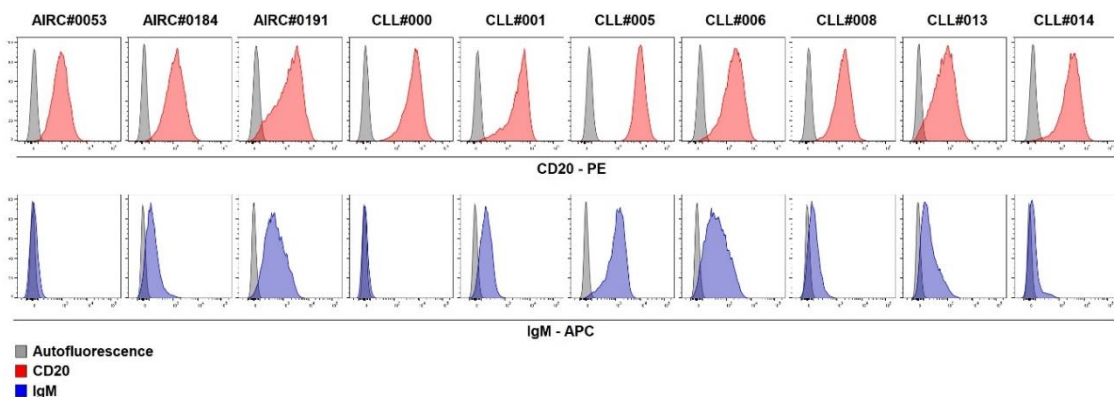


Figure 7. Expression of CD20 and IgM on CLL cells. Flow cytometry histograms of CD20 (red) and IgM (blue) expression compared to autofluorescence (gray) measured in CLL samples (n = 10).

Overall, BCR stimulation with anti-IgM antibodies induced a clear increase of the phosphorylation levels of BCR pathway phosphoproteins (**Figure 8, 9**). Specifically, for BTK, at the time point of analysis anti-IgM stimulation induced a

more pronounced increase of pBTK^{Y223} than pBTK^{Y551}, which indicates BTK increased activity (Ma et al. 2014).

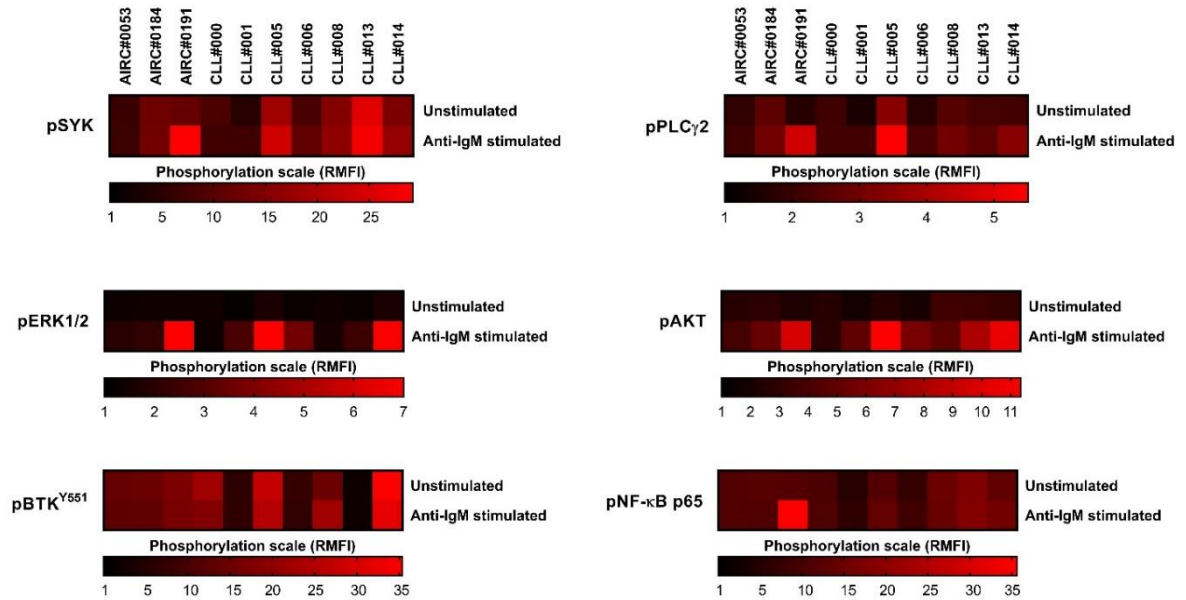


Figure 8. Functional characterization of BCR in CLL cells. BCR signaling profiles in basal condition or following stimulation with anti-IgM across CLL samples ($n = 10$). Data are expressed as median fluorescence intensity (MFI) divided by autofluorescence (relative median fluorescence intensity = RMFI) and represented as a pseudo-color map.

The phosphorylation responses to CD20 mAbs, measured as the log₂-fold change in phosphorylation between CD20-modulated and isotype-modulated signals, were heterogeneous across patients (**Figure 10 A**). Indeed, while for some phosphoproteins we documented a moderate or null modulation, for other phosphoproteins we detected a statistically significant phosphorylation reduction. Specifically, pBTK^{Y551} exhibited a clear-cut and significant decrease across CLL samples upon treatment with RTX or OFA in the unstimulated condition and with RTX, OFA or OBZ in the anti-IgM condition (**Figure 10 A**). In contrast, CD20 mAbs did not modulated phosphorylation of the Y223 residue of pBTK as shown in **Figure 9**.

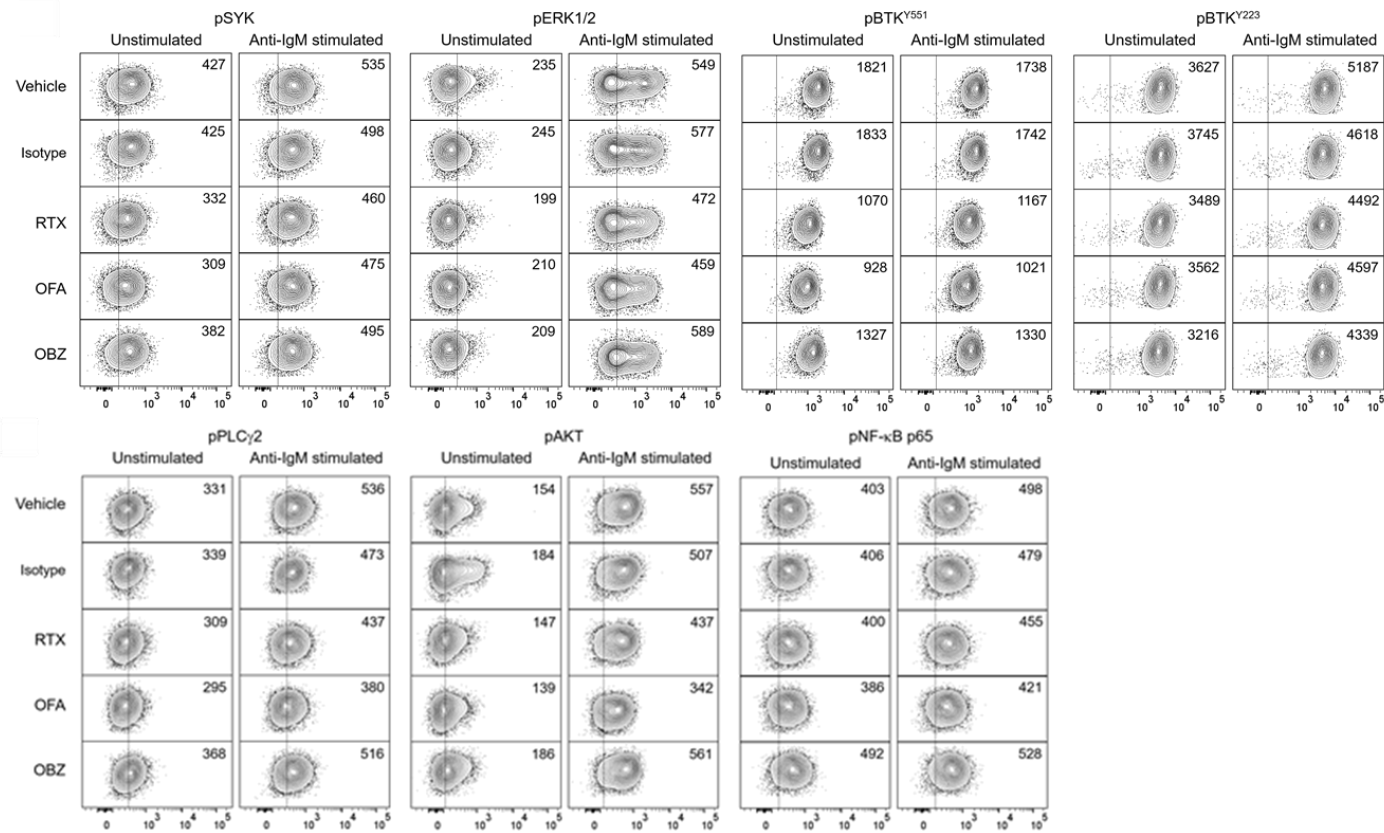


Figure 9. Responses of BCR signaling proteins to treatments with CD20 mAbs. Representative flow cytometry contour plots of phosphorylation levels of BCR proteins measured in CLL cells treated with CD20 mAbs or irrelevant IgG1 antibody as control in the unstimulated or anti-IgM stimulated conditions. Vertical line indicates autofluorescence upper limit. Median fluorescence intensity value is reported for each contour plot. BCR, B-cell receptor; CLL, chronic lymphocytic leukemia; RTX, rituximab; OFA, ofatumumab; OBZ, obinutuzumab.

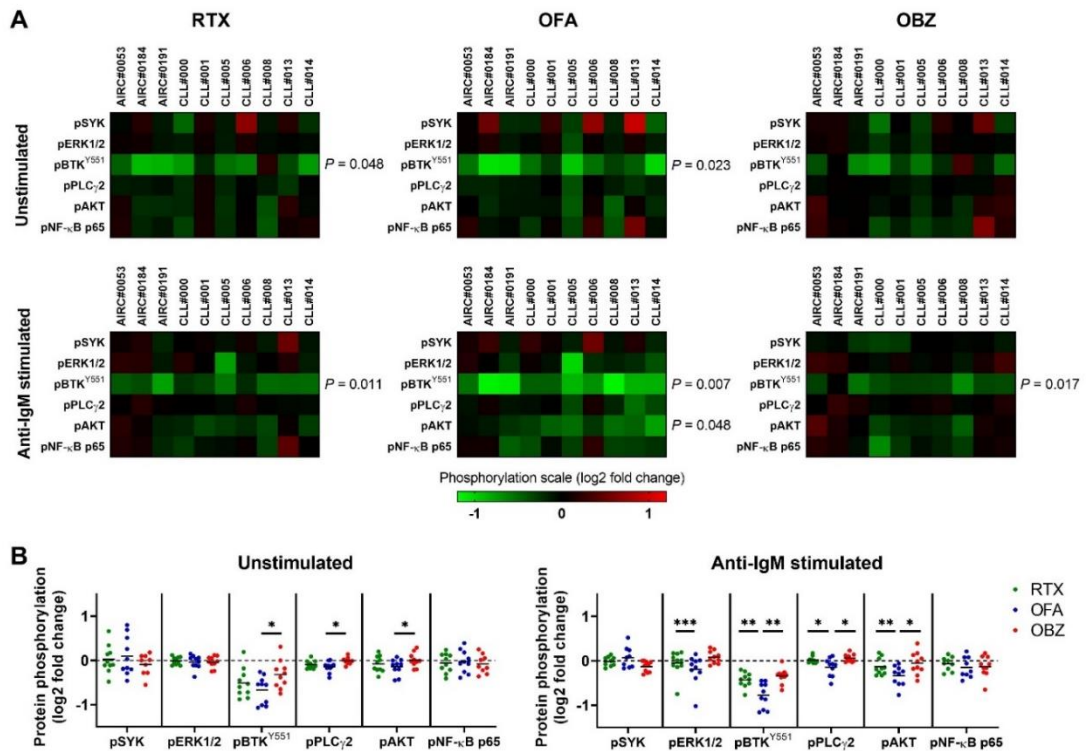


Figure 10. Responses of BCR signaling proteins to treatment with CD20 mAbs. CLL cell samples were thawed and rested for 24 h before treatment with 20 $\mu\text{g/ml}$ RTX, OFA, OBZ, or irrelevant isotype-matched control antibody (isotype) for 2 h, followed by stimulation with 20 $\mu\text{g/ml}$ anti-IgM (anti-IgM-stimulated) for 10 min or left unstimulated. (A) BCR signaling protein phosphorylation responses in CLL cell samples ($n = 10$) after treatment with RTX, OFA or OBZ, in the unstimulated or anti-IgM-stimulated conditions, were calculated as the log₂-fold change between CD20-treated and isotype-treated and represented as a pseudo-color map. Comparisons were performed using the one-way ANOVA and each P value was corrected for multiple comparison using the Sidak test. (B) Comparison of phosphorylation responses of BCR proteins to CD20 mAbs in CLL cell samples ($n = 10$) in the unstimulated or anti-IgM-stimulated conditions. Protein phosphorylation was measured as the log₂-fold change between CD20-treated and isotype-treated signals. Dashed line indicates the log₂ value = 0, corresponding to 'no change' with respect to the control. Comparisons were performed using the one-way ANOVA and each P value was corrected for multiple comparison using the Tukey multiple comparison test. *, $P \leq 0.050$; **, $P \leq 0.010$; ***, $P \leq 0.001$. BCR, B-cell receptor; CLL, chronic lymphocytic leukemia; RTX, rituximab; OFA, ofatumumab; OBZ, obinutuzumab.

We also showed a significant decrease of pAKT following treatment with OFA in the anti-IgM-stimulated condition (**Figure 9, 10 A**). The signaling responsiveness to CD20 mAbs in subgroups of patients defined by IGHV mutational status is reported in **Table 5** and **6**.

Table 5. Modulation of BCR signaling pathway induced by CD20 mAbs in mutated and unmutated CLL in unstimulated condition

		pSYK	pERK1/2	pBTK ^{Y551}	pPLC γ 2	pAKT	pNF- κ B p65
RTX	Mutated reduced*/total cases (%)	1/5 (20%)	0/5 (0%)	4/5 (80%)	0/5 (0%)	1/5 (20%)	1/5 (20%)
	Unmutated reduced*/total cases (%)	0/5 (0%)	0/5 (0%)	4/5 (80%)	0/5 (0%)	0/5 (0%)	0/5 (0%)
OFA	Mutated reduced*/total cases (%)	0/5 (0%)	1/5 (20%)	4/5 (80%)	1/5 (20%)	2/5 (40%)	2/5 (40%)
	Unmutated reduced*/total cases (%)	1/5 (20%)	0/5 (0%)	4/5 (80%)	0/5 (0%)	0/5 (0%)	0/5 (0%)
OBZ	Mutated reduced*/total cases (%)	1/5 (20%)	0/5 (0%)	3/5 (60%)	0/5 (0%)	0/5 (0%)	1/5 (20%)
	Unmutated reduced*/total cases (%)	0/5 (0%)	0/5 (0%)	2/5 (40%)	0/5 (0%)	0/5 (0%)	0/5 (0%)

*: phosphoproteins were considered reduced with a fold change ≤ 0.8 (corresponding to a 20% reduction of phosphorylation level with respect to vehicle).

Table 6. Modulation of BCR signaling pathway induced by CD20 mAbs in mutated and unmutated CLL in anti-IgM stimulated condition

		pSYK	pERK1/2	pBTK ^{Y551}	pPLC γ 2	pAKT	pNF- κ B p65
RTX	Mutated reduced*/total cases (%)	0/5 (0%)	1/5 (20%)	4/5 (80%)	0/5 (0%)	1/5 (20%)	0/5 (0%)
	Unmutated reduced*/total cases (%)	0/5 (0%)	0/5 (0%)	3/5 (60%)	0/5 (0%)	2/5 (40%)	0/5 (0%)
OFA	Mutated reduced*/total cases (%)	0/5 (0%)	1/5 (20%)	5/5 (100%)	2/5 (40%)	2/5 (40%)	2/5 (40%)
	Unmutated reduced*/total cases (%)	0/5 (0%)	1/5 (20%)	5/5 (100%)	2/5 (40%)	3/5 (60%)	1/5 (20%)
OBZ	Mutated reduced*/total cases (%)	0/5 (0%)	0/5 (0%)	2/5 (40%)	0/5 (0%)	2/5 (40%)	1/5 (20%)
	Unmutated reduced*/total cases (%)	0/5 (0%)	0/5 (0%)	4/5 (80%)	0/5 (0%)	0/5 (0%)	0/5 (0%)

*: phosphoproteins were considered reduced with a fold change ≤ 0.8 (corresponding to a 20% reduction of phosphorylation level with respect to vehicle).

The ability of phosphospecific flow cytometry to capture modulation of BCR signaling phosphoproteins induced by CD20 mAbs was also validated in Ramos B cells comparing flow cytometry with Western blotting analyses of pBTK^{Y551} following treatment with CD20 mAbs (**Figure 11**).



Figure 11. Comparison of Western blot (WB) and flow cytometry (FCM) analyses of pBTK^{Y551} modulation induced by CD20 mAbs. Ramos cells were incubated with CD20 mAbs rituximab (RTX), ofatumumab (OFA), obinutuzumab (OBZ) or left unstimulated (vehicle) for 2 hours. Cells were then divided and lysed for Western blot analysis or fixed and permeabilized for flow cytometry analysis. WB signals of pBTK^{Y551} are normalized dividing by GAPDH signals and FCM data are expressed as median fluorescence intensity divided by autofluorescence (relative median fluorescence intensity = RMFI). Modulation of pBTK^{Y551} in response to CD20 mAbs are represented as pseudo-color map setting the vehicle control to 100%. A representative experiment of 3 is shown.

Interestingly, the CD20-mAb-mediated decrease of pBTK^{Y551} in Ramos cells, which do not express Fc gamma receptor 2b (FCGR2B) (Lim et al. 2011), indicates that modulation of pBTK^{Y551} in the absence of FCGR2B is driven by CD20 and not FCGR2B engagement.

Then, comparison of phosphorylation responses across the three CD20 mAbs, measured as the log₂fold-change in phosphorylation between CD20-modulated and isotype-modulated signals in the unstimulated and anti-IgM-stimulated conditions, showed that in the unstimulated condition OFA induced a significant higher reduction of pBTK^{Y551}, pPLCγ2, and pAKT compared with OBZ whereas in the anti-IgM-stimulated condition OFA induced a significant higher reduction of pERK1/2, pBTK^{Y551}, pPLCγ2, and pAKT compared with RTX and of pBTK^{Y551}, pPLCγ2, and pAKT compared with OBZ (**Figure 10 B**)

Taken together, our results showed that CD20 ligation with therapeutic antibodies inhibits signalling of BCR proteins, preferentially targeting pBTK^{Y551} and, at a lesser extent, pAKT.

2.4.2. Combination of CD20 mAbs with BAKi enhances the BCR-inhibitory effects induced by single agents

We investigated the ability of CD20 mAbs in modulating the BCR-inhibitory activity of ibrutinib and idelalisib. First, we examined the effects of BAKi alone on phosphorylation levels of BCR proteins (**Figure 12**). Ibrutinib induced a significant reduction of pSYK both in the unstimulated and anti-IgM-stimulated conditions and of pBTK^{Y223} in the anti-IgM-stimulated condition. Idelalisib induced a significant decrease of pBTK^{Y223} and pAKT in the anti-IgM-stimulated condition (**Figure 12**).

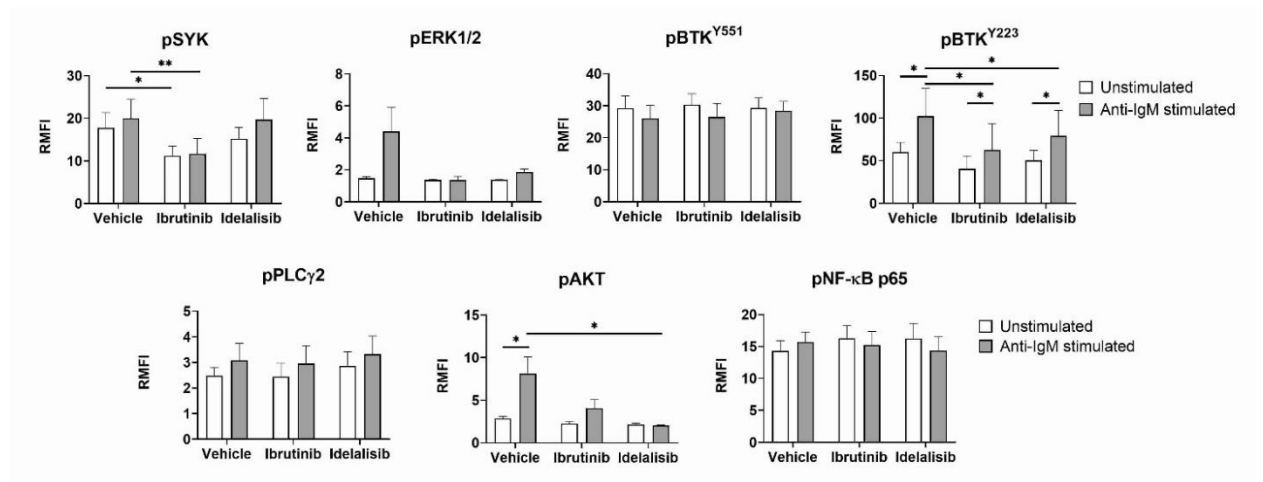


*Figure 12. Responses of BCR signaling proteins to BAKi. CLL cell samples (n = 4) were thawed and rested for 24 h before treatment with 1 μ M ibrutinib or idelalisib, and then stimulated with 20 μ g/ml anti-IgM (anti-IgM-stimulated) for 10 min or left unstimulated (vehicle). Data are expressed as median fluorescence intensity (MFI) divided by autofluorescence (relative median fluorescence intensity = RMFI). Comparisons were performed using the two-way ANOVA and each P value was corrected for multiple comparison using the Sidak test. *, $P \leq 0.050$; **, $P \leq 0.010$; ***, $P \leq 0.001$. BCR, B-cell receptor; CLL, chronic lymphocytic leukemia.*

Next, we compared responses of phosphoproteins to CD20 mAbs and BAKi combinations with CD20 mAbs or BAKi alone. We focused on those phosphoproteins that significantly responded to CD20 treatments, i.e. pBTK^{Y551} and pAKT (**Figure 10 A**). Although CD20 mAbs induced a significant reduction of pBTK^{Y551} (**Figure 10 A**), their combination with ibrutinib did not further potentiate the effects of CD20 mAbs alone, in both the unstimulated or anti-IgM-stimulated conditions (**Figure 13**). Remarkably, in the unstimulated condition

idelalisib combined with RTX or OFA potentiated the reduction induced by idelalisib or single CD20 mAbs (**Figure 13**).

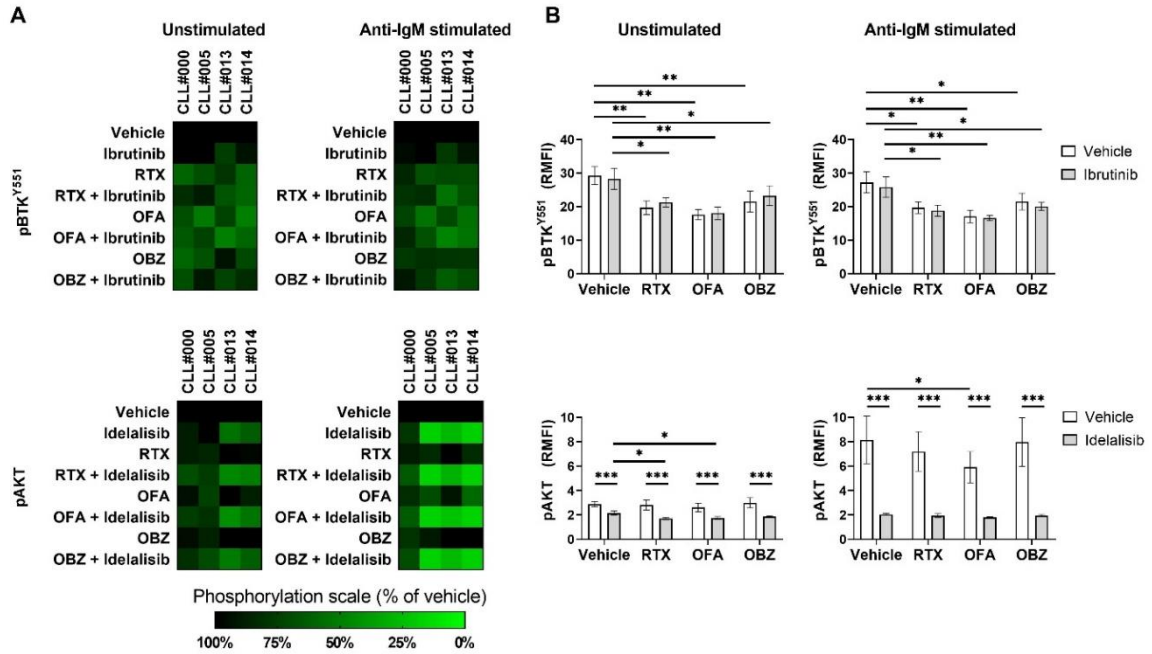


*Figure 13. Responses of BCR signaling proteins to combination of CD20 mAbs and BAKi. CLL cell samples ($n = 4$) were thawed and rested for 24 h before treatment with 1 μ M ibrutinib or idelalisib followed by stimulation with 20 μ g/ml of RTX, OFA, or OBZ for 2 h, and then stimulated with 20 μ g/ml anti-IgM (anti-IgM-stimulated) for 10 min or left unstimulated. Data are expressed as median fluorescence intensity divided by autofluorescence (relative median fluorescence intensity = RMFI), setting the vehicle control to 100%, and represented as a pseudo-color map (A) or as aggregate data expressed as mean \pm SEM (B). Comparisons were performed using the two-way ANOVA and each P value was corrected for multiple comparison using the Tukey test. *, $P \leq 0.050$; **, $P \leq 0.010$; ***, $P \leq 0.001$. BCR, B-cell receptor; CLL, chronic lymphocytic leukemia; RTX, rituximab; OFA, ofatumumab; OBZ, obinutuzumab; BAKi: BCR-associated kinase inhibitors.*

2.4.3. CD20 therapeutic antibodies inhibit LYN phosphorylation

LYN is a member of the SRC family kinases that plays a fundamental role in inducing the formation of the BCR signalosome leading to activation of downstream BCR signaling proteins, including SYK, BTK, PLC γ 2, and PI3K (Yamanashi et al. 1992; Monroe 2006). Moreover, there is evidence that RTX inhibits LYN phosphorylation, at least in lymphoma cell lines (Vega et al. 2009). To assess whether CD20 ligation could modulate LYN phosphorylation in CLL cells, we analyzed the phosphorylation level of LYN upon treatment with CD20 mAbs or the LYN inhibitor dasatinib as control. Phosphorylation level was measured in the unstimulated and anti-IgM-stimulated conditions at the single-cell level using phosphospecific flow cytometry and represented as the log₂fold-change in phosphorylation between CD20-modulated and unmodulated signals (**Figure 14**).

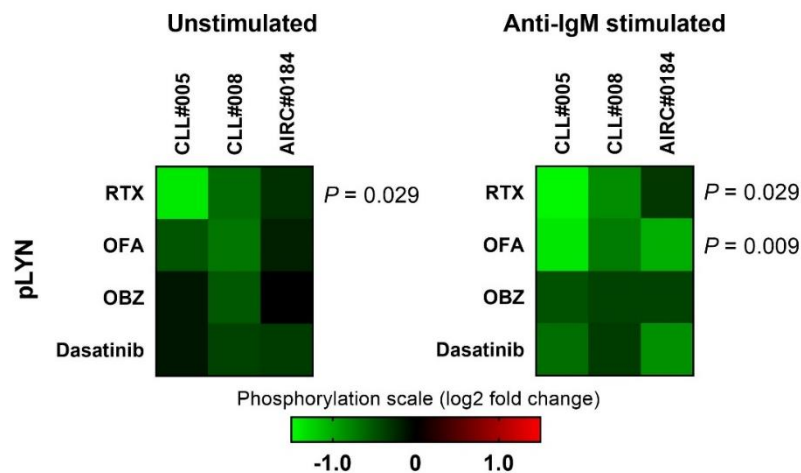


Figure 14. LYN phosphorylation response to treatments with CD20 mAbs. CLL cell samples were thawed and rested for 24 h before treatment with 20 μ g/ml of RTX, OFA, OBZ, or 0.1 μ M dasatinib for 2 h, followed by stimulation with 20 μ g/ml anti-IgM (anti-IgM-stimulated) for 10 min or left unstimulated. LYN protein phosphorylation responses in CLL cell samples ($n = 3$) were calculated as log₂-fold change between CD20-treated and untreated signals and represented as pseudo-color maps. Comparisons were performed using the one-way ANOVA and each P value was corrected for multiple comparison using the Dunnett test. CLL, chronic lymphocytic leukemia; RTX, rituximab; OFA, ofatumumab; OBZ, obinutuzumab.

Engagement of CD20 with monoclonal antibodies induced a reduction in phosphorylation of LYN that was statistically significant for RTX in the unstimulated condition and for RTX and OFA in the anti-IgM-stimulated condition (**Figure 14**). The CD20-induced concurrent phosphorylation inhibition of LYN and other BCR proteins suggests that inhibition of LYN mediated by CD20 mAbs can play a role in mediating the inhibitory effects of CD20 on BCR signaling in CLL cells.

2.4.4. Combination of CD20 mAbs with ibrutinib enhances the cell death induced by single agents

Inhibition of BCR signaling induces cell death in CLL cells (Sarah E.M. Herman et al. 2011; Lannutti et al. 2011). Moreover, there is evidence that binding of CD20 mediates direct apoptosis in malignant B cells, at least in some experimental systems (Okroj, Österborg, and Blom 2013). In CLL cells, binding of CD20 with RTX or OBZ induced cell death in the unstimulated and anti-IgM-stimulated conditions (**Figure 15, 17**).

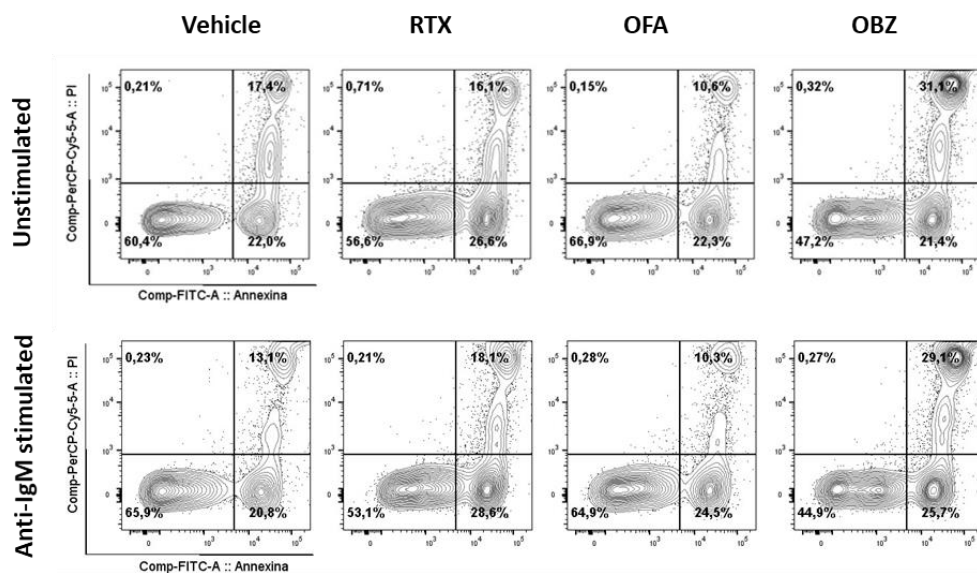


Figure 15. Annexin V/PI flow cytometry assay after CD20 mAb treatments. Representative flow cytometry analysis of leukemic cells from CLL patients stained with annexin V/PI. CLL cell sample was thawed and treated with 20 µg/ml of RTX, OFA or OBZ for 2 hours, followed by stimulation with 20 µg/ml anti-IgM for 24 hours or left unstimulated. CLL, chronic lymphocytic leukemia; RTX: rituximab; OFA: ofatumumab; OBZ: obinutuzumab.

As expected, anti-IgM stimulation induced a significant reduction of spontaneous cell death (**Figure 16**)

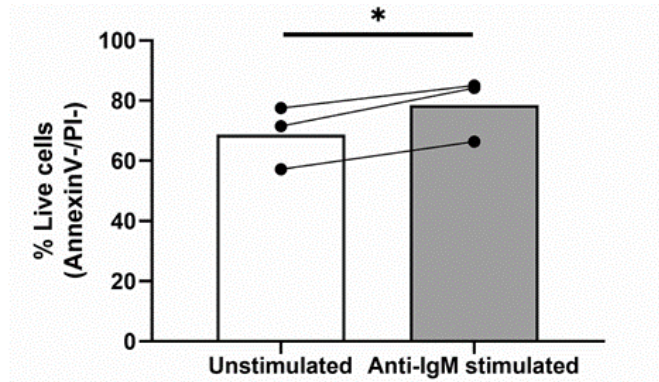


Figure 16. CLL cell survival after anti-IgM stimulation. CLL cell samples ($n = 3$) were thawed and stimulated with $20 \mu\text{g/ml}$ anti-IgM or left unstimulated for 24 hours. Spontaneous apoptosis in CLL cell samples was measured as annexin V-negative/PI-negative. Comparison was calculated by Student T test. *: $P \leq 0.050$. CLL, chronic lymphocytic leukemia.

However, only OBZ, in the basal condition and RTX, in the anti-IgM-stimulated condition, induced significant cell death levels in leukemic cells (**Figure 17**).

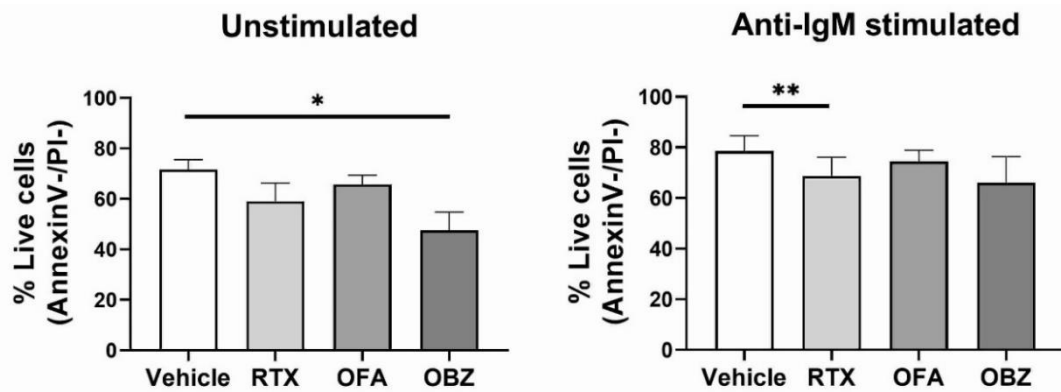


Figure 17. Effects of CD20 mAbs on CLL cell survival. CLL cell samples ($n = 5$) were thawed and treated with $20 \mu\text{g/ml}$ of RTX, OFA or OBZ for 2 hours, followed by stimulation with $20 \mu\text{g/ml}$ anti-IgM for 24 hours or left unstimulated. Percentage of live CLL cells was measured as annexin V-negative/PI-negative. Comparisons were performed using the one-way ANOVA and each P value was corrected for multiple comparisons using the Dunnett test. *, $P \leq 0.050$; **, $P \leq 0.010$; ***, $P \leq 0.001$. CLL, chronic lymphocytic leukemia; RTX: rituximab; OFA: ofatumumab; OBZ: obinutuzumab.

Moreover, the levels of cell death induced by CD20 ligation with RTX or OBZ were positively correlated with CD20 expression levels in CLL cells (**Figure 18**).

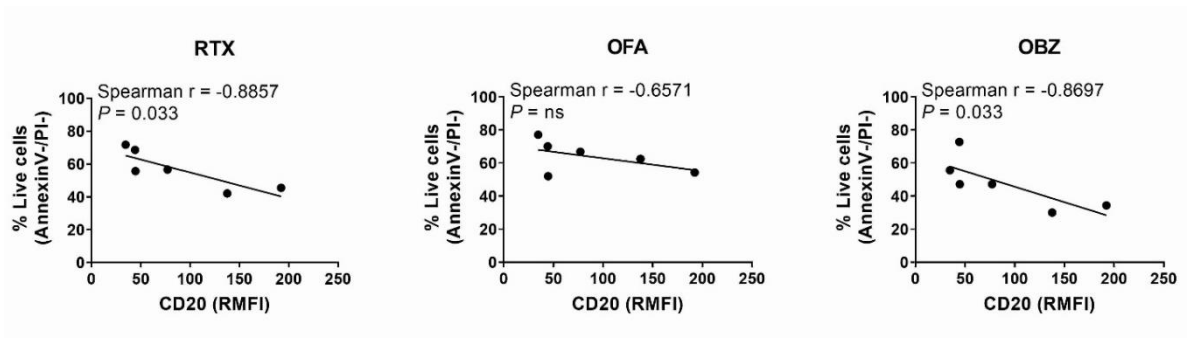


Figure 18. Association of CD20 cell surface expression with cell apoptosis induced by CD20 mAbs. CD20 expression level are expressed as RMFI (median fluorescence intensity (MFI) divided by autofluorescence (relative median fluorescence intensity = RMFI), and was correlated to CD20 mAbs-mediated apoptosis, measured using annexin V/PI staining and flow cytometry at 24 hours (n = 6).

In **Table 7** is reported the levels of cell death induced by CD20 ligation in subgroups of patients defined by IGHV mutational status, showing higher apoptosis levels in the mutated versus unmutated subset of CLL.

Table 7. Spontaneous apoptosis induced by CD20 mAbs in mutated and unmutated CLL

Apoptosis [#]		
RTX	Mutated	52.2±7.1%
	Unmutated	33.9±7.3%
OFA	Mutated	43.7±5.5%
	Unmutated	28.4±5.0%
OBZ	Mutated	62.8±8.9%
	Unmutated	41.3±12.8%

[#]: apoptosis is expressed as mean values ± SD of % apoptotic cells (sum of annexin V+/PI- and annexin V+/PI+ cells) (n = 3 for mutated cell samples and n = 3 unmutated).

Next, we measured cell death levels induced by combinations of each CD20 mAb (RTX, OFA, or OBZ) with each BAKi (ibrutinib or idelalisib) in CLL cells. Ibrutinib and idelalisib used *in vitro* as single agents induced cell death in CLL cells (**Figure 19 A**). Remarkably, combination of RTX or OBZ with ibrutinib induced a significantly higher cell death compared to those mediated by each single agent (**Figure 19 A**). Combination of OBZ with idelalisib induced a significantly higher cell death compared to that mediated by idelalisib alone and a trend toward an increase compared to cell death induced by OBZ alone (**Figure 19 A**). Analysis of the enhancement of cell death in these combinations revealed an approximately additive enhancement induced by combinations of RTX or OBZ with ibrutinib or idelalisib and a slightly less than additive enhancement induced by combinations of OFA with ibrutinib or idelalisib (**Figure 19 B**).

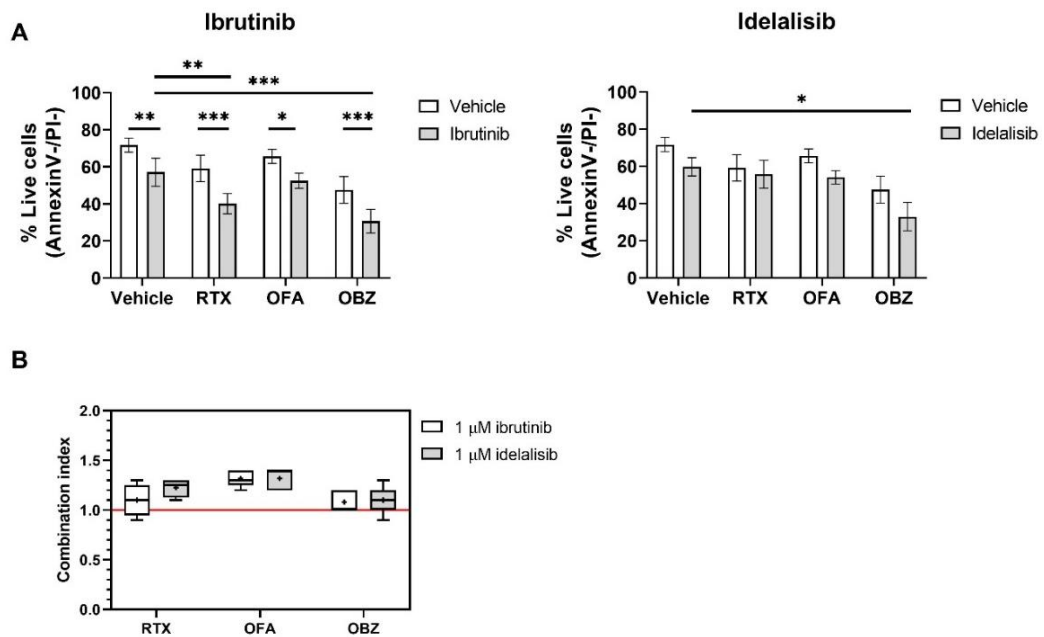


Figure 19. Effects of combination of CD20 mAbs and BAKi on CLL cell survival. CLL cell samples ($n = 5$) were thawed, pre-treated with $1 \mu\text{M}$ ibrutinib or $1 \mu\text{M}$ idelalisib for 30 min and then stimulated with $20 \mu\text{g/ml}$ of RTX, OFA or OBZ for 24 h. (A) Effect on CLL cell survival of CD20 in combination with BAKi. Percentage of live CLL cells was measured as annexin V-negative/PI-negative. Data were reported as mean \pm SEM. Comparisons were performed using the two-way ANOVA and each P value was corrected for multiple comparison using the Tukey test. $*P \leq 0.050$; $**P \leq 0.010$; $***P \leq 0.001$. (B) Combination index (CI) was calculated for five CLL samples for each drug combination. $CI = 1$ (red line) indicated additive effect; $CI > 1$ is considered less than additive. +, mean value. CLL, chronic lymphocytic leukemia; RTX, rituximab; OFA, ofatumumab; OBZ, obinutuzumab; BAKi: BCR-associated kinase inhibitors.

2.5. Discussion

This study shows that CD20 therapeutic antibodies inhibit BCR signaling and that the combination of CD20 mAbs and BAKi enhances the inhibitory effects induced on BCR by single agents. Moreover, combined administration of CD20 mAbs and BAKi augments apoptosis induced by the single agents in primary CLL cells. These findings are of clinical relevance since these agents are currently used in combination in several clinical trials (Burger and O'Brien 2018). The key advances of this study are identifying the ability of CD20 therapeutic antibodies to perturb BCR signaling and gaining insights into the effects of the combination of CD20 mAbs and BAKi on BCR signaling and cell death in CLL.

The finding that CD20 mAbs interfere with BCR signaling in leukemic cells from patients with CLL is in accordance with previous studies in lymphoma cell lines (Bonavida 2006; Vega et al. 2009; Kheirallah et al. 2010). Moreover, a convergence between CD20 and BCR signaling pathways has been suggested in lymphoma cell lines (Franke et al. 2011). Our study extends these previous data to primary CLL cells, also includes BTK among the analyzed BCR proteins, and compares the effects on BCR signaling of three CD20 monoclonal antibodies approved for use in cancer, namely rituximab, ofatumumab, and obinutuzumab. Interestingly, CD20 mAbs induce differential inhibitory effects on BCR signaling, with the higher level of inhibition mediated by OFA and the lower induced by OBZ. Although the extent of inhibition of phosphorylation is highly variable across patients and among phosphoproteins, a significant decrease in phosphorylation was observed more commonly for the Y551 site of BTK, which is trans-phosphorylated by the SRC family tyrosine kinases and is a major site involved in BTK catalytic activity (H. Park et al. 1996). In contrast, CD20 mAbs do not influence the major autophosphorylation site Y223 of BTK. Interestingly, the effects mediated by CD20 mAbs on the two major phosphorylation sites of BTK are opposite to those exerted by ibrutinib, which reduces pBTK^{Y223} to a higher extent than pBTK^{Y551}. In addition, BCR stimulation with anti-IgM induces a clear-cut and significant increase of pBTK^{Y223} while only moderately augmenting pBTK^{Y551}. Idelalisib induced a strong reduction of pAKT and also a significant decrease of pBTK^{Y223} in the anti-IgM-

stimulated condition. Interestingly, the CD20 mAbs RTX or OFA in the presence of PI3K δ inhibition potentiate the inhibition of AKT mediated by idelalisib or CD20 mAbs alone. Moreover, we document that CD20 mAbs induce BCR pathway inhibition both in the basal and anti-IgM-stimulated conditions, thus, showing that CD20 ligation can perturb ligand-independent tonic BCR signaling, which is mediated by PI3K α and PI3K δ functioning (Burger and Wiestner 2018), as well as activated BCR signaling. Taken together, these findings support the concept that CD20 and BCR share some signaling pathway components that activate regulatory mechanisms, including negative feedback control of the BCR signaling.

Activation of PI3K requires LYN-dependent phosphorylation of CD19, which induces recruitment and activation of PI3K. In turn, PI3K activates different downstream signaling proteins, including AKT and BTK (Marshall et al. 2000). Moreover, the tyrosine protein kinase LYN also directly phosphorylates BTK (Wahl et al. 1997; Baba et al. 2001). Remarkably, herein, we document that in primary CLL cells ligation of CD20 with monoclonal antibodies inhibits LYN phosphorylation at the activating site Y396 (Frezzato et al. 2014). Consistently, Vega et al showed that CD20 crosslinking with rituximab inhibits LYN phosphorylation in lymphoma cell lines (Vega et al. 2009). Although further studies are needed to decipher the molecular link between the CD20 and BCR signaling pathways, our findings suggest that LYN may be involved in the regulation of BTK and PI3K/AKT signaling pathways mediated by CD20 mAbs.

Beside effector mechanisms mediated by complement and immune cells, CD20 mAbs have been shown to induce direct apoptosis in lymphoma cell lines (Pedersen et al. 2002; Glennie et al. 2007) and in CLL patients' leukemia cells (Byrd et al. 2002; Krause et al. 2016). Consistently, our data show that RTX and OBZ induce cell death in CLL cells. Also, the BTK inhibitor ibrutinib and the PI3K-inhibitor idelalisib induce apoptosis in CLL, thus, confirming previous data (Sarah E.M. Herman et al. 2014; Lannutti et al. 2011). Combinations of RTX or OBZ with ibrutinib or idelalisib induce approximately additive enhancement of cell death levels compared to those mediated by each single agent, which is consistent with data from Krause et al. on combination of RTX or OBZ with idelalisib (Krause et

al. 2016). This finding is of clinical relevance as these agents are currently used in combination in several clinical trials with promising results (Yosifov et al. 2019). Preclinical studies have shown multiple negative interactions between these two classes of therapeutic agents. BAKi decreases CD20 expression on target cells in vitro, thus reducing CD20 mAb-mediated CDC (Bojarczuk et al. 2014). In addition, ibrutinib decreases antibody-mediated phagocytosis of target cells by macrophages and neutrophils (Borge et al. 2015; Da Roit et al. 2015) as well as ADCC (Kohrt et al. 2014). Positive interactions of BAKi with CD20 activity have also been described, such as inhibition of trogocytosis, a major contributor to antigen loss and leukemia escape during CD20 mAb therapy (Skarzynski et al. 2016). The enhanced direct cell death induced in primary CLL cells by combinations of CD20 mAbs with BAKi could balance some of the negative effects and inform on potential of combined therapies in ongoing and future clinical trials in patients with CLL.

3.CHAPTER 3: Regulation of catalase expression in CLL cells

3.1. Introduction

3.1.1. Human catalase characteristics

The human catalase gene is located on chromosome 11 (11p13) and consists of 12 introns and 13 exons coding for a single protein of 527 amino acids (NP_001743.1) (Kittur et al. 1985; Quan F.,Korneluk R.G. 1986). The complete genomic DNA coding sequence for human catalase (NC_000011.10) has 33,127 bp that generate a transcript of 2291 bp (NM_001752.4). The human catalase core promoter, located approximately in the first 200 bp region of the catalase promoter, has multiple start sites of transcription, is rich in GC residues, has no initiator element sequences, lacks a TATA box and contains both GGGCGG and CCAAT boxes (Quan F.,Korneluk R.G. 1986; Sato et al. 1992; Toda et al. 1997). Several single nucleotide polymorphisms (SNPs) have been described in the promoter, 5' and 3'- untranslated regions, exons and introns of human catalase gene, the most relevant are depicted in **Figure 20**.

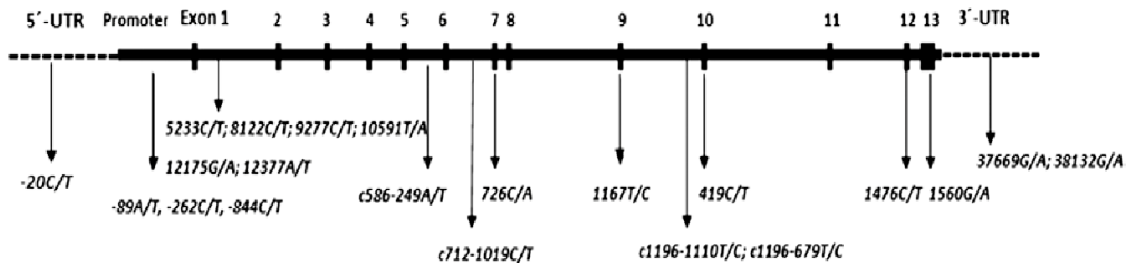


Figure 20. Schematic representation of human catalase gene and the most relevant SNPs. UTR – untranslated region (Kodydková et al. 2014).

Catalase is a key antioxidant enzyme in protecting cells against the toxic effects of hydrogen peroxide (H₂O₂). It takes its name from its catalytic action on H₂O₂ which is rapidly decomposed into O₂ and H₂O (Loew 1900). The human catalase belongs to typical catalases, it is a homotetramer of 240 kDa, composed by four subunits (62 kDa) with a ferric protoporphyrin IX in the active center (namely heme b) and NADPH (nicotinamide adenine dinucleotide phosphate hydrogen) as a cofactor. The heme-group, interacts with hydrogen peroxide for its detoxification activity

(Glorieux and Calderon 2017). During the dismutation of H_2O_2 reaction, catalase is first oxidized to a hypervalent iron intermediate, which is then reduced back to the resting state by a second H_2O_2 molecule (Jones and Dunford 2005).

3.1.2. Tissue and cellular distribution of catalase

Due to its central role in cell defense against oxidative stress, catalase is expressed in all major mammalian tissues, with the highest enzymatic activity in liver and erythrocytes (Winternitz and Meloy 1908). Relatively high catalase activity has been detected in kidney and adipose tissue, intermediate in lung and pancreas, and very low in heart and brain (Mueller, Riedel, and Stremmel 1997; Nishikawa, Hashida, and Takakura 2009; Deisseroth and Dounce 1970; Kirkman and Gaetani 2007; Goyal and Basak 2010). In human, catalase is not expressed in vascular smooth muscle cells and endothelial cells (Shingu et al. 1985).

Catalase is predominantly located in peroxisome in which high catalase activity is detected (Chance, Sies, and Boveris 1979). Targeting of human catalase to peroxisomes is mediated by a peroxisomal-targeting signal (PTS) that consists of four –COOH-terminus amino acids (-KANL) (Purdue et al. 1996). However, there is considerable evidence that catalase is also assembled outside of the peroxisomes. For instance, a functional catalase has also been detected in the cytosol (Middelkoop et al. 1993). More recently, it has been shown that catalase can be localized on the cytoplasmic membrane of cancer cells (Heinzelmann and Bauer 2010; Bauer 2012). In addition, a soluble catalase secreted by cancer cells has been described (Sandstrom and Buttke 1993; Moran et al. 2002; Böhm et al. 2015).

3.1.3. Physiological role of catalase

Mutations of catalase gene cause the human genetic disease known as acatalasemia, or Takahara's disease, an autosomal inherited rare disease characterized by the deficiency of erythrocyte catalase (Ogata 1991; Góth, Shemirani, and Kalmár 2000; Hirono et al. 1995; Wen et al. 1990). Catalase-deficient mice are viable and fertile and develop a normal hematological cell lineage although they can show defects in oxidative phosphorylation after oxidant injures (Y. S. Ho et al. 2004). Overall, these

phenotypes could be ascribed to the presence of other antioxidant enzymes able to decompose H_2O_2 , such as glutathione peroxidases (GPX) and peroxiredoxins. On the other hand, overexpression of catalase targeted to mitochondria induces extension of life span in mice (Schriner et al. 2005). In addition, a recent study shows that overexpression of human mitochondrial catalase in mice results in enhanced NF- κ B activation and increased glycolytic and oxidative metabolism in macrophages (Han et al. 2020).

Therefore, due to its ability to modulate H_2O_2 levels, catalase is involved in many processes regulated by H_2O_2 . H_2O_2 mediates toxic effects on cellular components due to its ability to form other reactive oxygen species (ROS) through the Fenton reaction (Kremer 1999). ROS are chemically unstable species that react with a wide spectrum of macromolecules, including lipids, proteins and nucleic acids, causing serious cellular damages; indeed, an imbalance between the production of ROS and the capacity of antioxidant defense mechanisms favoring oxidants leads to cellular oxidative stress (Pickering et al. 2013). Damaging ROS properties are also used by innate immune cells during the oxidative burst towards infective agents (Nathan and Cunningham-Bussel 2013). Thus, catalase plays a key role in protecting cells against cellular toxic effects mediated by ROS. Nevertheless, increasing evidence indicates that catalase is also involved in regulating various other cellular physiological processes, including signal transduction, proliferation, differentiation, apoptosis, in which H_2O_2 acts as a second messenger oxidizing signaling molecules (Sies, Berndt, and Jones 2017). At the low physiological levels in the nanomolar range, H_2O_2 is a major agent signaling via specific proteins involved in metabolic regulation and stress responses to support cellular adaptation to environmental changes and cellular stress (Sies, Berndt, and Jones 2017). During lymphocyte activation, H_2O_2 plays an important role as a secondary messenger in the initiation and amplification of signaling at the antigen receptor. Initiation, transmission, and strength of the antigen-receptor signaling are indeed regulated by the interplay between kinases and protein tyrosine phosphatases (PTPs), and the full activation of the signaling cascade requires not only activation of kinases but also inhibition of PTPs (Reth and Brummer 2004; Singh et al. 2005). PTPs may be

reversibly inhibited through oxidation of the catalytic cysteine by H_2O_2 , which is produced by calcium-dependent NOXes (NADPH oxidases) that are recruited in lymphocytes following antigen-receptor activation (Reth 2002). Besides antigen receptors, other protein tyrosine kinase (PTK) receptors are regulated by H_2O_2 including platelet-derived growth factor receptor (PDGFR) that, upon binding with its ligand, induces production of H_2O_2 and the inhibition of the receptor-associated PTP SHP-2 (SRC homology phosphatase 2) (Meng, Fukada, and Tonks 2002). It has been shown that NOXes are components of ROS-generating signaling endosome, namely redoxosome, which also comprises endocytosed receptors and receptor-associated signaling molecules. In redoxosome, ROS generated by NOXes amplify signaling of the endocytosed receptor (Tsubata 2020). Moreover, the oxidative burst in macrophages can play a role not only in pathogen killing but also in macrophages activation as well as neighboring cells (Nathan and Cunningham-Bussel 2013).

3.2. Regulation of catalase expression

Regulation of catalase expression comprises a wide range of mechanisms that are used to respond for instance to stress-stimuli or adapt to new condition. These regulatory mechanisms act at different levels (**Figure 21**) including:

- genetic modifications (SNPs and chromosome alterations)
- epigenetic modifications (histone deacetylation and CpGs methylation)
- transcriptional regulation (transcription factors)
- post-transcriptional regulation (miRNAs)
- post-translational regulation (phosphorylation, acetylation and ubiquitination)

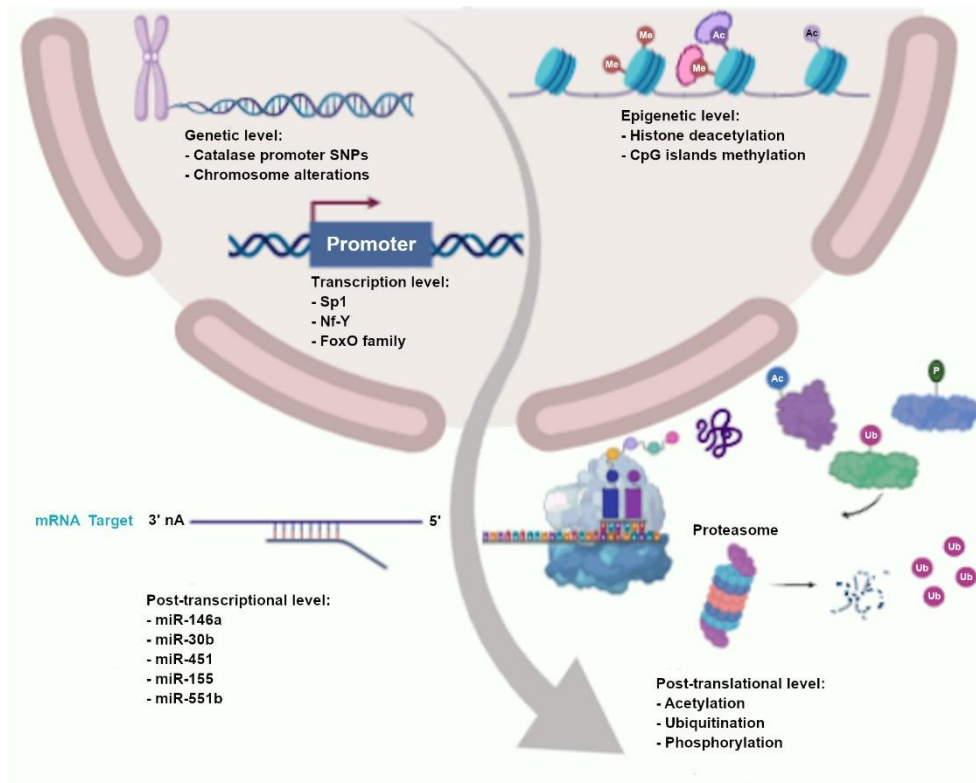


Figure 21. Various levels of catalase expression regulation. Regulation of catalase expression from genetic, transcriptional to RNA processing, and to the post-translational modification of protein. Abbreviations: specificity protein 1 (Sp1), nuclear factor Y (NFY), fork-head box protein O (FoxO) family, miR (miRNA), Single nucleotide polymorphisms (SNPs). Created with BioRender.com. Figure.

3.2.1. Genetic modifications

More than 245 single-nucleotide polymorphisms (SNPs) are described in different regions of the catalase (CAT) gene and its promoter (Crawford et al. 2012). However, only the C>T substitution in the catalase promoter at the -262 position from the transcription start, namely rs1001179 SNP, has been associated with altered catalase expression. Specifically, the T allele exhibits a significantly higher catalase expression associated with higher transcriptional activity of CAT gene (Forsberg et al. 2001; Saify, Saadat, and Saadat 2016; Schults et al. 2013). Although this SNP has been linked to several diseases (Geybels et al. 2015; Tsai et al. 2012), its role in cancer risk is unclear and controversial. There is evidence that the CAT -262C/T is associated with higher susceptibility to prostate cancer (Geybels et al.

2015), hepatocellular carcinoma (Ezzikouri et al. 2010; Yanqiong Liu et al. 2015; C. Di Wang et al. 2016) and skin cancer (C. Di Wang et al. 2016). Recently, meta-analysis studies demonstrated the association between the CAT -262C/T polymorphism and an increased cancer risk (K. Liu et al. 2016; C. Di Wang et al. 2016). Moreover the CAT -262C/C genotype is associated with a reduction in risk of breast cancer compared with the variant T allele (Ahn et al. 2005). However, the CAT -262C/T is not a risk factor for other cancers, such as non-Hodgkin lymphoma (Cosma et al. 2019). Besides the CAT rs1001179 SNP, which is the most characterized, other CAT SNPs have been described to be involved in cancer. In the meta-analysis from Liu et al., also the CAT rs794316 SNP has been associated with an increased cancer risk (K. Liu et al. 2016). Furthermore, the CAT rs769218 SNP has been proposed as prognostic marker in gastric cancer (Zhang et al. 2018). In addition, it has been described that the A allele within the CAT rs769214 SNP creates a binding site for paired box 6 (PAX6) transcription factor, which induces a higher transcriptional activity compared with the G allele in human hepatoblastoma cell (Hebert-Schuster et al. 2011).

Catalase expression is also influenced by alterations of the catalase gene. The major gene changes include gene amplification, loss of allele and deletion of chromosomal arms, which are common pro-tumorigenic alterations through which cancer cells take advantage for survival under stress condition (Matsui et al. 2013).

The chronic exposure of leukemia and fibroblast cell lines to increasing concentration of H₂O₂ results in the development of stable oxidative stress-resistant cells characterized by enhanced catalase levels, which correlate with an increased gene copy number compared with parental cell line (Hunt et al. 1998; Yamada et al. 1991).

On the contrary, the deletion of chromosome 11p is associated with a low catalase activity in the later passages of SV40-transformed human fibroblast (Hoffschir et al. 1993).

3.2.2. Epigenetic modifications

Database of CpG islands and analytical tools (DBCAT) indicates that the human catalase gene contains four CpG islands, among which the largest is the second one located between the promoter and the first exon (from 34416579 to 34417562) (Kuo et al. 2011). Some evidence indicates that epigenetic changes, such as histone modification and DNA methylation, contribute to the regulation of catalase gene expression. In the doxorubicin-resistant acute myelogenous leukemia (AML)-2/DX100 cell line model, catalase expression results significantly downregulated compared with the parental AML-2/ WT cells due to the histone H4 deacetylation (Kim, Lee, and Choi 2001; Lee, Moon, and Choi 2012). Moreover, it has been shown that chronic exposure to ROS induced a decrease of catalase promoter activity in hepatocarcinoma (HCC) cell line models, via hypermethylation of CpG Island II on its promoter (Min, Lim, and Jung 2010). Likewise, in human hepatic cell line WRL-98, it has been shown that ROS increase induced by CuO nanoparticles (NPs) is significantly associated with catalase promoter methylation and the transcriptional downregulation of catalase expression (Chibber, Sangeet, and Ansari 2017).

3.2.3. Transcriptional regulation

Catalase expression is predominantly controlled at the level of transcription by factors that positively or negatively regulate the activity of the promoter. The main factors involved in the regulation of human catalase transcription are: specificity protein 1 (Sp1), nuclear factor Y (NFY), Wilms tumor 1 (WT1), early growth response (Egr), X-box binding protein 1 (XBP-1), fork-head box protein M1 (FoxM1), silent mating type information regulator 2 homolog 1 (Sirt1), peroxisome proliferator-activated receptor- γ co-activator-1 α (PGC-1 α), signal transducer activator of transcription 3 (STAT3), octamer-binding transcription factor 1 (Oct-1), peroxisome proliferator-activated receptor gamma (PPAR γ), activator protein 1 (AP-1) member JunB, and retinoic acid receptor alpha (RAR α). (**Figure 22**).

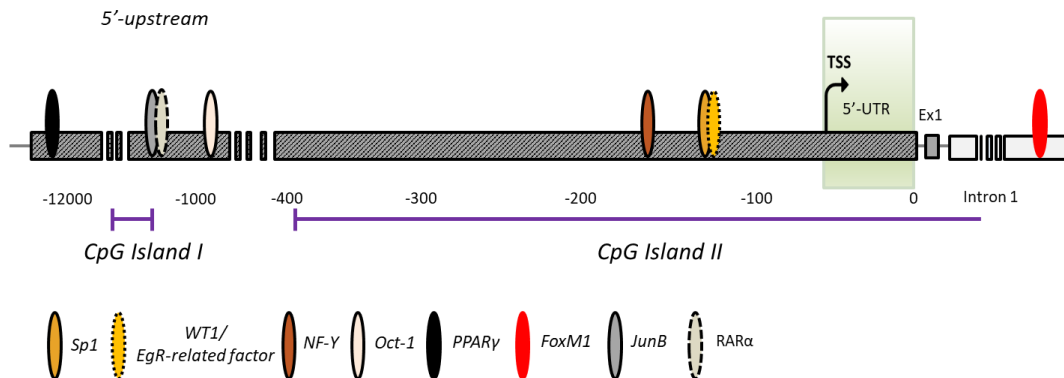


Figure 22. Schematic representation of human catalase promoter and the main DNA-binding transcription regulators. Abbreviations: specificity protein 1 (Sp1), nuclear factor Y (NF-Y), Wilms tumor 1 (WT1), early growth response (Egr), fork-head box protein M1 (FoxM1), octamer-binding transcription factor 1 (Oct-1), peroxisome proliferator-activated receptor gamma (PPAR γ), activator protein 1 (AP-1) member JunB, and retinoic acid receptor alpha (RAR α).

The human catalase core promoter, as previously described, contains both GGGCGG and CCAAT boxes (Quan F., Korneluk R.G. 1986; Sato et al. 1992; Toda et al. 1997). These boxes are DNA binding sites for the Sp1 and NF-Y transcription factors, respectively, which are known to regulate the transcription of several genes (Nenoi et al. 2001). In addition, due to the ability of Sp1 to bind the RNA polymerase II (Farnham and Cornwell 1991), this transcription factor is important in driving the transcription of genes lacking the TATA box (Farnham and Cornwell 1991). Consistently with the potential role of Sp1 in regulating catalase gene expression, it has been shown that the elevated expression of catalase is transcriptionally induced by both Sp1 and CCAAT-recognizing factors in H₂O₂-resistant variants of leukemia HL60 cell line (Nenoi et al. 2001). Moreover, catalase expression is downregulated by other transcription factors, such as WT1 and Egr-1, a member of the Egr protein family. These transcription factors lead to inactivation of the promoter by disturbing or competing with the transactivating ability of Sp1 (Nenoi et al. 2001).

NF-Y transcription factor plays a major role in regulating rat and mouse catalase gene directly binding to the CCAAT box (Taniguchi et al. 2005; Luo and Rando 2003). The binding of NF-Y to catalase promoter is enhanced by binding of XBP-1 to the CCAT box, which acts in a cooperative manner with NF-Y (Y. Liu et al.

2009). Interestingly, knockdown of XBP-1 in human retinal pigment epithelium (RPE) and glioma cell lines determines a decrease of catalase and SOD expression (Y. Liu et al. 2011; Zhong et al. 2012), thus suggesting that XBP-1 can influence also the activity of the human catalase promoter. Taken together, these findings indicate that the Sp1 and NF-Y as well as other CCAAT box-binding transcription factors play a central role in the transcriptional activation of the human catalase gene.

Forkhead box protein O (FOXO) transcription factor family members have been identified as positive regulators of catalase expression. Chromatin immunoprecipitation (ChIP) assay confirmed the presence of a FoxM1-binding site in the first intron that positively regulates human catalase expression (Park et al. 2009). Also, the FOXO family member Foxo3a is a direct transcriptional regulator of the human catalase gene in vascular endothelial cell. Suppression of endogenous Foxo3a resulted in reduced catalase mRNA expression, indicating that Foxo3a is necessary for the maintenance of catalase gene expression (Olmos et al. 2009). However, the knockdown and overexpression of FoxO3a did not affect catalase expression in breast cancer cell line (Glorieux et al. 2014). Moreover, Foxo3a activity is positively regulated by the NAD⁺-dependent protein Sirt1 deacetylase, which also transactivates catalase gene in normal and cancer (Olmos et al. 2013; Nemoto, Fergusson, and Finkel 2005; Olmos et al. 2009). Increased levels of Sirt1 have been documented in CLL cells compared with normal B cells (Bhalla and Gordon 2016). Interestingly, also catalase levels are higher in CLL cells than in normal B cells (Jitschin et al. 2014), thus suggesting a role for Sirt1 in regulating catalase gene expression also in leukemia.

The STAT3 transcription factor has been identified as a positive regulator of the catalase expression although no specific binding sites have been identified in the human catalase promoter. The inhibition of STAT3 prevents cell proliferation and induces ROS generation by suppressing catalase expression in human osteosarcoma cell line (Cai et al. 2017).

Oct-1, a member of the POU-domain transcription family, positively regulates catalase expression binding to the human catalase promoter at the octamer consensus sequence ATTAAATA. In human hepatocarcinoma cell line models, the exposure to H₂O₂ induces hypermethylation of the Oct-1 promoter decreasing catalase gene expression and protein levels, thus favoring ROS-mediated invasiveness (Quan, Lim, and Jung 2011).

PPAR γ regulates the expression of human catalase gene through the binding to the PPAR γ response element (PPRE) sequence TGACCTTTGCAAA in the catalase promoter (Okuno et al. 2010; W. Yang et al. 2011). PPAR γ activity is modulated by interacting with PGC-1 α , a transcriptional coactivator that plays a major role in cell metabolism regulation (Bost and Kaminski 2019). Intriguingly, also Foxo3a activity requires the transcriptional co-activator PGC-1 α . Foxo3a and PGC-1 α directly interact and are recruited to the same promoter regions (Olmos et al. 2009). Foxo3a and PGC-1 α have been shown to be deacetylated by Sirt1. Moreover, regulation of catalase mediated by Sirt1 depends on the formation of a FoxO3a/PGC-1 α complex (Olmos et al. 2013).

Recently, Glorieux et al. have identified a novel regulatory region in the human catalase promoter (-1518/-1226) that binds the AP-1 family member JunB and RAR α . Specifically, whilst JunB activates catalase transcription, RAR α mediates its repression through a histone deacetylases-dependent mechanism (Glorieux et al. 2016).

3.2.4. Post-transcriptional regulation

Catalase is also regulated at mRNA level through microRNAs, which influence mRNA stability, and in turn the transduction rate. miR-551b has been demonstrated to directly bind catalase 3'-UTR in lung cancer cell line models, A549 and H460-AR, suppressing catalase expression and causing ROS accumulation (Xu et al. 2014). In the same manner miR-30b family negatively regulates catalase expression in derived-human retinal pigment epithelium, ARPE-19, cells (Haque et al. 2012). Moreover, it has been suggested that the receptor-interacting protein 1 (RIP1)

downmodulates miR-146a expression which increases catalase expression in A549 and H460 cell line models (Q. Wang et al. 2014). In addition, overexpression of miR-155 inhibits Foxo3a inducing a decrease of catalase expression level (P. Wang et al. 2015). Conversely, the microRNA miR-451 indirectly enhances catalase expression by repressing an inhibitor of the FoxO3a pathway (Yu et al. 2010).

3.2.5. Post-translational regulation

Catalase activity also depends on post-translational modifications, which could influence the protein folding and tetramer formation, thus affecting the catalase enzymatic activity. Three different catalase phosphorylation sites have been identified. Phosphorylation in S167 by protein kinase C isoform delta (PKC δ) enhances catalase activity promoting the tetramerization of the enzyme (Rafikov et al. 2014). Catalase can be also phosphorylated in Y231 and Y386 by Abelson murine leukemia viral oncogene homolog 1 (c-Abl) and c-Abl-related gene (Arg) kinases that induce increase catalase activity. Moreover, it is described that the two overmentioned kinases exhibit differential activities depending on the levels of ROS. At lower levels of ROS, c-Abl and Arg kinases phosphorylate catalase, thus increasing its activity, whereas at higher levels of ROS the two kinases dissociate from catalase, and induce its ubiquitination and degradation through proteasome (Cao et al. 2003; Cao, Leng, and Kufe 2003). Catalase enzyme can undergo glycosylation (Yan and Harding 1997; Lortz, Lenzen, and Mehmeti 2015) and acetylation (Furuta et al. 1974). Both these modifications have been suggested to inhibit catalase activity.

3.3. Role of catalase in cancer

In spite of the existence of a multifaceted antioxidant enzyme system in mammalian cells, a wide consensus emerges from the literature on an alteration of redox homeostasis in cancer cells. Indeed, increased ROS levels have been detected in various cancers, where they activate protumorigenic signals; enhance cell survival, proliferation, migration and chemoresistance, and cause DNA damage and genetic instability (Moloney and Cotter 2018; Sullivan and Chandel 2014; Wu et al. 2006; Wu 2006). However, augmented levels of ROS can also promote antitumorigenic signals, resulting in an increase of oxidative stress and induction of cancer cell death (Trachootham et al. 2006; Moloney and Cotter 2018; Nogueira et al. 2008) (**Figure 23**). Accordingly, the expression of catalase and other antioxidant enzymes is often altered in cancer cells, and it is widely appreciated that catalase as well as other antioxidant enzymes, plays an important dichotomous role in cancer. Specifically, catalase can protect cells from tumor initiation and progression, due to its role in preventing the accumulation of dangerous levels of oxidants. Accordingly, some studies have reported a downregulation of catalase expression in some cancers (Baker, Oberley, and Cohen 1997; Lauer et al. 1999; J. C. Ho et al. 2001; Rawat et al. 2020). Moreover, catalase expression is highest in patients under complete remission compared with patients exhibiting treatment resistance in acute myeloid leukemia (Handschuh et al. 2018). By contrast, many cancer cells require oxidant detoxifying and upregulation of catalase for tumor progression and metastasis (Sander et al. 2003; Hwang, Choi, and Han 2007; Rainis et al. 2007; Jitschin et al. 2014). Coherently with this role of catalase, it has been recently documented that higher levels of catalase and decreased levels of cellular ROS are associated with a faster progression of chronic lymphocytic leukemia (CLL) (Cavallini et al. 2018). The dichotomous roles of catalase in cancers highlight the importance to investigate the role and regulation of this antioxidant enzyme. Moreover, therapies aimed at either reverting the increased or further escalating catalase levels could be effective, depending on the landscape of cancer cells.

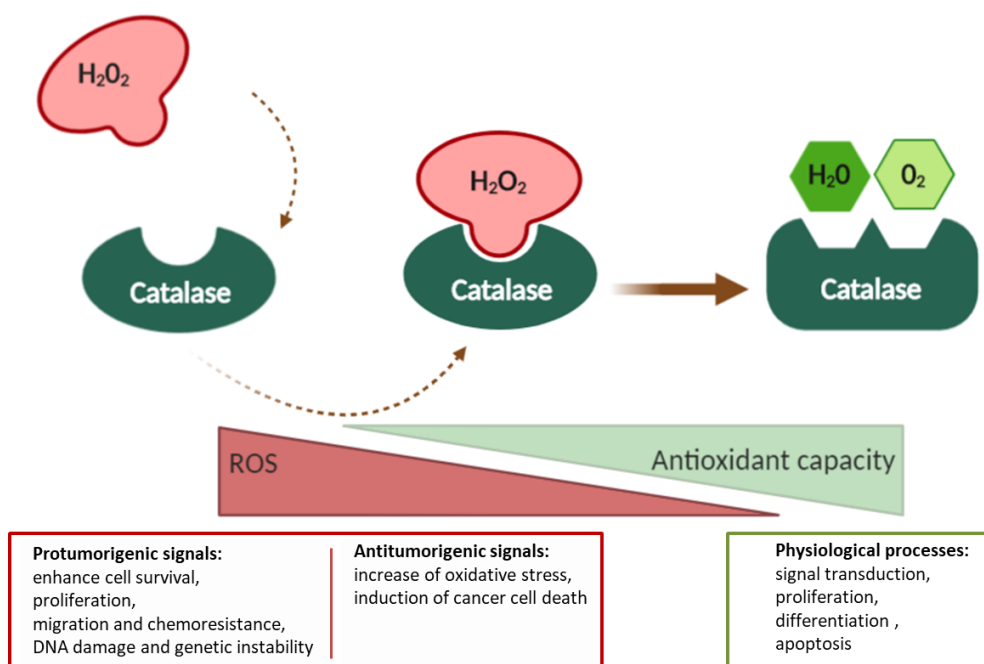
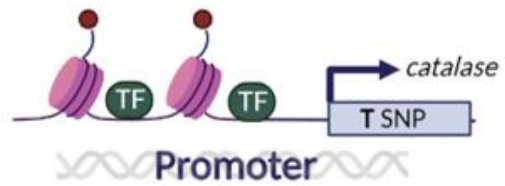


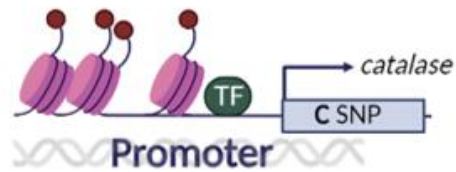
Figure 23. Biological function of catalase. Catalase modulate H₂O₂ levels, an imbalance between the production of ROS and the capacity of antioxidant defense mechanisms favoring oxidants leads to cellular oxidative stress. Under physiological conditions catalase is involved in regulating various cellular physiological processes, including signal transduction, proliferation, differentiation, apoptosis, in which H₂O₂ acts as a second messenger. Otherwise, ROS activate protumorigenic signals; enhance cell survival, proliferation, migration and chemoresistance; and cause DNA damage and genetic instability. However, increased levels of ROS can also promote antitumorigenic signals, resulting in an increase of oxidative stress and induction of cancer cell death. Created with BioRender.com.

High catalase



T rs 1001179 SNP and low methylation level enhances *CAT* expression

Low catalase



C rs 1001179 SNP and high methylation level reduces *CAT* expression

Figure 24. Graphical abstract. Regulation of catalase expression in CLL cells. *CAT*: catalase; *SNP*: single nucleotide polymorphism.

3.4. Aim of the study

Chronic lymphocytic leukemia is characterized by a highly variable clinical course. However, it remains an incurable disease characterized by an extremely variable clinical course and response to treatment, with some patients having indolent disease and others experiencing a more accelerated course, treatment resistance, and a dismal outcome (Hallek, Shanafelt, and Eichhorst 2018). In the last decades, advances in understanding the biological heterogeneity of the disease have led to identify molecules and signaling pathways involved in leukemia homing, survival, and proliferation. Along with the understanding of the molecular heterogeneity of the disease, growing interest is emerging in redox metabolism in CLL. Overall, altered expression of antioxidant enzymes have been observed in cancer, where increased enzyme expression has been associated with tumorigenic signals in some cancers but with antitumor functions in others (Hwang, Choi, and Han 2007; Ho et al. 2001; Glorieux et al. 2015; Tome et al. 2005). Downregulation of antioxidant enzymes in cancer is mainly associated with a high production of H₂O₂ and other ROS (Kang et al. 2013). Increased ROS levels have been detected in various cancers, but their role seems to be controversial. Increased ROS levels can activate protumorigenic signals as well as promote antitumorigenic signals, resulting in an increase of oxidative stress and induction of cancer cell death (Moloney and Cotter 2018; Dalla Pozza et al. 2012; Trachootham et al. 2006). However, in other cases increased ROS levels can activate signal transduction pathways, increase cell proliferation, promoting cell survival (Sullivan and Chandel 2014).

It has been described that in chronic lymphocytic leukemia (CLL) higher ROS levels are associated with favorable prognostic features and a slower disease progression (Linley et al. 2015). Accordingly, we have recently shown that higher levels of crucial antioxidant and detoxifying enzymes, such as catalase, are linked to lower ROS levels, unfavorable prognostic parameters, and faster progression of the disease (Cavallini et al. 2018). Differential catalase expression in CLL identifies two main disease subtypes characterized by a disparity in clinical outcome. The mechanisms controlling the transcription of catalase gene in pathological conditions are poorly understood (Glorieux et al. 2015). However, single nucleotide

polymorphism (SNP), rs1001179, in the catalase promoter C>T substitution in the -262 position from the transcription start site alters the expression as well as blood catalase levels (Forsberg et al. 2001; Saify 2016; Schults et al. 2013) and it has been linked to several diseases (Geybels et al. 2015; Tsai et al. 2012). Moreover, epigenetic modifications, such as DNA methylation, contribute to the regulation of catalase expression in several biological context.

In this study, we aim at investigating the mechanisms in regulating catalase expression in CLL. Therefore, we first confirmed that CLL patients expressed increased levels of catalase compared with the healthy donors (Jitschin et al. 2014). Then, we investigated the involvement of a genetic and epigenetic regulatory mechanism at the basis of differential catalase expression in CLL patients that that are associated with different clinical outcome (**Figure 24**).

3.5. Materials and Methods

3.5.1. Sampling and sample preparation

PBMCs were isolated by Ficoll-hypaque (Lymphoprep; Nicomed, Oslo, Norway) centrifugation and stored in liquid nitrogen. Upon thawing, only samples with at least 85% viability, assessed using 7-Amino-Actinomycin (7-AAD) dye (BD Biosciences, San Jose, CA) and flow cytometry (FACSCanto; Becton Dickinson, Franklin Lakes, NJ), were processed further. For quantitative RT-PCR, CLL cells from samples with <70% B cells were isolated by negative selection using Human B-Cell Enrichment Kit (Stem Cell Technologies, Vancouver, Canada). After separation, cell purity was routinely above 98%, as assessed with CD19 staining and flow cytometry (FACSCanto). Clinical annotations at diagnosis are summarized in **Table 8**. B cells from healthy-donor PBMCs were isolated with flow cytometry activated cell sorting (FACS) equipped with 85 µm nozzle (FACSAria, Becton Dickinson) using CD19-PerCpCy5.5 antibody (BD Biosciences) and purity mask. B cell purity post sorting was above 98%, as assessed with CD19 staining and flow cytometry (FACSAria).

Table 8. Clinical and biological characteristics of CLL patients

Patients	n=75
Gender	
Male	47 (62.7%)
Female	28 (37.3%)
Age at the diagnosis* (years)	
Median (range)	66 (36-92)
TTFT†† (months)	
Median (range)	64.6 (1.1-306.7)
Binet	
Binet A	56 (74.6%)
Binet B	15 (20.0%)
Binet C	2 (2.7%)
NA	2 (2.7%)
CD38§	
Negative	19 (25.3%)
Positive	55 (73.3%)
NA	1 (1.4%)
ZAP70‡	
Negative	20 (26.7%)
Positive	46 (61.3%)
NA	9 (12.0%)
IGHV†	
UM	25 (33.3%)
M	35 (46.7%)
NA	15 (20.0%)
Cytogenetic§§	
Favorable	20 (26.7%)
Neutral	27 (36.0%)
Unfavorable	13 (17.3%)
NA	15 (20.0%)

*diagnosed according to 2008 Guidelines for Diagnosis and Treatment of CLL (Hallek et al, 2008);

††TTFT: time-to-first-treatment;

§CD38 was determined using a 30% cut-off;

‡ZAP70 was determined using a 20% cut-off;

†IGHV sequencing utilized a 2% cut-off to discriminate mutated from unmutated IGHV; M: mutated; UM: unmutated;

§§Patients were stratified into major cytogenetic categories, based on NCCN CLL Guidelines (Hallek, Shanafelt, and Eichhorst 2018): favorable (del 13q as a sole aberration), neutral (normal karyotype, trisomy 12q), and unfavorable (11q and/or 17p deletion);

NA: not available.

3.5.2. Quantitative RT-PCR (qRT-PCR)

Total RNA was extracted using TRIzol Reagent (Thermo Fisher Scientific, Waltham, MA) and 1 µg of RNA was reverse transcribed using M-MLV Reverse Transcriptase (Invitrogen, Carlsbad, CA, USA). Samples were run in triplicate by SYBR Green detection chemistry with PowerUp SYBR Green Master Mix (Applied Biosystems, Foster City, CA, USA) on a Real-Time Quant Studio 3 (Thermo Fisher Scientific). The average of cycle threshold of each triplicate was analyzed according to the $2^{-\Delta\Delta C_t}$ method (Livak and Schmittgen 2001). The primers used were: Catalase F, 5'-GAACTGTCCCTACCGTGCTCGA-3'; Catalase R, 5'-CCAGAATATTGGATGCTGTGCTCCAGG-3'; normalization was performed analyzing the ribosomal protein large P0 (RPLP0) mRNA expression level. RPLP0 F, 5'-ACATGTTGCTGGCCAATAAGGT-3' and RPLP0 R, 5'-CCTAAAGCCTGGAAAAAGGAGG-3'. The thermal cycle reaction was performed as follows: 95°C for 10 minutes followed by 40 cycles at 95°C for 15 seconds and 60°C for 1 minute. Human embryonic kidney 293 cell line (HEK293) was used as calibrator and to normalize the expression values of the samples.

3.5.3. Flow cytometry

Flow cytometry was used to analyze the protein catalase levels. PBMCs from healthy donors were stained with: CD19-BV786, and CD3/14-APCCy7. PBMCs from CLL patients were stained with CD5-BV605, CD19-BV786, and CD3/14-APCCy7 (for details see **Table 8**). After incubation with antibodies for 15 min at rt in the dark, cells were washed, fixed with BD Phosflow™ Fix Buffer I (BD Biosciences) and permeabilized with PBS (1X) + 0,1% TritonX-100 for 15 min rt in the dark. Permeabilized cells were washed, pelleted, and stained with anti-cPARP-Alexa Fluor647 and anti-catalase-Alexa Fluor 488 (for details see **Table 9**). For catalase measurement, approximately 1.0×10^4 -gated events were acquired for each sample on a BD LSRFortessa flow cytometer (Becton Dickinson). Flow cytometry data were processed using FlowJo software (v10 TreeStar). For data analysis, identification of healthy and leukemic B cells was based on CD19 expression and CD5 and CD19 co-expression, respectively. Debris were excluded

based on forward-scatter and side-scatter and residual T and monocytes cells were excluded on the basis of CD3 and CD14 signal, respectively. Viable cells were defined as c-PARP negative cells.

Table 9. Antibodies used for catalase detection

Antibody	Fluorochrome	Clone	Manufacturer
Catalase	Alexa Fluor488	EP1929Y	Abcam
Cleaved PARP (cPARP)	Alexa Fluor647	F21-852	BD Biosciences
CD19	BV786	SJ25C1	BD Biosciences
CD3	APCCy7	UCHT1	BioLegend
CD14	APCCy7	M5E2	BioLegend
CD5	BV605	UCHT2	BD Biosciences

3.5.4. Catalase activity assay

Catalase activity and protein levels were measured using a catalase-specific activity kit (ab118184 Abcam, Cambridge, UK), according to the manufacturer, as previously described by Lespay-Rebolledo et al. (Lespay-Rebolledo et al. 2018). Briefly, PBMCs from CLL patients and purified B cells from HD were thawed and the pellets were processed according to the manufacturer's protocol. Catalase activity and protein levels were detected by luminescence and absorbance, respectively, in a microplate reader (Parkin Elmer, Victor 3, Waltham, Massachusetts, USA). Catalase activity, corresponding to the exponential decay of H₂O₂, was detected in a time interval of 10 minutes. Catalase protein levels were detected at wavelength of 450 nm in an end point mode. The rate constant (k), reflecting catalase activity, was calculated considering the equation:

$$k = \frac{\ln(S1/S2)}{\Delta t}$$

where Δt was the time interval (10 min), S1 and S2 are the H₂O₂ levels (from the luminescence data) at time t1 and t2, respectively. Specific catalase activity was obtained by dividing k by absorbance values of catalase and total protein, expressed in milligrams.

3.5.5. DNA extraction and genotyping by restriction fragment length polymorphism (RFLP)-PCR

Genomic DNA extraction was performed using salting-out method. DNA was isolated from PBMCs samples collected from 55 CLL patients and 50 HD. Genotyping was assessed by RFLP-PCR as previously described (Zarei, Saadat, and Farvardin-Jahromi 2015). The primers used were: Catalase F, 5'-CTGATAACCGGGAGCCCCGCCCTGGGTTCGGATAT-3', Catalase R, 5'-CTAGGCAGGCCAAGATTGGAAGCCCAATGG-3'. The thermal cycle reaction was performed as follows: 95°C for 15' followed by 35 cycles at 94°C for 1', 68°C for 1' and 72°C for 1' followed by 72°C for 15'. PCR products (191 bp) were digested by restriction endonuclease EcoR V (New England Biolabs, Ipswich, MA) for 1h at 37°C. DNA fragments were separated on 4% agarose gel.

3.5.6. Pyrosequencing analysis / CpG sites methylation analysis

Quantified methylation level of eight CpG sites in the catalase promoter region (from the transcription start site (TSS) -277 to -226, or from ATG -357 to -306, (ref. seq. GRCh38 (+) - Chr11: 34438657-34438708) was determined by pyrosequencing of bisulfite-converted DNA. Sample bisulfite treatment, PCR amplification, pyrosequencing, and quantification of percent methylation were performed by EpigenDx (Worcester, MA, USA). Degree of methylation is analyzed as a "C/T SNP". Software provides the percentage of Cytosine methylation calculated according to the formula:

$$\% \text{ methylation} = \frac{\text{C peak height}}{\text{C peak height} + \text{T peak height}}$$

3.5.7. Inhibition of DNA methyltransferase in CLL cells

MEC-1 cell lines were maintained in Iscove's Modified Dulbecco's Medium (IMDM) supplemented with 10% heat inactivated fetal bovine serum (FBS), 2 mM L-glutamine and 2 mM penicillin/streptomycin and were maintained at 37 °C in 5% CO₂. Cells were seeded at concentration of 0,5x10⁶ cell/ml of appropriate culture

media. Cells were treated for 96 hours in a medium containing DMSO vehicle or 2 μ M of DNA methyltransferase inhibitor 5-aza-20-deoxycytidine (DAC). After treatment, catalase gene expression was assessed using qRT-PCR.

3.5.8. Software and statistical analysis

To evaluate the risk of CLL among different genotypes, odds ratios and 95% confidence intervals (95% CI) were calculated, and P-values were estimated by Fisher's exact test. Consistency of the control population with Hardy–Weinberg equilibrium was investigated by χ^2 test (Hardy–Weinberg Calculator by Michael H. Court). For comparisons, unpaired Student's t-test, Mann-Whitney test and, Wilcoxon matched-pairs signed rank test were used depends on data distribution evaluated with D'Agostino & Pearson normality test. Correlation analysis was performed calculating Spearman correlation coefficient (Spearman r). A P-value of < 0.05 was considered statistically significant. Graphing and statistical analyses were performed using GraphPad Prism software (v. 7.03, GraphPad Software Inc., La Jolla, CA). For flow cytometry data FlowJo software v.10 was used. Multiple sequence alignment was conducted using online MUSCLE software (<https://www.ebi.ac.uk/Tools/msa/muscle/>). Jalview software was used to calculate the percent identity among sequences. (v. 2.11.1.3, Jalview Software Barton Group, University of Dundee, Scotland, UK). Linear regression analyses were carried out using the open source platform for statistical computing R (version 3.6.0) run under the free integrated development environment RStudio (version 1.0.153, <https://rstudio.com>). We developed several models to study the effects of the interactions between genotypes and methylation levels, measured within the promoter region of the catalase gene, on the regulation of catalase mRNA transcription in CLL patients, and the goodness of the different fits was determined by ANOVA. The R package *ggeffects* (Lüdtke 2018) was also used to compute the marginal effects, i.e. the mean response of the factor variable (i.e. genotype) adjusted for the covariate (methylation levels), and the corresponding 95% confidence intervals.

3.6. Results

3.6.1. CLL cells express higher levels of catalase than normal B cells

We assessed catalase mRNA levels in leukemic cell samples from 54 CLL patients and in B cells from 18 healthy donors (HDs) isolated from PBMCs. Catalase protein expression level was analyzed using flow cytometry in 20 CLL samples and in 10 HDs.

Although the levels of catalase expression were highly heterogeneous among CLL samples (coefficients of variation: CV=74.72% for CLL *versus* CV=49.37% for HDs) (**Figure 25 A**), CLL cells expressed higher mRNA levels of catalase compared with healthy donors. Moreover, CLL cells exhibited an overall higher and more heterogeneous catalase protein levels than HD B cells (CV=35.75 for CLL *versus* CV=23.99% for HDs) (**Figure 25 B**).

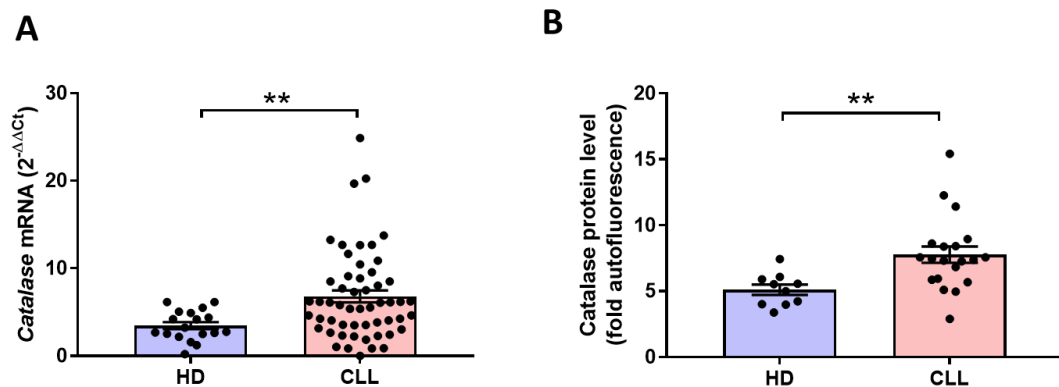


Figure 25. Catalase levels in B cells from HDs and leukemic cells from CLL patients. A) The relative catalase gene expression in CLL samples ($n = 54$) compared with healthy donors ($n = 18$). B) Catalase protein expression in CLL cells ($n = 20$) compared with HD B cells ($n = 10$). Data are expressed as relative median fluorescence intensity (RMFI) calculated as median fluorescence intensity (MFI) divided by fluorescence-minus-one (FMO). Data are expressed as mean \pm SEM. Comparisons were performed with Mann Whitney test. **: $P < 0.01$. CLL, chronic lymphocytic leukemia; HDs, healthy donors.

These data highlight the importance of studying CLL cells' redox metabolism and its role in the clinical course of the disease, supporting the hypothesis that catalase plays a role in CLL pathology.

3.6.2. Differential catalase expression in CLL associates with divergent clinical behaviors

We evaluated the distribution of catalase expression data in order to cluster patients into groups with high or low expression levels and investigate the potential correlation between catalase expression levels and disease behavior.

The levels of catalase mRNA among CLL patients were not normally distributed and exhibited a tail to the right (skewness = 1.488, Kurtosis = 2.733, **Figure 26 A, C**). Likewise, catalase protein data in CLL cells showed a skewness of 1.123 and Kurtosis of 2.216 (**Figure 26 B, D**).

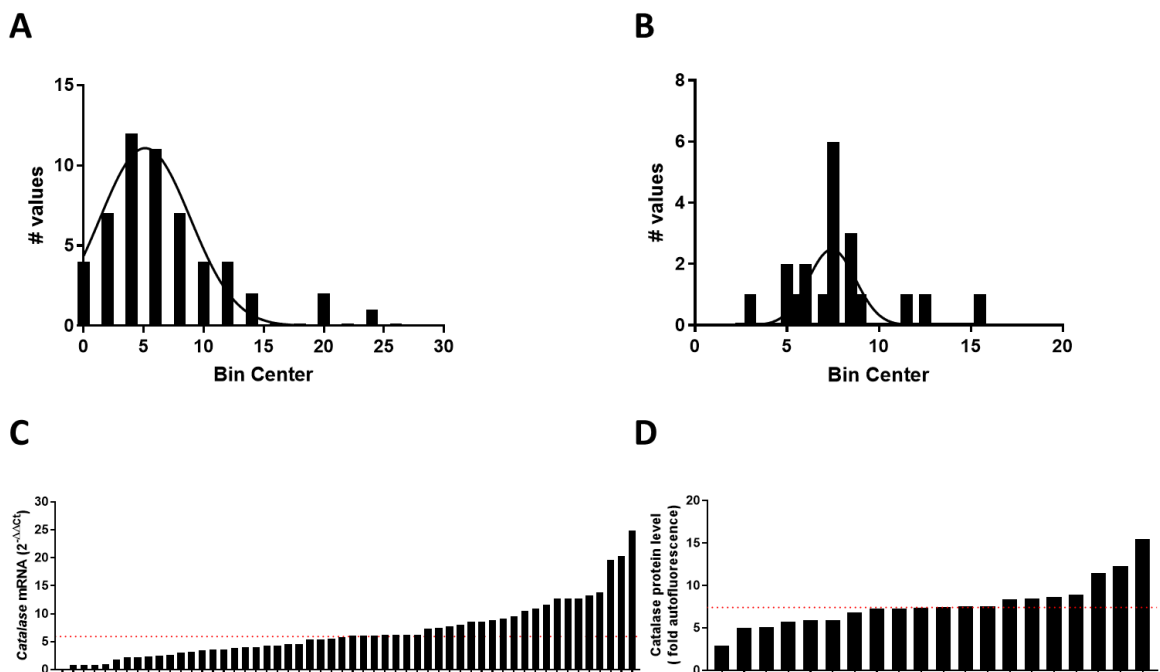


Figure 26. Catalase data distribution in CLL patients. A) Frequency distribution of mRNA expression data set. B) Frequency distribution of protein catalase expression data set. C) Ordered mRNA expression data set. D) Ordered protein expression data set. Red dotted line indicates median value (for mRNA = 5.943; for protein = 7.425). D'Agostino & Pearson normality test was used to evaluate the data distribution. CLL, chronic lymphocytic leukemia.

Based on distribution data, we used the median value of catalase expression (red dotted line in **Figures 26 C, D**) as a cut-off to cluster patients into groups with high or low catalase levels.

Kaplan-Meier curves showed that differential catalase expression in CLL identified two main disease subtypes characterized by a disparity in clinical outcome (**Figures 27 A, B**). In particular, low levels of catalase were significantly associated with a longer TTFT that reflects a better clinical course.

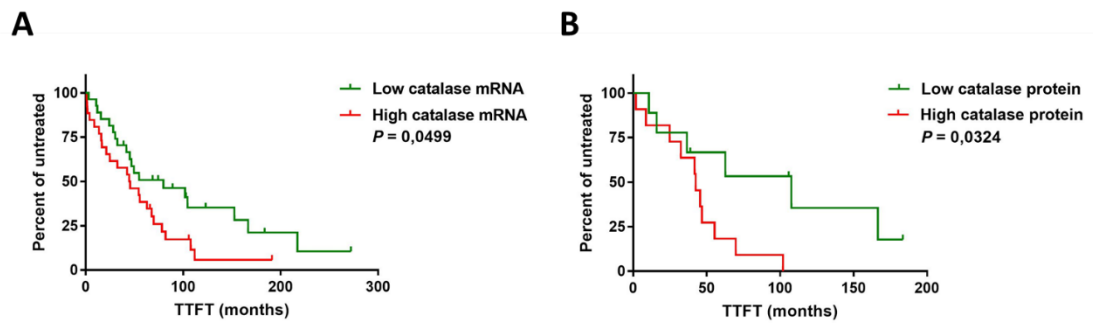


Figure 27. Association between catalase expression levels and time-to-first-treatment (TTFT) in CLL. A) Kaplan-Meier curves of TTFT for subgroups of CLL patients distinguished by low ($n = 27$) and high ($n = 26$) catalase mRNA levels B) Kaplan-Meier curves of TTFT for subgroups of CLL patients distinguished by low ($n = 9$) and high ($n = 11$) catalase protein levels. High and low enzyme expression values were referred to the median expression values. Difference between the two curves was calculated with log-rank test.

These data, confirmed previously results on mRNA catalase expression (Cavallini et al. 2018) (**Figure 27 A**) and extended these findings also at a protein level (**Figure 27 B**).

Given the difference of catalase protein expression between CLL patients and the normal counterpart, to investigate possible differences in the catalase specific activities linked to the leukemia transformation, we evaluated the specific catalase activity in 14 CLL samples and in 5 HDs. Interestingly, given the same amount of protein, no significant differences were found between CLL patients and healthy donors (**Table 10**), thus indicating that the enzyme has the same capacity in decompose H_2O_2 in CLL samples as well as in HDs. These findings imply that differences in catalase protein levels correspond to different cellular catalase activities.

Table 10. Catalase activity in CLL and HD reported as mean±SD

Samples	Activity (k/catalase/total protein in mg)	P value
Healthy donors	0.0017±0.0003	ns
CLL samples	0.002±0.0002	

3.6.3. The rs1001179 SNP is not a risk factor for CLL

The rs1001179 SNP (-262 C/T) in the catalase promoter region is associated with susceptibility to cancer risk in some cancers, including prostate cancer (Geybels et al. 2015) and, hepatocellular carcinoma (Ezzikouri et al. 2010; C. Di Wang et al. 2016). In contrast, this SNP is not a risk factor for non-Hodgkin lymphoma development (Cosma et al. 2019).

In order to evaluate a possible association between the rs1001179 SNP and susceptibility in CLL risk, 55 CLL patients and 50 HDs were genotyped for rs1001179 polymorphism (Table 11).

Table 11. Distributions of CAT rs1001179 genotypes in CLL patients and HD.

Polymorphisms	CLL (%)	HD (%)	OR	95% CI	P-value
CAT -262 C/T					
CC	24 (43.6)	25 (50)	1.00	-	-
CT	26 (47.3)	21 (42)	1.29	0.559 – 2.771	ns
TT	5 (9.1)	4 (8)	1.30	0.323 – 4.632	ns
CT+TT	31	25	1.29	0.599 – 2.823	ns
C	74 (67.3)	71 (71)	1.00		
T	36 (32.7)	29 (29)	1.19	0.667 – 2.166	ns

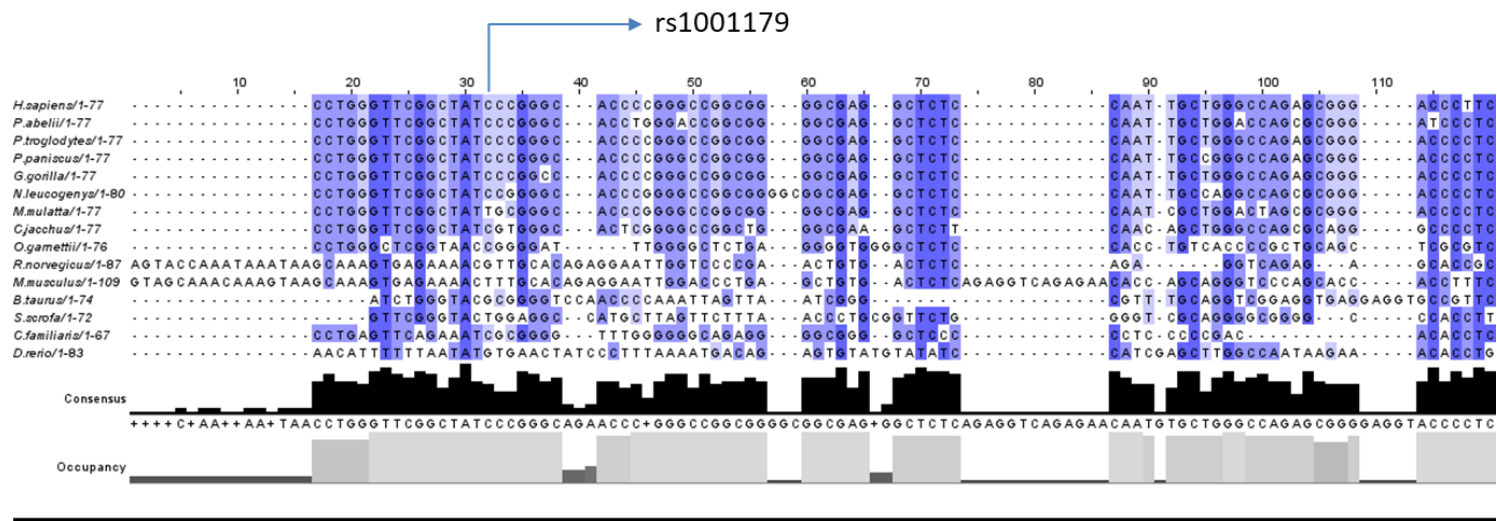
The distribution of genotypes was consistent with the Hardy–Weinberg equilibrium among CLL patients and HDs (for CLL patients' rs1001179 polymorphism, $\chi^2 = 0.2977$, $P > 0.05$; for HDs' rs1001179 polymorphism, $\chi^2 = 0.0198$, $P > 0.05$). Genotype frequencies among CLL patients were 43.6% for CC, 47.3% for CT and 9% for TT; genotype frequencies in HD (n=50) were 50% for CC, 42% for CT and 8% for TT. Moreover, the catalase rs1001179 polymorphism was not associated

with CLL risk in the analyzed cohort (CT vs CC: OR = 1.29, 95% CI: 0.559- 2.771, P = ns; TT vs CC: OR = 1.30, 95% CI: 0.323- 4.632, P = ns; CT+TT vs CC: OR = 1.29, 95% CI: 0.599-2.823, P = ns) (**Table 11**).

3.6.4. The rs1001179 SNP influences catalase gene expression

We have recently shown and confirmed in the present study that higher levels of catalase expression in CLL cells is linked to a faster progression of the disease. It is known that the rs1001179 SNP alters catalase expression in some cell types (Forsberg et al. 2001; Saify, Saadat, and Saadat 2016; Schults et al. 2013). Therefore, we investigated the role of the rs1001179 SNP in catalase expression in CLL cells.

First, we conducted a multiple sequence alignment of a selected upstream promoter region surrounding the analyzed rs1001179 SNP among 15 catalase genes. The multiple alignment analysis showed that the region surrounding the rs1001179 is conserved among species, thus suggesting a possible role of this SNP in catalase expression (**Figure 28**).



Color intensity represents the percentage identity

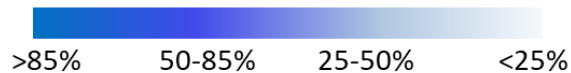


Figure 28. Multiple sequence alignment of a selected upstream promoter region among 15 catalase genes. Multiple sequence alignment was conducted using the online MUSCLE software (<https://www.ebi.ac.uk/Tools/msa/muscle/>). Jalview software was used to calculate the percent identity among sequences. Multiple sequence alignment was conducted considering the upstream promoter region of 15 catalase genes that include primates, no-primate mammals, rodents, and zebrafish. Color intensity, from a deeper blue (>85%) to a fainter one (<25%), represent the percentage identity. GenBank accession references: *Homo sapiens* (human), NC_000011.10; *Pongo abelii* (orangutan), NC_036914.1; *Pan troglodytes* (chimpanzee), NC_036890.1; *Pan paniscus* (pygmychimpanzee), NC_048250.1; *Gorilla gorilla* (gorilla), NC_044613.1; *Nomascus leucogenys* (white-cheeked gibbon), NC_044395.1; *Macaca mulatta* (rhesus macaque), NC_041767.1; *Callithrix jacchus* (common marmoset), NC_048393.1; *Otolemur garnettii* (greatergalago), NW_003852396.1; *Rattus norvegicus* (brownrat), NC_005102.4; *Mus musculus* (house mouse), NC_000068.8; *Bos taurus* (cattle), NC_037342.1; *Sus scrofa* (wild boar), NC_010444.4; *Canis lupus familiaris* (dog), NC_006600.3; and *Danio rerio* (zebrafish), NC_007136.7.

To investigate the genetic influence of the rs1001179 SNP in the differential catalase expression in CLL subtypes, we determine relative catalase gene expression in 34 CLL cell samples selected on the basis of their genotype (15 CC, 14 CT + 5 TT genotypes, **Figure 29**). Next, we compared the catalase gene expression levels between the CC and CT/TT genotype subgroups of CLL samples (**Figure 29 B**). Due to the limited number of homozygous patients harboring the minor T allele, we grouped together the CT and TT genotypes.

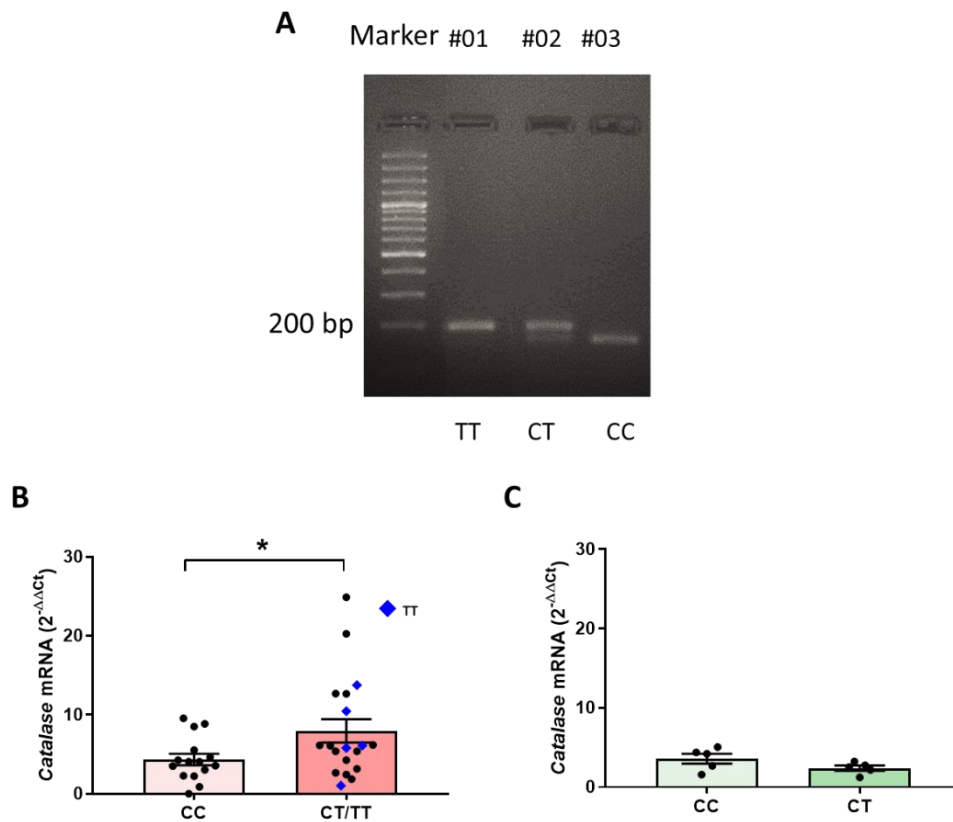


Figure 29. Association between catalase gene expression and rs1001179 SNP. A) Representative genotypes for the rs1001179 SNP. From left to right the lanes show: Marker) DNA size marker (100 bp ladder), #01) TT genotype (191 bp), #02) CT genotype (191, 157 and 34 bp) and #03) CC genotype (157 and 34 bp). B) Comparison of catalase mRNA expression between CC and CT/TT genotypes for rs1001179 SNP in CLL (n=34). C) Comparison of catalase mRNA expression between CC and CT genotypes for rs1001179 SNP in HDs (n=10). Data are expressed as mean \pm SEM; Comparison was performed with Mann Whitney test, *: $P < 0.05$.

The catalase expression levels were highly heterogeneous among CLL samples compared with HDs. For the CC genotypes, CV was 64.40% across CLL samples versus 39.43% among HD samples, **Figure 29 B, C**). Similarly, for cell samples harboring the T allele, CV was 85.95% in CLL and 31.01% in HD (**Figure 29 B, C**). Nevertheless, CLL cells harboring the T allele exhibited a significantly higher catalase expression compared with cells bearing the CC genotype (**Figure 29 B**). However, the TT genotype did not show higher levels of catalase mRNA compared with the CT genotype (**Figure 29 B**). In contrast, comparison of the catalase gene expression levels between the CC and CT genotype subgroups in HDs did not show significant differences (**Figure 29 C**). The HD samples lacked the TT genotype because of the limited number of HDs analyzed.

Next, in order to investigate the influence of the studied SNP at protein level we assessed the protein catalase expression levels in 16 CLL cell samples. Among them 6 samples exhibited the CC genotype, 8 the CT and 2 the TT genotype. Although CLL cells showed a trend towards higher protein catalase expression in the CT/TT genotypes compared with CC genotypes, this did not reach statistical significance in this small set of samples (**Figure 30**).

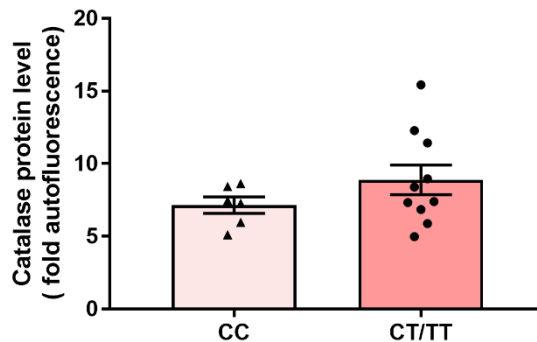


Figure 30. Association of protein catalase expression and rs1001179 SNP in CLL cells. Comparison of protein catalase expression between CC and CT/TT genotypes for rs1001179 SNP. Data are expressed as relative median fluorescence intensity (RMFI) calculated as median fluorescence intensity (MFI) divided by fluorescence-minus-one (FMO). Data are expressed as mean±SEM (n=16); Comparison was performed with Mann Whitney test.

3.6.5. Methylation influences catalase gene expression

In order to investigate the involvement of epigenetic regulatory mechanisms in the control of catalase expression, we quantified the methylation levels in a defined catalase promoter region (GRCh38 (+) - Chr11:34438657-34438708). Using bisulfite pyrosequencing we analyzed the methylation levels of 8 CpG sites within the CpG island II of the human catalase gene promoter in 21 CLL and 10 HD samples (**Figure 31, 32 and Table 12**). This region was selected because it surrounds the analyzed rs1001179 SNP and because it has been shown to be differentially methylated in different cell contexts, thus influencing catalase expression (Min, Lim, and Jung 2010; Chibber, Sangeet, and Ansari 2017) (**Figure 29**).

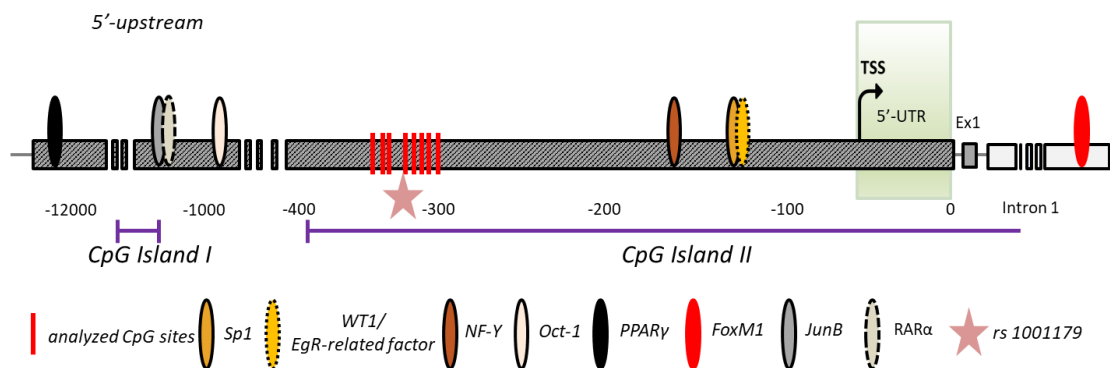


Figure 31. Schematic representation of human catalase promoter and location of the analyzed CpG sites. Location of the main DNA-binding transcription regulators and the CpG islands in the promoter region of human catalase gene. Red bars represent the location of the 8 CpG sites, on the proximal region of human catalase promoter, analyzed for bisulfite pyrosequencing. The analyzed CpGs sites range from ATG -357 to -306. This region covers or is directly adjacent to rs1001179 SNP (-330 bp upstream of the ATG translation start). Abbreviations: specificity protein 1 (Sp1), nuclear factor Y (NFY), Wilms tumor 1 (WT1), early growth response (Egr), fork-head box protein M1 (FoxM1), octamer-Binding transcription factor 1 (Oct-1), peroxisome proliferator-activated receptor gamma (PPAR γ), activator protein 1 (AP-1) member JunB, and retinoic acid receptor alpha (RAR α).

The methylation levels, in each site (CpG#-n) and the mean methylation level of the analyzed sites are expressed in percentage and shown in **Table 12** for CLL samples and in **Table 13** for HD samples.

Table 12. DNA methylation percentage in CLL samples.

Human CAT Methylation Analysis - Results in % Methylation									
From ATG	-357	-348	-337	-328	-319	-314	-311	-306	-357 to -306
GRCh38	Chr11:657	Chr11:666	Chr11:677	Chr11:686	Chr11:695	Chr11:700	Chr11:703	Chr11:708	Chr11:34438657-34438708
Sample ID	CpG#-25	CpG#-24	CpG#-23	CpG#-22	CpG#-21	CpG#-20	CpG#-19	CpG#-18	Mean
CLLV#009	1,5	3,8	2,6	1,6	1,6	0,0	0,0	0,0	1,4
CLLV#017	4,8	4,3	4,5	3,4	4,6	3,9	2,3	2,1	3,7
CLL#08a	4,0	3,4	4,9	0,0	4,3	6,4	2,8	3,7	3,7
CLLV#033	5,4	3,5	5,3	4,1	4,9	5,9	3,3	0,0	4,0
CLLV#014	4,6	3,2	4,4	2,8	4,1	4,3	1,9	0,0	3,1
CLLV#034	1,8	1,9	3,4	0,0	2,1	0,0	0,0	0,0	1,1
CLLV#035	4,5	4,0	3,4	0,0	0,0	3,0	0,0	0,0	1,9
CLLV#012	1,9	1,6	3,0	1,7	1,8	0,0	0,0	0,0	1,2
CLL#04a	3,7	3,4	2,9	3,0	2,6	0,0	0,0	0,0	1,9
CLLV#027	5,1	5,6	5,1	6,3	0,0	0,0	0,0	0,0	2,7
AIRC-0047	2,3	3,8	4,0	3,1	2,6	2,7	1,6	0,0	2,5
AIRC-0105	2,6	3,4	3,2	2,4	3,3	3,4	1,5	0,0	2,5
AIRC-0028	3,1	3,5	4,8	3,1	2,9	2,7	1,7	0,0	2,7
AIRC-0112	3,0	2,9	2,7	2,3	3,3	2,5	0,0	0,0	2,1
AIRC-0100	2,6	3,1	3,2	2,6	2,8	2,5	1,6	1,7	2,5
AIRC-0102	3,5	2,9	4,0	3,3	4,3	3,5	2,6	0,0	3,0
AIRC-0180	1,6	2,7	3,5	2,1	2,1	2,9	0,0	0,0	1,9
AIRC-0157	0,0	2,2	0,0	0,0	2,4	0,0	0,0	0,0	0,6
AIRC-0061	2,3	3,0	3,4	2,7	2,3	2,0	1,7	1,6	2,4
AIRC-0029	1,9	2,0	2,3	1,9	2,2	2,5	1,6	0,0	1,8
AIRC-0002	1,7	3,2	3,2	1,8	1,7	2,3	0,0	0,0	1,7

Table 13. DNA methylation percentage in HD samples.

Human CAT Methylation Analysis - Results in % Methylation									
From ATG	-357	-348	-337	-328	-319	-314	-311	-306	-357 to -306
GRCh38	Chr11:657	Chr11:666	Chr11:677	Chr11:686	Chr11:695	Chr11:700	Chr11:703	Chr11:708	Chr11:34438657-34438708
Sample ID	CpG#-25	CpG#-24	CpG#-23	CpG#-22	CpG#-21	CpG#-20	CpG#-19	CpG#-18	Mean
HD#012	9,3	9,4	9,8	9,2	9,6	9,2	6,1	8,1	8,8
HD#017	1,3	3,9	2,3	1,9	1,3	2,3	0,0	0,0	1,6
HD#022	10,0	10,5	11,7	10,7	11,3	8,9	7,7	8,2	9,9
HD#023	0,0	3,3	3,1	1,9	1,8	2,0	0,0	0,0	1,5
HD#024	3,0	5,5	4,6	3,3	3,4	3,3	2,6	2,8	3,6
HD#025	1,6	1,9	2,6	1,7	1,4	1,7	0,0	0,0	1,4
HD#026	4,1	4,4	4,7	3,9	3,0	4,1	2,8	2,5	3,7
HD#027	2,4	3,9	3,9	3,7	3,4	3,5	2,3	2,6	3,2
HD#028	5,2	4,7	5,4	4,9	5,1	5,4	3,8	4,5	4,9
HD#033	9,4	11,1	11,6	10,7	10,1	10,4	8,0	9,3	10,1

The sites highlighted in red are the sites surrounding the rs1001179 SNP. The site CpG#22 is the closest to rs1001179 SNP.

An example of pyrogram is shown in **Figure 32**.

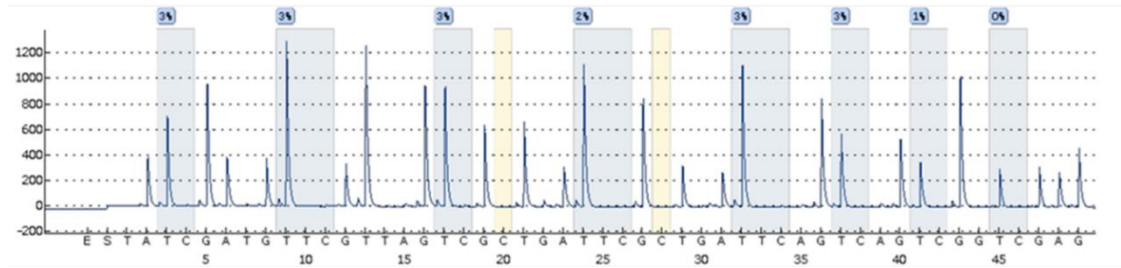


Figure 32. Example of pyrogram reporting the DNA methylation status on eight CpG site in the catalase promoter region. Blue boxes highlighted the eight CpG sites analyzed for cytosine methylation percentage degree; yellow boxes represent bisulfite conversion efficacy control.

Then, we compared the overall methylation levels between HDs and CLL samples, measured as mean of all the analyzed CpG sites. As shown in **Figure 33**, CLL cells showed lower methylation levels compared with HDs, in line with the differential catalase gene expression documented in CLL and HDs (**Figure 25**).

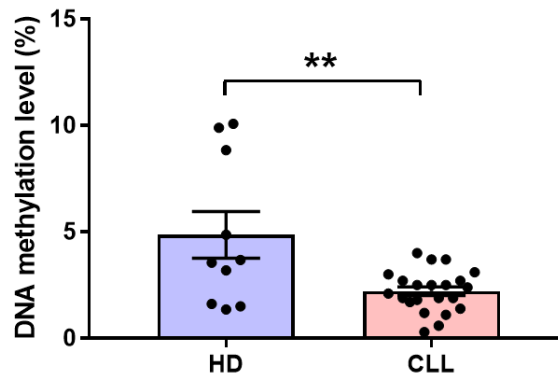


Figure 33. Methylation levels of catalase promoter region in HDs and CLL patients. Methylation levels of the analyzed catalase promoter in CLL samples ($n=21$) compared with HDs ($n=10$). DNA methylation levels are measured as mean among the analyzed sites. Data are expressed as mean \pm SEM. Comparisons were performed with Student T tests. **: $P < 0.01$. CLL, chronic lymphocytic leukemia; HDs, healthy donors.

Then, we investigated the relationship between DNA methylation level and catalase gene expression across CLL samples. First, we correlated the methylation levels of each CpG site with the catalase gene expression levels. Remarkably, the

methylation level at CpG#21 site negatively correlated with the catalase gene expression level (**Figure 34**).

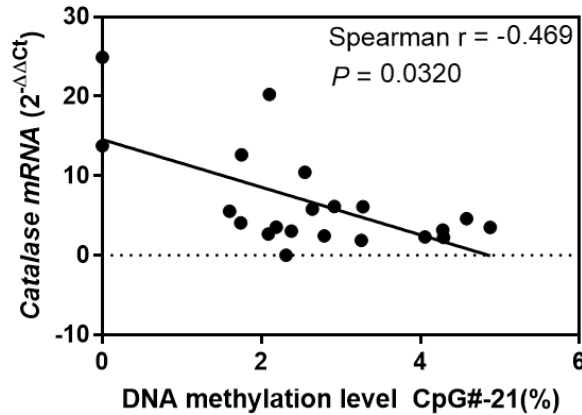


Figure 34. Correlation between DNA methylation levels in CpG#21 site and catalase gene expression in CLL samples. DNA methylation levels in CpG#21 site, in the catalase promoter region, was expressed in percentage and correlated to catalase gene expression (n = 21). The comparisons indicated the Spearman correlation coefficient.

Next, we evaluated the correlation between mean percentage methylation levels and the catalase expression level, considering the mean percent methylation of all sites and different combinations of them. Although the mean percent methylation of all sites did not significantly correlate with catalase gene expression (data not shown), the mean percentage methylation of sites CpG#22 to CpG#18 (CpG#22-18) (**Figure 35 A**), sites CpG#21 to CpG#18 (CpG#21-18) (**Figure 35 B**), sites CpG#20 to CpG#18 (CpG#20-18) (**Figure 35 C**) and sites CpG#19 and CpG#18 (CpG#19-18) (**Figure 35 D**) showed statistically significant negative relationships with the catalase gene expression levels.

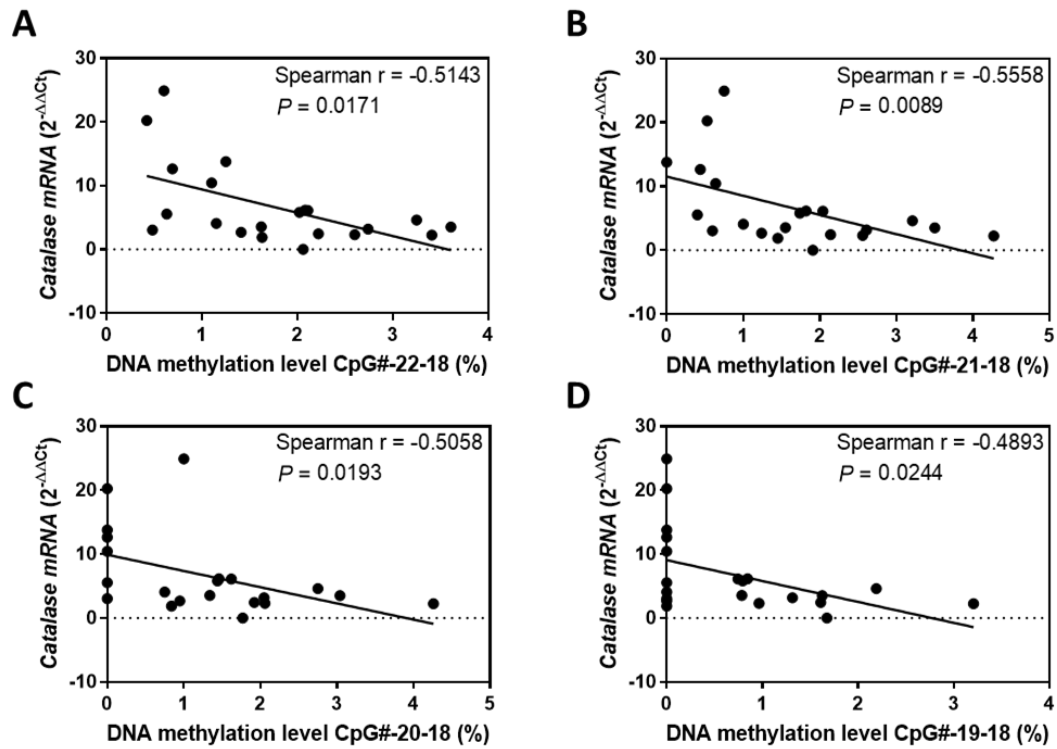
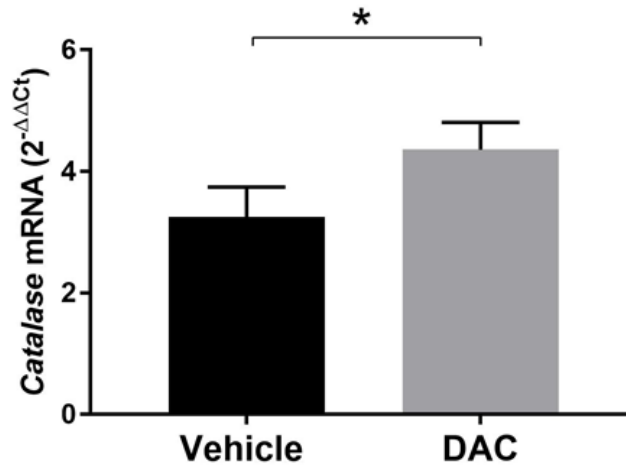


Figure 35. Correlation between mean percentage methylation levels with catalase expression level in CLL samples. DNA methylation levels expressed as mean percentage methylation. A) DNA methylation percentage of sites CpG#22 to CpG#18 correlated to catalase gene expression ($n = 21$). B) DNA methylation percentage of sites CpG#21 to site CpG#18 correlated to catalase gene expression ($n = 21$). C) DNA methylation percentage of sites CpG#20 to site CpG#18 was correlated to catalase gene expression ($n = 21$). D) DNA methylation percentage of sites CpG#19 and CpG#18 was correlated to catalase gene expression ($n = 21$). The comparisons indicated the Spearman correlation coefficient.

The next step was to functionally validate the influence of methylation in regulating catalase gene expression in CLL. For this purpose, we analyzed catalase gene expression after treatment with the DNA methyltransferase inhibitor 5-aza-20-deoxycytidine (DAC) of MEC-1 cell line. As shown in **Figure 36**, inhibiting methyltransferase activity in CLL cells induced an increase in catalase expression.



*Figure 36. Catalase expression levels after DNA methyltransferase inhibitor (DAC) treatment in MEC-1 CLL cell line. Comparison of catalase gene expression between MEC-1 cells treated with 2 μ M 5-aza-20-deoxycytidine (DAC) or left unstimulated (vehicle) for 96 hours. Value bars represent the mean \pm SEM of 5 independent experiments. Comparison was performed with Wilcoxon matched-pairs signed rank test, *: $P < 0.05$.*

Taken together, these data showed that methylation as well as the rs1001179 SNP within the catalase promoter play a role in the regulation of catalase gene expression in CLL cells.

3.6.6. Methylation and rs1001179 T allele influences catalase gene expression

In this study, we showed as the rs1001179 SNP on the one hand and methylation on the other one influence catalase gene expression in CLL cells. Based on these findings, we wondered about a possible interaction between these two regulatory levels in controlling catalase expression. Therefore, we developed a Linear model in order to investigate the interactions between the independent variable "genotypes" - a factor variable with 2 levels, the "CC" and "CT/TT" - and the methylation levels - a continuous covariate - on catalase gene expression. We grouped together the CT and TT genotypes due to the limited number of homozygous patients harboring the minor T allele. We found a significant inverse linear relationship between mean percent methylation across sites CpG#22-CpG#18 and catalase gene expression in CLL cells harboring CT/TT genotypes (**Figure 37**, **Table 14** and **Table 15**), thus indicating that the CT/TT genotypes show a lower methylation levels and a highest catalase gene expression level.

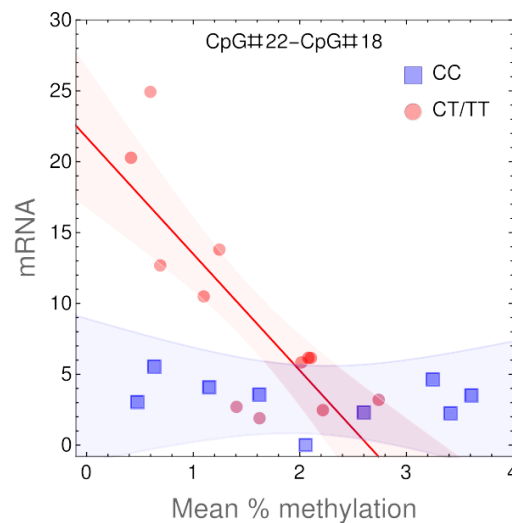


Figure 37. Effects of the interaction of genotype with mean methylation levels on catalase mRNA expression. The interaction has been investigated within the context of linear models. We found significant regression results when methylation from site CpG#22 to site CpG#18 was averaged and stratified for the two genotypes CC and CT/TT. The line shows the marginal effects (i.e. predicted values) for the significant interaction between genotype CT/TT and methylation on mRNA expression (detailed in Table 13 and Table 14). Shaded colored areas indicate the 95% confidence intervals for all interactions. Measurements stratified by genotypes are shown as points.

Moreover, in this study we confirmed that high catalase expression levels were associated to a more severe prognosis in CLL. Therefore, these analyses indicate that a lower level of mean methylation value across CpG#22-CpG#18 sites may constitute a risk factor in CLL harboring the minor T allele.

Table 14. Coefficients and goodness-of-fit statistics for the linear regression model shown in Figure 37

	Estimate	SE	t value	P-value
intercept	3.87	2.58	1.50	0.15
methylation	-0.32	1.09	-0.29	0.77
CT/TT	17.84	3.63	4.92	1.3 10 ⁻⁴
methylation: CT/TT	-7.91	1.87	-4.23	5.6 10 ⁻⁴
Adj. r^2			0.67	
¹ $F_{3,17}$			14.3 ($P=6.45 \cdot 10^{-5}$)	
² KS-test			$P=0.67$	

¹F statistics for the linear regression.

²Kolmogorov-Smirnov test assessing whether the residuals of the fit e_i were normally distributed, i.e. $e_i \sim \mathcal{N}(0, \sigma_e)$. Please note that high P values indicate that it is unlikely that the residuals were drawn from a different distribution.

Table 15. ANOVA table for the linear regression model shown in Figure 37

	Df	Sum of Sq.	Mean Sq.	F	P-value
genotype	1	183.65	183.65	13.48	1.9 10 ⁻³
methylation	1	156.67	156.67	11.50	3.5 10 ⁻³
meth.: genotype	1	244.12	244.12	17.92	5.6 10 ⁻⁴
residuals	17	231.59	13.623		

These data point toward genetic and epigenetic regulatory mechanisms of catalase expression that may contribute to disease severity.

3.7. Discussion

This study shows that CLL cells express higher levels of catalase compared with healthy donors, both at mRNA and protein level. Catalase levels are heterogeneous among patients and differential catalase (CAT) expression associated with divergent clinical behaviors and progression. Herein, we show for the first time that the rs1001179 SNP in the catalase promoter is associated with modulation of catalase expression. Moreover, we show that methylation of catalase promoter influences catalase expression in CLL. Furthermore, methylation and the rs1001179 T allele interact in regulating catalase gene expression. The key advantage of this study is to provide new insights into the knowledge of genetic and epigenetic mechanisms at the basis of differential expression of catalase in CLL.

In this study, we show that CLL cells express increased levels of catalase compared with healthy donors, both at mRNA and protein level. Deregulation in antioxidant enzymes expression has been often observed in cancer. Increased enzyme expression has been associated with tumorigenic signals in some cancers, but with antitumor functions in others (Hwang, Choi, and Han 2007; Glorieux et al. 2015). For instance, catalase is increased in gastric carcinoma and malignant melanoma cells compared to the normal counterpart (Hwang, Choi, and Han 2007; Sander et al. 2003). Moreover, Jitschin et al. reported increased levels of catalase in CLL compared with normal B cells (Jitschin et al. 2014). On the contrary, catalase expression results decreased in lung cancer respect to the healthy adjacent airway epithelial cells (J. C. Ho et al. 2001). These contrasting data on catalase expression in different cancer types reflect a dichotomous role of catalase in cancer.

Herein, we also document that higher catalase, both a mRNA and protein level, is associated with a faster progression of CLL, thus confirming and extending previous data. Moreover, we show that the higher catalase protein levels correspond to higher enzymatic activity of catalase. These data are in agreement with the finding that many cancer cells require oxidant detoxifying and upregulation of catalase for tumor progression and metastasis (Wu 2006; Sander et al. 2003; Jitschin et al. 2014). The hypothesis on the role of catalase in CLL is that altered antioxidant

enzymes could have a critical role in regulating ROS, which in turn can mediate antitumor signals in leukemic cells, i.e. cell death or susceptibility to apoptosis, thus influencing disease progression. Consistently, it has been recently documented that higher levels of catalase and decreased levels of cellular ROS are associated with a faster progression of CLL (Cavallini et al. 2018). Moreover, Linley et al. recently showed an inverse correlation between ROS levels and the proportion of viable cells in CLL (Linley et al. 2015).

The dual role of catalase in cancer underlines the importance to investigate the role and the regulation of this antioxidant enzyme. Since catalase has a pivotal role in controlling the concentration of H₂O₂, polymorphisms in the CAT gene promoter provide useful information in association studies with oxidative stress-related diseases. There are several lines of evidence suggesting that oxidative stress is involved in key steps of cancer development, including CLL, even if the precise pathogenic mechanisms remain still poorly understood (D'Avola et al. 2016). Many previous studies have suggested a possible correlation between a single nucleotide polymorphism (SNP) in the catalase promoter region (rs1001179; -262 C/T) and susceptibility to cancers, such as prostate cancer and hepatocellular carcinoma (Geybels et al. 2015; Ezzikouri et al. 2010; C. Di Wang et al. 2016). Thus, first we investigated the genetic susceptibility of this SNP in CLL. However, we observed no significant association between CAT -262 C/T polymorphism and susceptibility to CLL risk in the analyzed cohort. Similarly, the CAT -262C/T is not a risk factor for non-Hodgkin lymphoma development (Cosma et al. 2019). Then, in order to explore the molecular mechanisms underlying differential expression of catalase in CLL subtypes, we investigated the influence of rs1001179 SNP on catalase gene expression. Remarkably, our data showed for the first time that CLL cells harboring the variant T allele exhibit higher expression of catalase compared with cells carrying the wild-type C allele. This finding is in accordance with previous studies (Forsberg et al. 2001; Saify, Saadat, and Saadat 2016; Schults et al. 2013) and suggests that this SNP lies on a putative consensus sequence for specific transcription-factor binding. Further studies will provide new insights on this aspect. Forsberg et al. had predicted a different affinity for the proteins GATA-1,

Lmo2, and c-Rel in the presence of two polymorphic promoter variants. However, the involvement of these transcription factors has been excluded (Forsberg et al. 2001). Moreover, further bioinformatics analysis predicted a STAT4 binding site in presence of the T allele and a putative binding site for TFII-1 transcription factor in presence of C allele (Saify 2016). Nevertheless, the STAT4 and TFII-1 influence on catalase expression needs to be functionally validated. Taken together, these data point to genetic polymorphism as a possible mechanism underlying the heterogeneous expression of CAT associated with variable CLL clinical behavior. However, we do not document an association between the rs1001179 SNP and clinical progression, measured as TTFT (data not shown). This finding could be explained by the multifactorial pattern of CAT expression regulation in cancer, which include not only genetic but also epigenetic changes and transcriptional regulation (Glorieux et al. 2015).

Besides genetic alterations and posttranscriptional modification, epigenetic processes have been revealed as crucial actors in the regulation of catalase expression, although still poorly investigated. It is known that CpG islands in the human promoter of catalase are methylated in human hepatocarcinoma cell lines; the methylation correlates with decreased catalase expression (Min, Lim, and Jung 2010). Moreover, Chibber et al. demonstrated that CuO nanoparticles induced hypermethylation of CpG island II on the catalase promoter and downregulated catalase expression at the transcriptional level (Chibber, Sangeet, and Ansari 2017). Herein, we show for the first time that CLL cells present lower catalase promoter methylation levels compared with healthy donors. Moreover, catalase promoter hypomethylation is associated with higher catalase gene expression levels. Consistently, it has been shown that CLL cells display massive hypomethylation compared to normal B cells (Oakes et al. 2016). We also show that catalase promoter methylation negatively correlates with catalase gene expression levels. Specifically, methylation of the single CpG site at position -319 from ATG as well as the mean percentage of 5 CpG sites, which include also the CpG site at position -319 from ATG, show a significant negative correlation with catalase expression. Interestingly, these CpG sites are the closest to the core promoter. Moreover,

inhibition of DNA methyltransferase in the MEC-1 CLL cell line induces augment of catalase mRNA levels, thus functionally confirming the role of methylation in regulating catalase gene expression in CLL. This evidence points to the hypothesis that catalase promoter methylation influences the binding of transcriptional factors to the promoter, thus reducing the level of catalase transcription.

Taken together, these data show the involvement of methylation processes in the regulation of catalase expression in CLL. We also documented the interaction between rs1001179 SNP and methylation level in regulating catalase expression. CLL cells carrying the T allele showed a lower methylation level and a higher catalase gene expression, which is associated with a faster disease progression. Consistently with this finding, the methylation changes represent a powerful predictor of clinical aggressiveness in CLL and in mantle cell lymphoma (MCL) (Tsagiopoulou et al. 2019; Queirós et al. 2016; Oakes et al. 2016).

In conclusion, our data provide new insights into the knowledge of genetic and epigenetic mechanisms regulating the catalase expression in CLL. Moreover, these data form the basis for future studies aimed at dissecting molecular mechanisms that regulate catalase expression, which could be of crucial relevance for the development of therapies targeting redox pathways.

4. References

- Ahn, Jiyoung, Marilie D. Gammon, Regina M. Santella, Mia M. Gaudet, Julie A. Britton, Susan L. Teitelbaum, Mary Beth Terry, et al. 2005. "Associations between Breast Cancer Risk and the Catalase Genotype, Fruit and Vegetable Consumption, and Supplement Use." *American Journal of Epidemiology* 162 (10): 943–52. <https://doi.org/10.1093/aje/kwi306>.
- Allsup, David J., Aura S. Kamiguti, Ke Lin, Paul D. Sherrington, Zoltan Matrai, Joseph R. Slupsky, John C. Cawley, and Mirko Zuzel. 2005. "B-Cell Receptor Translocation to Lipid Rafts and Associated Signaling Differ between Prognostically Important Subgroups of Chronic Lymphocytic Leukemia." *Cancer Research* 65 (16): 7328–37. <https://doi.org/10.1158/0008-5472.CAN-03-1563>.
- Austen, Belinda, Anna Skowronska, Claire Baker, Judith E. Powell, Anne Gardiner, David Oscier, Aneela Majid, et al. 2007. "Mutation Status of the Residual ATM Allele Is an Important Determinant of the Cellular Response to Chemotherapy and Survival in Patients with Chronic Lymphocytic Leukemia Containing an 11q Deletion." *Journal of Clinical Oncology* 25 (34): 5448–57. <https://doi.org/10.1200/JCO.2007.11.2649>.
- Baba, Yoshihiro, Shoji Hashimoto, Masato Matsushita, Dai Watanabe, Tadimitsu Kishimoto, Tomohiro Kurosaki, and Satoshi Tsukada. 2001. "BLNK Mediates Syk-Dependent Btk Activation." *Proceedings of the National Academy of Sciences of the United States of America* 98 (5): 2582–86. <https://doi.org/10.1073/pnas.051626198>.
- Baker, Andrew M., Larry W. Oberley, and Michael B. Cohen. 1997. "Expression of Antioxidant Enzymes in Human Prostatic Adenocarcinoma." *Prostate* 32 (4): 229–33. [https://doi.org/10.1002/\(SICI\)1097-0045\(19970901\)32:4<229::AID-PROS1>3.0.CO;2-E](https://doi.org/10.1002/(SICI)1097-0045(19970901)32:4<229::AID-PROS1>3.0.CO;2-E).
- Bauer, Georg. 2012. "Tumor Cell-Protective Catalase as a Novel Target for Rational Therapeutic Approaches Based on Specific Intercellular ROS Signaling." *Anticancer Research* 32 (7): 2599–2624.
- Beers, Stephen A., Ruth R. French, H. T. Claude Chan, Sean H. Lim, Timothy C. Jarrett, Regina Mora Vidal, Sahan S. Wijayaweera, et al. 2010. "Antigenic Modulation Limits the Efficacy of Anti-CD20 Antibodies: Implications for Antibody Selection." *Blood* 115 (25): 5191–5201. <https://doi.org/10.1182/blood-2010-01-263533>.
- Bhalla, Savita, and Leo I. Gordon. 2016. "Functional Characterization of NAD Dependent De-Acetylases SIRT1 and SIRT2 in B-Cell Chronic Lymphocytic Leukemia (CLL)." *Cancer Biology and Therapy* 17 (3): 300–309. <https://doi.org/10.1080/15384047.2016.1139246>.
- Böhm, Britta, Sonja Heinzelmann, Manfred Motz, and Georg Bauer. 2015. "Extracellular Localization of Catalase Is Associated with the Transformed State of Malignant Cells." *Biological Chemistry* 396 (12): 1339–56. <https://doi.org/10.1515/hsz-2014-0234>.
- Bojarczuk, K., M. Siernicka, M. Dwojak, M. Bobrowicz, B. Pyrzynska, P. Gaj, M. Karp, et al. 2014. "B-Cell Receptor Pathway Inhibitors Affect CD20 Levels and Impair Antitumor Activity of Anti-CD20 Monoclonal Antibodies." *Leukemia*. Nature Publishing Group. <https://doi.org/10.1038/leu.2014.12>.
- Bonavida, Benjamin. 2006. "What Signals Are Generated by Anti-CD20 Antibody Therapy?" *Current Hematologic Malignancy Reports* 1 (4): 205–13. <https://doi.org/10.1007/s11899-006-0001-z>.
- Borge, Mercedes, María Belén Almejún, Enrique Podaza, Ana Colado, Horacio Fernández Grecco, María Cabrejo, Raimundo F. Bezares, Mirta Giordano, and Romina Gamberale. 2015. "Ibrutinib Impairs the Phagocytosis of Rituximab-Coated Leukemic Cells from Chronic Lymphocytic Leukemia Patients by Human

- Macrophages.” *Haematologica*. Ferrata Storti Foundation.
<https://doi.org/10.3324/haematol.2014.119669>.
- Bost, Frederic, and Lisa Kaminski. 2019. “The Metabolic Modulator PGC-1 α in Cancer.” *American Journal of Cancer Research* 9 (2): 198–211.
<http://www.ncbi.nlm.nih.gov/pubmed/30906622><http://www.pubmedcentral.nih.gov/articlerender.fcgi?artid=PMC6405967>.
- Brown, Jennifer R. 2008. “Inherited Predisposition to Chronic Lymphocytic Leukemia.” *Expert Review of Hematology*. NIH Public Access.
<https://doi.org/10.1586/17474086.1.1.51>.
- Burger, Jan A. 2020. “Treatment of Chronic Lymphocytic Leukemia.” Edited by Dan L. Longo. *New England Journal of Medicine* 383 (5): 460–73.
<https://doi.org/10.1056/NEJMra1908213>.
- Burger, Jan A., and Nicholas Chiorazzi. 2013. “B Cell Receptor Signaling in Chronic Lymphocytic Leukemia.” *Trends in Immunology*. Trends Immunol.
<https://doi.org/10.1016/j.it.2013.07.002>.
- Burger, Jan A., Michael J. Keating, William G. Wierda, Elena Hartmann, Julia Hoellenriegel, Nathalie Y. Rosin, Iris de Weerd, et al. 2014. “Safety and Activity of Ibrutinib plus Rituximab for Patients with High-Risk Chronic Lymphocytic Leukaemia: A Single-Arm, Phase 2 Study.” *The Lancet Oncology* 15 (10): 1090–99.
[https://doi.org/10.1016/S1470-2045\(14\)70335-3](https://doi.org/10.1016/S1470-2045(14)70335-3).
- Burger, Jan A., and Susan O’Brien. 2018. “Evolution of CLL Treatment — from Chemoimmunotherapy to Targeted and Individualized Therapy.” *Nature Reviews Clinical Oncology* 15 (8): 510–27. <https://doi.org/10.1038/s41571-018-0037-8>.
- Burger, Jan A., and Adrian Wiestner. 2018. “Targeting B Cell Receptor Signalling in Cancer: Preclinical and Clinical Advances.” *Nature Reviews Cancer*. Nature Publishing Group. <https://doi.org/10.1038/nrc.2017.121>.
- Byrd, John C., Richard R. Furman, Steven E. Coutre, Ian W. Flinn, Jan A. Burger, Kristie A. Blum, Barbara Grant, et al. 2013. “Targeting BTK with Ibrutinib in Relapsed Chronic Lymphocytic Leukemia.” *New England Journal of Medicine* 369 (1): 32–42. <https://doi.org/10.1056/NEJMoa1215637>.
- Byrd, John C., Shinichi Kitada, Ian W. Flinn, Jennifer L. Aron, Michael Pearson, David Lucas, and John C. Reed. 2002. “The Mechanism of Tumor Cell Clearance by Rituximab in Vivo in Patients with B-Cell Chronic Lymphocytic Leukemia: Evidence of Caspase Activation and Apoptosis Induction.” *Blood* 99 (3): 1038–43.
<https://doi.org/10.1182/blood.V99.3.1038>.
- Cai, Nan, Wei Zhou, Lan Lan Ye, Jun Chen, Qiu Ni Liang, Gang Chang, and Jia Jie Chen. 2017. “The STAT3 Inhibitor Pimozide Impedes Cell Proliferation and Induces ROS Generation in Human Osteosarcoma by Suppressing Catalase Expression.” *American Journal of Translational Research* 9 (8): 3853–66.
- Cao, Cheng, Yumei Leng, and Donald Kufe. 2003. “Catalase Activity Is Regulated by C-Abl and Arg in the Oxidative Stress Response.” *Journal of Biological Chemistry* 278 (32): 29667–75. <https://doi.org/10.1074/jbc.M301292200>.
- Cao, Cheng, Yumei Leng, Xuan Liu, Yanping Yi, Ping Li, and Donald Kufe. 2003. “Catalase Is Regulated by Ubiquitination and Proteosomal Degradation. Role of the c-Abl and Arg Tyrosine Kinases.” *Biochemistry* 42 (35): 10348–53.
<https://doi.org/10.1021/bi035023f>.
- Cavallini, Chiara, Roberto Chignola, Ilaria Dando, Omar Perbellini, Elda Mimiola, Ornella Lovato, Carlo Laudanna, Giovanni Pizzolo, Massimo Donadelli, and Maria Teresa Scupoli. 2018. “Low Catalase Expression Confers Redox Hypersensitivity and Identifies an Indolent Clinical Behavior in CLL.” *Blood* 131 (17): 1942–54.
<https://doi.org/10.1182/blood-2017-08-800466>.
- Cavallini, Chiara, Marilisa Galasso, Elisa Dalla Pozza, Roberto Chignola, Ornella

- Lovato, Ilaria Dando, Maria G. Romanelli, et al. 2020. “Effects of CD20 Antibodies and Kinase Inhibitors on B-cell Receptor Signalling and Survival of Chronic Lymphocytic Leukaemia Cells.” *British Journal of Haematology*, November, bjh.17139. <https://doi.org/10.1111/bjh.17139>.
- Cavallini, Chiara, Carlo Visco, Santosh Putta, Davide Rossi, Elda Mimiola, Norman Purvis, Ornella Lovato, et al. 2017. “Integration of B-Cell Receptor-Induced ERK1/2 Phosphorylation and Mutations of SF3B1 Gene Refines Prognosis in Treatment-Naïve Chronic Lymphocytic Leukemia.” *Haematologica*. Ferrata Storti Foundation. <https://doi.org/10.3324/haematol.2016.154450>.
- Cesano, Alessandra, Omar Perbellini, Erik Evensen, Charles C. Chu, Federica Cioffi, Jason Ptacek, Rajendra N. Damle, et al. 2013. “Association between B-Cell Receptor Responsiveness and Disease Progression in B-Cell Chronic Lymphocytic Leukemia: Results from Single Cell Network Profiling Studies.” *Haematologica* 98 (4): 626–34. <https://doi.org/10.3324/haematol.2012.071910>.
- Chan, David Hughes, Ruth R. French, Alison L. Tutt, Claire A. Walshe, Jessica L. Teeling, and Mark S. Cragg Martin J. Glennie. n.d. “CD20-Induced Lymphoma Cell Death Is Independent of Both Caspases and Its Redistribution into Triton X-100 Insoluble Membrane Rafts - PubMed.” Accessed November 10, 2020. <https://pubmed.ncbi.nlm.nih.gov/14500384/>.
- Chance, B., H. Sies, and A. Boveris. 1979. “Hydroperoxide Metabolism in Mammalian Organs.” *Physiological Reviews* 59 (3): 527–605. <https://doi.org/10.1152/physrev.1979.59.3.527>.
- Chibber, Sandesh, Ameer Sangeet, and Shakeel Ahmed Ansari. 2017. “Downregulation of Catalase by CuO Nanoparticles via Hypermethylation of CpG Island II on the Catalase Promoter.” *Toxicology Research* 6: 305. <https://doi.org/10.1039/c6tx00416d>.
- Chou, Ting Chao. 2010. “Drug Combination Studies and Their Synergy Quantification Using the Chou-Talalay Method.” *Cancer Research*. Cancer Res. <https://doi.org/10.1158/0008-5472.CAN-09-1947>.
- “Chronic Lymphocytic Leukemia — Cancer Stat Facts.” n.d. Accessed November 3, 2020. <https://seer.cancer.gov/statfacts/html/clyl.html>.
- Cimmino, Amelia, George Adrian Calin, Muller Fabbri, Marilena V. Iorio, Manuela Ferracin, Masayoshi Shimizu, Sylwia E. Wojcik, et al. 2005. “MiR-15 and MiR-16 Induce Apoptosis by Targeting BCL2.” *Proceedings of the National Academy of Sciences of the United States of America* 102 (39): 13944–49. <https://doi.org/10.1073/pnas.0506654102>.
- Coscia, M., F. Pantaleoni, C. Riganti, C. Vitale, M. Rigoni, S. Peola, B. Castella, et al. 2011. “IGHV Unmutated CLL B Cells Are More Prone to Spontaneous Apoptosis and Subject to Environmental Prosurvival Signals than Mutated CLL B Cells.” *Leukemia* 25 (5): 828–37. <https://doi.org/10.1038/leu.2011.12>.
- Cosma, Adriana-Stela, Cristina Radu, Alexandra Moldovan, Alina Bogliș, George Andrei Crauciuc, Emőke Horváth, Marcela Căndea, and Florin Tripon. 2019. “The Influence of GPX1 Pro198Leu, CAT C262T and MnSOD Ala16Val Gene Polymorphisms on Susceptibility for Non-Hodgkin Lymphoma and Overall Survival Rate at Five Years from Diagnosis.” *Acta Medica Marisiensis* 65 (1): 25–30. <https://doi.org/10.2478/amma-2019-0005>.
- Crawford, Amanda, Robert G. Fassett, Dominic P. Geraghty, Dale A. Kunde, Madeleine J. Ball, Iain K. Robertson, and Jeff S. Coombes. 2012. “Relationships between Single Nucleotide Polymorphisms of Antioxidant Enzymes and Disease.” *Gene*. Elsevier. <https://doi.org/10.1016/j.gene.2012.04.011>.
- Cunha-Bang, Caspar da, and Carsten Utoft Niemann. 2018. “Targeting Bruton’s Tyrosine Kinase Across B-Cell Malignancies.” *Drugs* 78 (16): 1653–63.

- <https://doi.org/10.1007/s40265-018-1003-6>.
- D'Avola, Annalisa, Samantha Drennan, Ian Tracy, Isla Henderson, Laura Chiecchio, Marta Larrayoz, Matthew Rose-Zerilli, et al. 2016. "Surface IgM Expression and Function Are Associated with Clinical Behavior, Genetic Abnormalities, and DNA Methylation in CLL." *Blood* 128 (6): 816–26. <https://doi.org/10.1182/blood-2016-03-707786>.
- Dal Bo, Michele, Francesca Maria Rossi, Davide Rossi, Clara Deambrogi, Francesco Bertoni, Ilaria Del Giudice, Giuseppe Palumbo, et al. 2011. "13q14 Deletion Size and Number of Deleted Cells Both Influence Prognosis in Chronic Lymphocytic Leukemia." *Genes, Chromosomes and Cancer* 50 (8): 633–43. <https://doi.org/10.1002/gcc.20885>.
- Dalla Pozza, Elisa, Claudia Fiorini, Ilaria Dando, Marta Menegazzi, Anna Sgarbossa, Chiara Costanzo, Marta Palmieri, and Massimo Donadelli. 2012. "Role of Mitochondrial Uncoupling Protein 2 in Cancer Cell Resistance to Gemcitabine." *Biochimica et Biophysica Acta - Molecular Cell Research* 1823 (10): 1856–63. <https://doi.org/10.1016/j.bbamcr.2012.06.007>.
- Dalle, Stephane, Lina Reslan, Timothee Besseyre De Horts, Stephanie Herveau, Frank Herting, Adriana Plesa, Thomas Friess, Pablo Umana, Christian Klein, and Charles Dumontet. 2011. "Preclinical Studies on the Mechanism of Action and the Anti-Lymphoma Activity of the Novel Anti-CD20 Antibody GA101." *Molecular Cancer Therapeutics* 10 (1): 178–85. <https://doi.org/10.1158/1535-7163.MCT-10-0385>.
- Damle, Rajendra N., Tarun Wasil, Franco Fais, Fabio Ghiotto, Angelo Valetto, Steven L. Allen, Aby Buchbinder, et al. 1999. "Ig V Gene Mutation Status and CD38 Expression as Novel Prognostic Indicators in Chronic Lymphocytic Leukemia." *Blood* 94 (6): 1840–47. https://doi.org/10.1182/blood.v94.6.1840.418k06_1840_1847.
- Darwiche, Walaa, Brigitte Gubler, Jean Pierre Marolleau, and Hussein Ghamlouch. 2018. "Chronic Lymphocytic Leukemia B-Cell Normal Cellular Counterpart: Clues from a Functional Perspective." *Frontiers in Immunology*. Frontiers Media S.A. <https://doi.org/10.3389/fimmu.2018.00683>.
- Deisseroth, A., and A. L. Dounce. 1970. "Catalase: Physical and Chemical Properties, Mechanism of Catalysis, and Physiological Role." *Physiological Reviews*. <https://doi.org/10.1152/physrev.1970.50.3.319>.
- Döhner, Hartmut, Stephan Stilgenbauer, Axel Benner, Elke Leupolt, Alexander Kröber, Lars Bullinger, Konstanze Döhner, Martin Bentz, and Peter Lichter. 2000. "Genomic Aberrations and Survival in Chronic Lymphocytic Leukemia." *New England Journal of Medicine* 343 (26): 1910–16. <https://doi.org/10.1056/nejm200012283432602>.
- Du, Fanny Huynh, Elizabeth A. Mills, and Yang Mao-Draayer. 2017. "Next-Generation Anti-CD20 Monoclonal Antibodies in Autoimmune Disease Treatment." *Autoimmunity Highlights*. Springer-Verlag Italia s.r.l. <https://doi.org/10.1007/s13317-017-0100-y>.
- Edelmann, Jennifer, Karlheinz Holzmann, Florian Miller, Dirk Winkler, Andreas Bühler, Thorsten Zenz, Lars Bullinger, et al. 2012. "High-Resolution Genomic Profiling of Chronic Lymphocytic Leukemia Reveals New Recurrent Genomic Alterations." *Blood* 120 (24): 4783–94. <https://doi.org/10.1182/blood-2012-04-423517>.
- Einfeld, D A, J P Brown, M A Valentine, E A Clark, and J A Ledbetter. 1988. "Molecular Cloning of the Human B Cell CD20 Receptor Predicts a Hydrophobic Protein with Multiple Transmembrane Domains." *The EMBO Journal* 7 (3): 711–17. <http://www.ncbi.nlm.nih.gov/pubmed/2456210>.
- Evans, PharmD, Sarah S., and Amber B. Clemmons, PharmD, BCOP. 2015. "Obinutuzumab: A Novel Anti-CD20 Monoclonal Antibody for Chronic

- Lymphocytic Leukemia.” *Journal of the Advanced Practitioner in Oncology* 6 (4). <https://doi.org/10.6004/jadpro.2015.6.4.7>.
- Ezzikouri, Sayeh, Abdellah Essaid El Feydi, Rajae Afifi, Mustapha Benazzouz, Mohammed Hassar, Pascal Pineau, and Soumaya Benjelloun. 2010. “Polymorphisms in Antioxidant Defence Genes and Susceptibility to Hepatocellular Carcinoma in a Moroccan Population.” *Free Radical Research* 44 (2): 208–16. <https://doi.org/10.3109/10715760903402906>.
- Fabbri, Giulia, and Riccardo Dalla-Favera. 2016. “The Molecular Pathogenesis of Chronic Lymphocytic Leukaemia.” *Nature Reviews Cancer*. Nature Publishing Group. <https://doi.org/10.1038/nrc.2016.8>.
- Fabbri, Giulia, Silvia Rasi, Davide Rossi, Vladimir Trifonov, Hossein Khiabani, Jing Ma, Adina Grunn, et al. 2011. “Analysis of the Chronic Lymphocytic Leukemia Coding Genome: Role of NOTCH1 Mutational Activation.” *Journal of Experimental Medicine* 208 (7): 1389–1401. <https://doi.org/10.1084/jem.20110921>.
- Farnham, P. J., and M. M. Cornwell. 1991. “Sp1 Activation of RNA Polymerase II Transcription Complexes Involves a Heat-Labile DNA-Binding Component.” *Gene Expression* 1 (2): 137–48. [/pmc/articles/PMC5952208/?report=abstract](https://pubmed.ncbi.nlm.nih.gov/10552208/).
- Forsberg, Lena, Louise Lyrenäs, Ulf De Faire, and Ralf Morgenstern. 2001. “A Common Functional C-T Substitution Polymorphism in the Promoter Region of the Human Catalase Gene Influences Transcription Factor Binding, Reporter Gene Transcription and Is Correlated to Blood Catalase Levels.” *Free Radical Biology and Medicine* 30 (5): 500–505. [https://doi.org/10.1016/S0891-5849\(00\)00487-1](https://doi.org/10.1016/S0891-5849(00)00487-1).
- Franke, Andreas, Gerhard J. Niederfellner, Christian Klein, and Helmut Burtscher. 2011. “Antibodies against CD20 or B-Cell Receptor Induce Similar Transcription Patterns in Human Lymphoma Cell Lines.” *PLoS ONE* 6 (2): 1–11. <https://doi.org/10.1371/journal.pone.0016596>.
- Frezzato, Federica, Valentina Trimarco, Veronica Martini, Cristina Gattazzo, Elisa Ave, Andrea Visentin, Anna Cabrelle, et al. 2014. “Leukaemic Cells from Chronic Lymphocytic Leukaemia Patients Undergo Apoptosis Following Microtubule Depolymerization and Lyn Inhibition by Nocodazole.” *British Journal of Haematology* 165 (5): 659–72. <https://doi.org/10.1111/bjh.12815>.
- Furman, Richard R., Jeff P. Sharman, Steven E. Coutre, Bruce D. Cheson, John M. Pagel, Peter Hillmen, Jacqueline C. Barrientos, et al. 2014. “Idelalisib and Rituximab in Relapsed Chronic Lymphocytic Leukemia.” *New England Journal of Medicine* 370 (11): 997–1007. <https://doi.org/10.1056/NEJMoa1315226>.
- Furuta, Hiroaki, Akira HACHIMORI, Yuraiko OHTA, and Tatsuya SAMEJIMA. 1974. “Dissociation of Bovine Liver Catalase into Subunits on Acetylation.” *The Journal of Biochemistry* 76 (3): 481–91. <https://doi.org/10.1093/oxfordjournals.jbchem.a130592>.
- Geybels, Milan S., Piet A. Van Den Brandt, Frederik J. Van Schooten, and Bas A.J. Verhage. 2015. “Oxidative Stress-Related Genetic Variants, pro-and Antioxidant Intake and Status, and Advanced Prostate Cancer Risk.” *Cancer Epidemiology Biomarkers and Prevention* 24 (1): 178–86. <https://doi.org/10.1158/1055-9965.EPI-14-0968>.
- Glennie, Martin J., Ruth R. French, Mark S. Cragg, and Ronald P. Taylor. 2007. “Mechanisms of Killing by Anti-CD20 Monoclonal Antibodies.” *Molecular Immunology* 44 (16): 3823–37. <https://doi.org/10.1016/j.molimm.2007.06.151>.
- Glorieux, Christophe, Julien Auquier, Nicolas Dejeans, Brice Sid, Jean Baptiste Demoulin, Luc Bertrand, Julien Verrax, and Pedro Buc Calderon. 2014. “Catalase Expression in MCF-7 Breast Cancer Cells Is Mainly Controlled by PI3K/Akt/MTor Signaling Pathway.” *Biochemical Pharmacology* 89 (2): 217–23. <https://doi.org/10.1016/j.bcp.2014.02.025>.

- Glorieux, Christophe, and Pedro Buc Calderon. 2017. "Catalase, a Remarkable Enzyme: Targeting the Oldest Antioxidant Enzyme to Find a New Cancer Treatment Approach." *Biological Chemistry* 398 (10): 1095–1108. <https://doi.org/10.1515/hsz-2017-0131>.
- Glorieux, Christophe, Juan Marcelo Sandoval, Antoine Fattaccioli, Nicolas Dejeans, James C. Garbe, Marc Dieu, Julien Verrax, Patricia Renard, Peng Huang, and Pedro Buc Calderon. 2016. "Chromatin Remodeling Regulates Catalase Expression during Cancer Cells Adaptation to Chronic Oxidative Stress." *Free Radical Biology and Medicine* 99: 436–50. <https://doi.org/10.1016/j.freeradbiomed.2016.08.031>.
- Glorieux, Christophe, Marcel Zamocky, Juan Marcelo Sandoval, Julien Verrax, and Pedro Buc Calderon. 2015. "Regulation of Catalase Expression in Healthy and Cancerous Cells." *Free Radical Biology and Medicine* 87: 84–97. <https://doi.org/10.1016/j.freeradbiomed.2015.06.017>.
- Gorter, David J.J. de, Esther A. Beuling, Rogier Kersseboom, Sabine Middendorp, Janine M. van Gils, Rudolf W. Hendriks, Steven T. Pals, and Marcel Spaargaren. 2007. "Bruton's Tyrosine Kinase and Phospholipase C γ 2 Mediate Chemokine-Controlled B Cell Migration and Homing." *Immunity* 26 (1): 93–104. <https://doi.org/10.1016/j.immuni.2006.11.012>.
- Góth, László, Amir Shemirani, and Tibor Kalmár. 2000. "A Novel Catalase Mutation (a GA Insertion) Causes the Hungarian Type of Acatlasemia." *Blood Cells, Molecules, and Diseases* 26 (2): 151–54. <https://doi.org/10.1006/bcmd.2000.0288>.
- Goyal, Madhur M, and Anjan Basak. 2010. "Human Catalase: Looking for Complete Identity." *Protein and Cell*. <https://doi.org/10.1007/s13238-010-0113-z>.
- Hallek, Michael. 2019. "Chronic Lymphocytic Leukemia: 2020 Update on Diagnosis, Risk Stratification and Treatment." *American Journal of Hematology* 94 (11): 1266–87. <https://doi.org/10.1002/ajh.25595>.
- Hallek, Michael, Bruce D. Cheson, Daniel Catovsky, Federico Caligaris-Cappio, Guillermo Dighiero, Hartmut Döhner, Peter Hillmen, et al. 2018. "IWCLL Guidelines for Diagnosis, Indications for Treatment, Response Assessment, and Supportive Management of CLL." *Blood* 131 (25): 2745–60. <https://doi.org/10.1182/blood-2017-09-806398>.
- Hallek, Michael, Tait D. Shanafelt, and Barbara Eichhorst. 2018. "Chronic Lymphocytic Leukaemia." *The Lancet* 391 (10129): 1524–37. [https://doi.org/10.1016/S0140-6736\(18\)30422-7](https://doi.org/10.1016/S0140-6736(18)30422-7).
- Hamblin, Terry J., Zandie Davis, Anne Gardiner, David G. Oscier, and Freda K. Stevenson. 1999. "Unmutated Ig V(H) Genes Are Associated with a More Aggressive Form of Chronic Lymphocytic Leukemia." *Blood* 94 (6): 1848–54. <https://doi.org/10.1182/blood.v94.6.1848>.
- Han, Wei, Joshua P. Fessel, Taylor Sherrill, Emily G. Kocurek, Fiona E. Yull, and Timothy S. Blackwell. 2020. "Enhanced Expression of Catalase in Mitochondria Modulates NF-KB[1] W. Han, J.P. Fessel, T. Sherrill, E.G. Kocurek, F.E. Yull, T.S. Blackwell, Enhanced Expression of Catalase in Mitochondria Modulates NF-KB–Dependent Lung Inflammation through Alteration Of." *The Journal of Immunology* 205 (4): 1125–34. <https://doi.org/10.4049/jimmunol.1900820>.
- Handsuh, Luiza, Maciej Kazmierczak, Marek C. Milewski, Michal Goralski, Magdalena Luczak, Marzena Wojtaszewska, Barbara Uszczyńska-Ratajczak, Krzysztof Lewandowski, Mieczysław Komarnicki, and Marek Figlerowicz. 2018. "Gene Expression Profiling of Acute Myeloid Leukemia Samples from Adult Patients with AML-M1 and -M2 through Boutique Microarrays, Real-Time PCR and Droplet Digital PCR." *International Journal of Oncology* 52 (3): 656–78. <https://doi.org/10.3892/ijo.2017.4233>.
- Haque, Rashidul, Eugene Chun, Jennifer C. Howell, Trisha Sengupta, Dan Chen, and

- Hana Kim. 2012. "MicroRNA-30b-Mediated Regulation of Catalase Expression in Human ARPE-19 Cells." *PLoS ONE* 7 (8).
<https://doi.org/10.1371/journal.pone.0042542>.
- Hashimoto, An, Hidetaka Okada, Aimin Jiang, Mari Kurosaki, Steven Greenberg, Edward A. Clark, and Tomohiro Kurosaki. 1998. "Involvement of Guanosine Triphosphatases and Phospholipase C- Γ 2 in Extracellular Signal-Regulated Kinase, c-Jun NH2-Terminal Kinase, and P38 Mitogen-Activated Protein Kinase Activation by the B Cell Antigen Receptor." *Journal of Experimental Medicine* 188 (7): 1287–95. <https://doi.org/10.1084/jem.188.7.1287>.
- Hebert-Schuster, M., C. H. Cottart, C. Laguillier-Morizot, A. Raynaud-Simon, J. L. Golmard, L. Cynober, J. L. Beaudoux, E. E. Fabre, and V. Nivet-Antoine. 2011. "Catalase Rs769214 SNP in Elderly Malnutrition and during Renutrition: Is Glucagon to Blame?" *Free Radical Biology and Medicine* 51 (8): 1583–88. <https://doi.org/10.1016/j.freeradbiomed.2011.07.016>.
- Heinzelmanna, Sonja, and Georg Bauer. 2010. "Multiple Protective Functions of Catalase against Intercellular Apoptosis-Inducing ROS Signaling of Human Tumor Cells." *Biological Chemistry* 391 (6): 675–93. <https://doi.org/10.1515/BC.2010.068>.
- Herman, S. E.M., C. U. Niemann, M. Farooqui, J. Jones, R. Z. Mustafa, A. Lipsky, N. Saba, et al. 2014. "Ibrutinib-Induced Lymphocytosis in Patients with Chronic Lymphocytic Leukemia: Correlative Analyses from a Phase II Study." *Leukemia* 28 (11): 2188–96. <https://doi.org/10.1038/leu.2014.122>.
- Herman, Sarah E.M., Amber L. Gordon, Erin Hertlein, Asha Ramanunni, Xiaoli Zhang, Samantha Jaglowski, Joseph Flynn, et al. 2011. "Bruton Tyrosine Kinase Represents a Promising Therapeutic Target for Treatment of Chronic Lymphocytic Leukemia and Is Effectively Targeted by PCI-32765." *Blood* 117 (23): 6287–96. <https://doi.org/10.1182/blood-2011-01-328484>.
- Herman, Sarah E.M., Amber L. Gordon, Amy J. Wagner, Nyla A. Heerema, Weiqiang Zhao, Joseph M. Flynn, Jeffrey Jones, et al. 2010. "Phosphatidylinositol 3-Kinase- δ Inhibitor CAL-101 Shows Promising Preclinical Activity in Chronic Lymphocytic Leukemia by Antagonizing Intrinsic and Extrinsic Cellular Survival Signals." *Blood* 116 (12): 2078–88. <https://doi.org/10.1182/blood-2010-02-271171>.
- Herman, Sarah E.M., Rashida Z. Mustafa, Jennifer A. Gyamfi, Stefania Pittaluga, Stella Chang, Betty Chang, Mohammed Farooqui, and Adrian Wiestner. 2014. "Ibrutinib Inhibits BCR and NF-KB Signaling and Reduces Tumor Proliferation in Tissue-Resident Cells of Patients with CLL." *Blood* 123 (21): 3286–95. <https://doi.org/10.1182/blood-2014-02-548610>.
- Hill, Brian T., and Matt Kalaycio. 2015. "Profile of Obinutuzumab for the Treatment of Patients with Previously Untreated Chronic Lymphocytic Leukemia." *Oncotargets and Therapy*. Dove Medical Press Ltd. <https://doi.org/10.2147/OTT.S68770>.
- Hirono, Akira, Fumika Sasaya-Hamada, Hitoshi Kanno, Hisaichi Fujii, Tomoyuki Yoshida, and Shiro Miwa. 1995. "A Novel Human Catalase Mutation (358 T_{del}) Causing Japanese-Type Acatlasemia." *Blood Cells, Molecules and Diseases* 21 (3): 232–34. <https://doi.org/10.1006/bcmd.1995.0026>.
- Ho, James Chung-man, Shuo Zheng, Suzy A. A. Comhair, Carol Farver, and Serpil C. Erzurum. 2001. "Differential Expression of Manganese Superoxide Dismutase and Catalase in Lung Cancer." *Cancer Research* 61 (23).
- Ho, Ye Shih, Ye Xiong, Wanchao Ma, Abraham Spector, and Dorothy S. Ho. 2004. "Mice Lacking Catalase Develop Normally but Show Differential Sensitivity to Oxidant Tissue Injury." *Journal of Biological Chemistry* 279 (31): 32804–12. <https://doi.org/10.1074/jbc.M404800200>.
- Hoellenriegel, Julia, Sarah A. Meadows, Mariela Sivina, William G. Wierda, Hagop Kantarjian, Michael J. Keating, Neill Giese, et al. 2011. "The Phosphoinositide 3'-

- Kinase Delta Inhibitor, CAL-101, Inhibits B-Cell Receptor Signaling and Chemokine Networks in Chronic Lymphocytic Leukemia.” *Blood* 118 (13): 3603–12. <https://doi.org/10.1182/blood-2011-05-352492>.
- Hoffschir, F., M. Vuillaume, L. Sabatier, M. Ricoul, L. Daya-grosjean, S. Estrade, R. Cassingena, R. Calvayrac, A. Sarasin, and B. Dutrillaux. 1993. “Decrease in Catalase Activity and Loss of the 11p Chromosome Arm in the Course of SV40 Transformation of Human Fibroblasts.” *Carcinogenesis* 14 (8): 1569–72. <https://doi.org/10.1093/carcin/14.8.1569>.
- Hunt, Clayton R., Julia E. Sim, Shannon J. Sullivan, Terence Featherstone, Wendy Golden, Chris Von Kapp-Herr, Randy A. Hock, R. Ariel Gomez, Azemat J. Parsian, and Douglas R. Spitz. 1998. “Genomic Instability and Catalase Gene Amplification Induced by Chronic Exposure to Oxidative Stress.” *Cancer Research* 58 (17): 3986–92.
- HWANG, JOYCE K., FREDERICK W. ALT, and LENG-SIEW YEAP. 2015. “Related Mechanisms of Antibody Somatic Hypermutation and Class Switch Recombination.” In *Mobile DNA III*, 3:325–48. American Society of Microbiology. <https://doi.org/10.1128/microbiolspec.mdna3-0037-2014>.
- Hwang, T. S., H. K. Choi, and H. S. Han. 2007. “Differential Expression of Manganese Superoxide Dismutase, Copper/Zinc Superoxide Dismutase, and Catalase in Gastric Adenocarcinoma and Normal Gastric Mucosa.” *European Journal of Surgical Oncology* 33 (4): 474–79. <https://doi.org/10.1016/j.ejso.2006.10.024>.
- Jaglowksi, Samantha M., Jeffrey A. Jones, Veena Nagar, Joseph M. Flynn, Leslie A. Andritsos, Kami J. Maddocks, Jennifer A. Woyach, et al. 2015. “Safety and Activity of BTK Inhibitor Ibrutinib Combined with Ofatumumab in Chronic Lymphocytic Leukemia: A Phase 1b/2 Study.” *Blood* 126 (7): 842–50. <https://doi.org/10.1182/blood-2014-12-617522>.
- Jitschin, Regina, Andreas D. Hofmann, Heiko Bruns, Andreas Gießl, Juliane Bricks, Jana Berger, Domenica Saul, Michael J. Eckart, Andreas Mackensen, and Dimitrios Mougiakakos. 2014. “Mitochondrial Metabolism Contributes to Oxidative Stress and Reveals Therapeutic Targets in Chronic Lymphocytic Leukemia.” *Blood* 123 (17): 2663–72. <https://doi.org/10.1182/blood-2013-10-532200>.
- Jones, Jeffrey A., Tadeusz Robak, Jennifer R. Brown, Farrukh T. Awan, Xavier Badoux, Steven Coutre, Javier Loscertales, et al. 2017. “Efficacy and Safety of Idelalisib in Combination with Ofatumumab for Previously Treated Chronic Lymphocytic Leukaemia: An Open-Label, Randomised Phase 3 Trial.” *The Lancet Haematology* 4 (3): e114–26. [https://doi.org/10.1016/S2352-3026\(17\)30019-4](https://doi.org/10.1016/S2352-3026(17)30019-4).
- Jones, Peter, and H. Brian Dunford. 2005. “The Mechanism of Compound I Formation Revisited.” *Journal of Inorganic Biochemistry* 99 (12): 2292–98. <https://doi.org/10.1016/j.jinorgbio.2005.08.009>.
- Jou, Shiann-Tarnng, Nick Carpino, Yutaka Takahashi, Roland Piekorz, Jyh-Rong Chao, Neena Carpino, Demin Wang, and James N. Ihle. 2002. “Essential, Nonredundant Role for the Phosphoinositide 3-Kinase P110 δ in Signaling by the B-Cell Receptor Complex.” *Molecular and Cellular Biology* 22 (24): 8580–91. <https://doi.org/10.1128/mcb.22.24.8580-8591.2002>.
- Kang, M. Y., H. B. Kim, C. Piao, K. H. Lee, J. W. Hyun, I. Y. Chang, and H. J. You. 2013. “The Critical Role of Catalase in Prooxidant and Antioxidant Function of P53.” *Cell Death and Differentiation* 20 (1): 117–29. <https://doi.org/10.1038/cdd.2012.102>.
- Kheirallah, Samar, Pierre Caron, Emilie Gross, Anne Quillet-Mary, Justine Bertrand-Michel, Jean Jacques Fournié, Guy Laurent, and Christine Bezombes. 2010. “Rituximab Inhibits B-Cell Receptor Signaling.” *Blood* 115 (5): 985–94. <https://doi.org/10.1182/blood-2009-08-237537>.

- Kikushige, Yoshikane, Fumihiko Ishikawa, Toshihiro Miyamoto, Takahiro Shima, Shingo Urata, Goichi Yoshimoto, Yasuo Mori, et al. 2011. "Self-Renewing Hematopoietic Stem Cell Is the Primary Target in Pathogenesis of Human Chronic Lymphocytic Leukemia." *Cancer Cell* 20 (2): 246–59. <https://doi.org/10.1016/j.ccr.2011.06.029>.
- Kim, Hyang Suk, Tae Bum Lee, and Cheol Hee Choi. 2001. "Down-Regulation of Catalase Gene Expression in the Doxorubicin-Resistant Aml Subline Am 1-2/Dx100." *Biochemical and Biophysical Research Communications* 281 (1): 109–14. <https://doi.org/10.1006/bbrc.2001.4324>.
- Kirkman, Henry N., and Gian F. Gaetani. 2007. "Mammalian Catalase: A Venerable Enzyme with New Mysteries." *Trends in Biochemical Sciences*. Elsevier. <https://doi.org/10.1016/j.tibs.2006.11.003>.
- Kittur, S. D., J. W.M. Hoppener, S. E. Antonarakis, J. D. Daniels, D. A. Meyers, N. E. Maestri, M. Jansen, R. G. Korneluk, B. D. Nelkin, and H. H. Kazazian. 1985. "Linkage Map of the Short Arm of Human Chromosome 11: Location of the Genes for Catalase, Calcitonin, and Insulin-like Growth Factor II." *Proceedings of the National Academy of Sciences of the United States of America* 82 (15): 5064–67. <https://doi.org/10.1073/pnas.82.15.5064>.
- Klein, Christian, Alfred Lammens, Wolfgang Schäfer, Guy Georges, Manfred Schwaiger, Ekkehard Mössner, Karl Peter Hopfner, Pablo Umaña, and Gerhard Niederfellner. 2013. "Epitope Interactions of Monoclonal Antibodies Targeting CD20 and Their Relationship to Functional Properties." *MAbs* 5 (1): 22–33. <https://doi.org/10.4161/mabs.22771>.
- Klein, Ulf, Yuhai Tu, Gustavo A. Stolovitzky, Michela Mattioli, Giorgio Cattoretti, Hervé Husson, Arnold Freedman, et al. 2001. "Gene Expression Profiling of B Cell Chronic Lymphocytic Leukemia Reveals a Homogeneous Phenotype Related to Memory B Cells." *Journal of Experimental Medicine* 194 (11): 1625–38. <https://doi.org/10.1084/jem.194.11.1625>.
- Kodydková, J., L. Vávrová, M. Kocík, and A. Žák. 2014. "Human Catalase, Its Polymorphisms, Regulation and Changes of Its Activity in Different Diseases." *Folia Biologica (Czech Republic)* 60 (4): 153–67.
- Kohrt, Holbrook E., Idit Sagiv-Barfi, Sarwish Rafiq, Sarah E.M. Herman, Jonathon P. Butchar, Carolyn Cheney, Xiaoli Zhang, et al. 2014. "Ibrutinib Antagonizes Rituximab-Dependent NK Cell-Mediated Cytotoxicity." *Blood*. American Society of Hematology. <https://doi.org/10.1182/blood-2014-01-547869>.
- Krause, Günter, Imaan Baki, Susan Kerwien, Eva Knödgen, Lars Neumann, Elisa Göckeritz, Thomas Landwehr, Karl Heinz Heider, and Michael Hallek. 2016. "Cytotoxicity of the CD37 Antibody BI 836826 against Chronic Lymphocytic Leukaemia Cells in Combination with Chemotherapeutic Agents or PI3K Inhibitors." *British Journal of Haematology*. Blackwell Publishing Ltd. <https://doi.org/10.1111/bjh.13635>.
- Kremer, Mordechai L. 1999. "Mechanism of the Fenton Reaction. Evidence for a New Intermediate." *Physical Chemistry Chemical Physics* 1 (15): 3595–3605. <https://doi.org/10.1039/a903915e>.
- Krüber, Alexander, Till Seiler, Axel Benner, Lars Bullinger, Elsbeth Brückle, Peter Lichter, Hartmut Döhner, and Stephan Stilgenbauer. 2002. "VH Mutation Status, CD38 Expression Level, Genomic Aberrations, and Survival in Chronic Lymphocytic Leukemia." *Blood* 100 (4): 1410–16. https://doi.org/10.1182/blood.v100.4.1410.h81602001410_1410_1416.
- Kuo, Hsien-Chi, Po-Yu Lin, Ting-Chiun Chung, Chin-Mei Chao, Liang-Chuan Lai, Mong-Hsun Tsai, and Eric Y. Chuang. 2011. "DBCAT: Database of CpG Islands and Analytical Tools for Identifying Comprehensive Methylation Profiles in Cancer

- Cells.” *Journal of Computational Biology* 18 (8): 1013–17.
<https://doi.org/10.1089/cmb.2010.0038>.
- Landgren, Ola, Maher Albitar, Wanlong Ma, Fatima Abbasi, Richard B. Hayes, Paolo Ghia, Gerald E. Marti, and Neil E. Caporaso. 2009. “B-Cell Clones as Early Markers for Chronic Lymphocytic Leukemia.” *New England Journal of Medicine* 360 (7): 659–67. <https://doi.org/10.1056/nejmoa0806122>.
- Lannutti, Brian J., Sarah A. Meadows, Sarah E.M. Herman, Adam Kashishian, Bart Steiner, Amy J. Johnson, John C. Byrd, et al. 2011. “CAL-101, a P110 δ Selective Phosphatidylinositol-3-Kinase Inhibitor for the Treatment of B-Cell Malignancies, Inhibits PI3K Signaling and Cellular Viability.” *Blood* 117 (2): 591–94.
<https://doi.org/10.1182/blood-2010-03-275305>.
- Lauer, Christoph, Alfred Völkl, Stefan Riedl, H. Dariush Fahimi, and Konstantin Beier. 1999. “Impairment of Peroxisomal Biogenesis in Human Colon Carcinoma.” *Carcinogenesis* 20 (6): 985–89. <https://doi.org/10.1093/carcin/20.6.985>.
- Lee, Tae Bum, Young Sook Moon, and Cheol Hee Choi. 2012. “Histone H4 Deacetylation Down-Regulates Catalase Gene Expression in Doxorubicin-Resistant AML Subline.” *Cell Biology and Toxicology* 28 (1): 11–18.
<https://doi.org/10.1007/s10565-011-9201-y>.
- Lespay-Rebolledo, Carolyne, Ronald Perez-Lobos, Andrea Tapia-Bustos, Valentina Vio, Paola Morales, and Mario Herrera-Marschitz. 2018. “Regionally Impaired Redox Homeostasis in the Brain of Rats Subjected to Global Perinatal Asphyxia: Sustained Effect up to 14 Postnatal Days.” *Neurotoxicity Research* 34 (3): 660–76.
<https://doi.org/10.1007/s12640-018-9928-9>.
- Lim, Sean H., Stephen A. Beers, Ruth R. French, Peter W.M. Johnson, Martin J. Glennie, and Mark S. Cragg. 2010. “Anti-CD20 Monoclonal Antibodies: Historical and Future Perspectives.” *Haematologica*.
<https://doi.org/10.3324/haematol.2008.001628>.
- Lim, Sean H., Andrew T. Vaughan, Margaret Ashton-Key, Emily L. Williams, Sandra V. Dixon, H. T. Claude Chan, Stephen A. Beers, et al. 2011. “Fc Gamma Receptor IIb on Target B Cells Promotes Rituximab Internalization and Reduces Clinical Efficacy.” *Blood* 118 (9): 2530–40. <https://doi.org/10.1182/blood-2011-01-330357>.
- Linley, Adam, Beatriz Valle-Argos, Andrew J. Steele, Freda K. Stevenson, Francesco Forconi, and Graham Packham. 2015. “Higher Levels of Reactive Oxygen Species Are Associated with Anergy in Chronic Lymphocytic Leukemia.” *Haematologica* 100 (7): e265–68. <https://doi.org/10.3324/haematol.2014.120824>.
- Liu, Kang, Xinghan Liu, Meng Wang, Xijing Wang, Huafeng Kang, Shuai Lin, Pengtao Yang, et al. 2016. “Two Common Functional Catalase Gene Polymorphisms (Rs1001179 and Rs794316) and Cancer Susceptibility: Evidence from 14,942 Cancer Cases and 43,285 Controls.” *Oncotarget* 7 (39): 62954–65.
<https://doi.org/10.18632/oncotarget.10617>.
- Liu, Y., M. Adachi, S. Zhao, M. Hareyama, A. C. Koong, Dan Luo, T. A. Rando, K. Imai, and Y. Shinomura. 2009. “Preventing Oxidative Stress: A New Role for XBP1.” *Cell Death and Differentiation* 16 (6): 847–57.
<https://doi.org/10.1038/cdd.2009.14>.
- Liu, Y., X. Zhang, Y. Liang, H. Yu, X. Chen, T. Zheng, B. Zheng, et al. 2011. “Targeting X Box-Binding Protein-1 (XBP1) Enhances Sensitivity of Glioma Cells to Oxidative Stress.” *Neuropathology and Applied Neurobiology* 37 (4): 395–405.
<https://doi.org/10.1111/j.1365-2990.2010.01155.x>.
- Liu, Yanqiong, Li Xie, Jiangyang Zhao, Xiuli Huang, Liuying Song, Jingrong Luo, Liping Ma, Shan Li, and Xue Qin. 2015. “Association between Catalase Gene Polymorphisms and Risk of Chronic Hepatitis B, Hepatitis B Virus-Related Liver Cirrhosis and Hepatocellular Carcinoma in Guangxi Population.” *Medicine (United*

- States*) 94 (13): 1–8. <https://doi.org/10.1097/MD.0000000000000702>.
- Livak, Kenneth J., and Thomas D. Schmittgen. 2001. “Analysis of Relative Gene Expression Data Using Real-Time Quantitative PCR and the 2- $\Delta\Delta$ CT Method.” *Methods* 25 (4): 402–8. <https://doi.org/10.1006/meth.2001.1262>.
- LOEW, O. 1900. “A NEW ENZYME OF GENERAL OCCURRENCE IN ORGANISMIS.” *Science* 11 (279): 701–2. <https://doi.org/10.1126/science.11.279.701>.
- Lortz, S., S. Lenzen, and I. Mehmeti. 2015. “N-Glycosylation-Negative Catalase: A Useful Tool for Exploring the Role of Hydrogen Peroxide in the Endoplasmic Reticulum.” *Free Radical Biology and Medicine* 80 (March): 77–83. <https://doi.org/10.1016/j.freeradbiomed.2014.11.024>.
- Lüdecke, Daniel. 2018. “Ggeffects: Tidy Data Frames of Marginal Effects from Regression Models.” *Journal of Open Source Software* 3 (26): 772. <https://doi.org/10.21105/joss.00772>.
- Luo, Dan, and Thomas A. Rando. 2003. “The Regulation of Catalase Gene Expression in Mouse Muscle Cells Is Dependent on the CCAAT-Binding Factor NF-Y.” *Biochemical and Biophysical Research Communications* 303 (2): 609–18. [https://doi.org/10.1016/S0006-291X\(03\)00397-8](https://doi.org/10.1016/S0006-291X(03)00397-8).
- M E Reff, K Carner, K S Chambers, P C Chinn, J E Leonard, R Raab, R A Newman, N Hanna, D R Anderson. 1994. “Depletion of B Cells in Vivo by a Chimeric Mouse Human Monoclonal Antibody to CD20 - PubMed.” *Blood*, 435–45. <https://pubmed.ncbi.nlm.nih.gov/7506951/>.
- Ma, Jiao, Pin Lu, Ailin Guo, Shuhua Cheng, Hongliang Zong, Peter Martin, Morton Coleman, and Y. Lynn Wang. 2014. “Characterization of Ibrutinib-Sensitive and -Resistant Mantle Lymphoma Cells.” *British Journal of Haematology* 166 (6): 849–61. <https://doi.org/10.1111/bjh.12974>.
- Marcotte, Douglas J., Yu Ting Liu, Robert M. Arduini, Catherine A. Hession, Konrad Miatkowski, Craig P. Wildes, Patrick F. Cullen, et al. 2010. “Structures of Human Bruton’s Tyrosine Kinase in Active and Inactive Conformations Suggest a Mechanism of Activation for TEC Family Kinases.” *Protein Science* 19 (3): 429–39. <https://doi.org/10.1002/pro.321>.
- Marshall, A. J., H. Niuro, T. J. Yun, and E. A. Clark. 2000. “Regulation of B-Cell Activation and Differentiation by the Phosphatidylinositol 3-Kinase and Phospholipase C γ Pathways.” *Immunological Reviews*. Blackwell Munksgaard. <https://doi.org/10.1034/j.1600-065X.2000.00611.x>.
- Marshall, Michael J.E., Richard J. Stopforth, and Mark S. Cragg. 2017. “Therapeutic Antibodies: What Have We Learnt from Targeting CD20 and Where Are We Going?” *Frontiers in Immunology* 8 (OCT). <https://doi.org/10.3389/fimmu.2017.01245>.
- Matsui, Atsuka, Tatsuya Ihara, Hiraku Suda, Hirofumi Mikami, and Kentaro Semba. 2013. “Gene Amplification: Mechanisms and Involvement in Cancer.” *Biomolecular Concepts*. Biomol Concepts. <https://doi.org/10.1515/bmc-2013-0026>.
- Meng, Tzu Ching, Toshiyuki Fukada, and Nicholas K. Tonks. 2002. “Reversible Oxidation and Inactivation of Protein Tyrosine Phosphatases in Vivo.” *Molecular Cell* 9 (2): 387–99. [https://doi.org/10.1016/S1097-2765\(02\)00445-8](https://doi.org/10.1016/S1097-2765(02)00445-8).
- Middelkoop, Esther, Erik A.C. Wiemer, D. E. Tycho Schoenmaker, Anneke Strijland, and Joseph M. Tager. 1993. “Topology of Catalase Assembly in Human Skin Fibroblasts.” *BBA - Molecular Cell Research* 1220 (1): 15–20. [https://doi.org/10.1016/0167-4889\(93\)90091-3](https://doi.org/10.1016/0167-4889(93)90091-3).
- Min, Ji Young, Seung Oe Lim, and Guhung Jung. 2010. “Downregulation of Catalase by Reactive Oxygen Species via Hypermethylation of CpG Island II on the Catalase Promoter.” *FEBS Letters* 584 (11): 2427–32.

- <https://doi.org/10.1016/j.febslet.2010.04.048>.
- Moloney, Jennifer N., and Thomas G. Cotter. 2018. "ROS Signalling in the Biology of Cancer." *Seminars in Cell and Developmental Biology*. Elsevier Ltd. <https://doi.org/10.1016/j.semcd.2017.05.023>.
- Monroe, John G. 2006. "ITAM-Mediated Tonic Signalling through Pre-BCR and BCR Complexes." *Nature Reviews Immunology*. Nat Rev Immunol. <https://doi.org/10.1038/nri1808>.
- Moran, Elizabeth C., Aura S. Kamiguti, John C. Cawley, and Andrew R. Pettitt. 2002. "Cytoprotective Antioxidant Activity of Serum Albumin and Autocrine Catalase in Chronic Lymphocytic Leukaemia." *British Journal of Haematology* 116 (2): 316–28. <https://doi.org/10.1046/j.1365-2141.2002.03280.x>.
- Moreno, Carol, Richard Greil, Fatih Demirkan, Alessandra Tedeschi, Bertrand Anz, Loree Larratt, Martin Simkovic, et al. 2019. "Ibrutinib plus Obinutuzumab versus Chlorambucil plus Obinutuzumab in First-Line Treatment of Chronic Lymphocytic Leukaemia (ILLUMINATE): A Multicentre, Randomised, Open-Label, Phase 3 Trial." *The Lancet Oncology* 20 (1): 43–56. [https://doi.org/10.1016/S1473-2045\(18\)30788-5](https://doi.org/10.1016/S1473-2045(18)30788-5).
- Mössner, Ekkehard, Peter Brünker, Samuel Moser, Ursula Püntener, Carla Schmidt, Sylvia Herter, Roger Grau, et al. 2010. "Increasing the Efficacy of CD20 Antibody Therapy through the Engineering of a New Type II Anti-CD20 Antibody with Enhanced Direct and Immune Effector Cell - Mediated B-Cell Cytotoxicity." *Blood* 115 (22): 4393–4402. <https://doi.org/10.1182/blood-2009-06-225979>.
- Mueller, Sebastian, Hans Dieter Riedel, and Wolfgang Stremmel. 1997. "Direct Evidence for Catalase as the Predominant H₂O₂-Removing Enzyme in Human Erythrocytes." *Blood* 90 (12): 4973–78. https://doi.org/10.1182/blood.v90.12.4973.4973_4973_4978.
- Muzio, Marta, Benedetta Apollonio, Cristina Scielzo, Michela Frenquelli, Irene Vandoni, Vassiliki Boussiotis, Federico Caligaris-Cappio, and Paolo Ghia. 2008. "Constitutive Activation of Distinct BCR-Signaling Pathways in a Subset of CLL Patients: A Molecular Signature of Anergy." *Blood* 112 (1): 188–95. <https://doi.org/10.1182/blood-2007-09-111344>.
- Nathan, Carl, and Amy Cunningham-Bussel. 2013. "Beyond Oxidative Stress: An Immunologist's Guide to Reactive Oxygen Species." *Nature Reviews Immunology*. NIH Public Access. <https://doi.org/10.1038/nri3423>.
- Nemoto, Shino, Maria M. Fergusson, and Toren Finkel. 2005. "SIRT1 Functionally Interacts with the Metabolic Regulator and Transcriptional Coactivator PGC-1 α ." *Journal of Biological Chemistry* 280 (16): 16456–60. <https://doi.org/10.1074/jbc.M501485200>.
- Nenoi, Mitsuru, Sachiko Ichimura, Osami Yukawa, Kazuei Mita, and Iain L. Cartwright. 2001. "Regulation of the Catalase Gene Promoter by Sp1, CCAAT-Recognizing Factors, and a WT1/Egr-Related Factor in Hydrogen Peroxide-Resistant HP100 Cells." *Cancer Research* 61 (15): 5885–94.
- Nishikawa, Makiya, Mitsuru Hashida, and Yoshinobu Takakura. 2009. "Catalase Delivery for Inhibiting ROS-Mediated Tissue Injury and Tumor Metastasis." *Advanced Drug Delivery Reviews* 61 (4): 319–26. <https://doi.org/10.1016/j.addr.2009.01.001>.
- Nogueira, Veronique, Youngkyu Park, Chia Chen Chen, Pei Zhang Xu, Mei Ling Chen, Ivana Tonic, Terry Unterman, and Nissim Hay. 2008. "Akt Determines Replicative Senescence and Oxidative or Oncogenic Premature Senescence and Sensitizes Cells to Oxidative Apoptosis." *Cancer Cell* 14 (6): 458–70. <https://doi.org/10.1016/j.ccr.2008.11.003>.
- O'Brien, Susan M., Nicole Lamanna, Thomas J. Kipps, Ian Flinn, Andrew D. Zelenetz,

- Jan A. Burger, Michael Keating, et al. 2015. “A Phase 2 Study of Idelalisib plus Rituximab in Treatment-Naïve Older Patients with Chronic Lymphocytic Leukemia.” *Blood* 126 (25): 2686–94. <https://doi.org/10.1182/blood-2015-03-630947>.
- Oakes, Christopher C., Marc Seifert, Yassen Assenov, Lei Gu, Martina Przekopowicz, Amy S. Ruppert, Qi Wang, et al. 2016. “DNA Methylation Dynamics during B Cell Maturation Underlie a Continuum of Disease Phenotypes in Chronic Lymphocytic Leukemia.” *Nature Genetics* 48 (3): 253–64. <https://doi.org/10.1038/ng.3488>.
- Ogata, Masana. 1991. “Acatalasemia.” *Human Genetics*. Springer-Verlag. <https://doi.org/10.1007/BF00201829>.
- Okkenhaug, Klaus, Antonio Bilancio, Géraldine Farjot, Helen Priddle, Sara Sancho, Emma Peskett, Wayne Pearce, et al. 2002. “Impaired B and T Cell Antigen Receptor Signaling in P110 δ PI 3-Kinase Mutant Mice.” *Science* 297 (5583): 1031–34. <https://doi.org/10.1126/science.1073560>.
- Okroj, Marcin, Anders Österborg, and Anna M. Blom. 2013. “Effector Mechanisms of Anti-CD20 Monoclonal Antibodies in B Cell Malignancies.” *Cancer Treatment Reviews* 39 (6): 632–39. <https://doi.org/10.1016/j.ctrv.2012.10.008>.
- Okuno, Yosuke, Morihiro Matsuda, Yugo Miyata, Atsunori Fukuhara, Ryutaro Komuro, Michio Shimabukuro, and Iichiro Shimomura. 2010. “Human Catalase Gene Is Regulated by Peroxisome Proliferator Activated Receptor-Gamma through a Response Element Distinct from That of Mouse.” *Endocrine Journal* 57 (4): 303–9. <https://doi.org/10.1507/endocrj.K09E-113>.
- Oldham, Robert J., Kirstie L.S. Cleary, and Mark S. Cragg. 2014. “CD20 and Its Antibodies: Past, Present, and Future.” *Forum on Immunopathological Diseases and Therapeutics*. Begell House Inc. <https://doi.org/10.1615/ForumImmunDisTher.2015014073>.
- Olmos, Yolanda, Francisco J. Sánchez-Gómez, Brigitte Wild, Nieves García-Quintans, Sofía Cabezudo, Santiago Lamas, and María Monsalve. 2013. “SirT1 Regulation of Antioxidant Genes Is Dependent on the Formation of a FoxO3a/PGC-1 α Complex.” *Antioxidants and Redox Signaling* 19 (13): 1507–21. <https://doi.org/10.1089/ars.2012.4713>.
- Olmos, Yolanda, Inmaculada Valle, Sara Borniquel, Alberto Tierrez, Estrella Soria, Santiago Lamas, and Maria Monsalve. 2009. “Mutual Dependence of Foxo3a and PGC-1 α in the Induction of Oxidative Stress Genes.” *Journal of Biological Chemistry* 284 (21): 14476–84. <https://doi.org/10.1074/jbc.M807397200>.
- Ouillette, Peter, Roxane Collins, Sajid Shakhani, Jinghui Li, Cheng Li, Kerby Shedden, and Sami N. Malek. 2011. “The Prognostic Significance of Various 13q14 Deletions in Chronic Lymphocytic Leukemia.” *Clinical Cancer Research* 17 (21): 6778–90. <https://doi.org/10.1158/1078-0432.CCR-11-0785>.
- Packham, Graham, Serge Krysov, Alex Allen, Natalia Savelyeva, Andrew J. Steele, Francesco Forconi, and Freda K. Stevenson. 2014. “The Outcome of B-Cell Receptor Signaling in Chronic Lymphocytic Leukemia: Proliferation or Anergy.” *Haematologica* 99 (7): 1138–48. <https://doi.org/10.3324/haematol.2013.098384>.
- Pal Singh, Simar, Floris Dammeijer, and Rudi W. Hendriks. 2018. “Role of Bruton’s Tyrosine Kinase in B Cells and Malignancies.” *Molecular Cancer* 17 (1): 1–23. <https://doi.org/10.1186/s12943-018-0779-z>.
- Park, Hyun Jung, Janai R. Carr, Zebin Wang, Veronique Nogueira, Nissim Hay, Angela L. Tyner, Lester F. Lau, Robert H. Costa, and Pradip Raychaudhuri. 2009. “FoxM1, a Critical Regulator of Oxidative Stress during Oncogenesis.” *EMBO Journal* 28 (19): 2908–18. <https://doi.org/10.1038/emboj.2009.239>.
- Park, Hyunsun, Matthew I. Wahl, Daniel E.H. Afar, Christoph W. Turck, David J. Rawlings, Christina Tam, Andrew M. Scharenberg, Jean Pierre Kinet, and Owen N.

- Witte. 1996. "Regulation of Btk Function by a Major Autophosphorylation Site within the SH3 Domain." *Immunity* 4 (5): 515–25. [https://doi.org/10.1016/S1074-7613\(00\)80417-3](https://doi.org/10.1016/S1074-7613(00)80417-3).
- Pavlasova, Gabriela, Marek Borsky, Veronika Svobodova, Jan Oppelt, Katerina Cerna, Jitka Novotna, Vaclav Seda, et al. 2018. "Rituximab Primarily Targets an Intra-Clonal BCR Signaling Proficient CLL Subpopulation Characterized by High CD20 Levels." *Leukemia* 32 (9): 2028–31. <https://doi.org/10.1038/s41375-018-0211-0>.
- Pavlasova, Gabriela, and Marek Mraz. 2020. "The Regulation and Function of CD20: An 'Enigma' of B-Cell Biology and Targeted Therapy." *Haematologica* 105 (6): 1494–1506. <https://doi.org/10.3324/haematol.2019.243543>.
- Pawluczko, Andrew W., Frank J. Beurskens, Paul V. Beum, Margaret A. Lindorfer, Jan G. J. van de Winkel, Paul W. H. I. Parren, and Ronald P. Taylor. 2009. "Binding of Submaximal C1q Promotes Complement-Dependent Cytotoxicity (CDC) of B Cells Opsonized with Anti-CD20 MAbs Ofatumumab (OFA) or Rituximab (RTX): Considerably Higher Levels of CDC Are Induced by OFA than by RTX." *The Journal of Immunology* 183 (1): 749–58. <https://doi.org/10.4049/jimmunol.0900632>.
- Pedersen, Irene Munk, Anne Mette Buhl, Pia Klausen, Christian H. Geisler, and Jesper Jurlander. 2002. "The Chimeric Anti-CD20 Antibody Rituximab Induces Apoptosis in B-Cell Chronic Lymphocytic Leukemia Cells through a P38 Mitogen Activated Protein-Kinase-Dependent Mechanism." *Blood* 99 (4): 1314–19. <https://doi.org/10.1182/blood.V99.4.1314>.
- Petrie, Ryan J., and Julie P. Deans. 2002. "Colocalization of the B Cell Receptor and CD20 Followed by Activation-Dependent Dissociation in Distinct Lipid Rafts." *The Journal of Immunology* 169 (6): 2886–91. <https://doi.org/10.4049/jimmunol.169.6.2886>.
- Pickering, Andrew M., Lesya Vojtovich, John Tower, and Kelvin J.A. Davies. 2013. "Oxidative Stress Adaptation with Acute, Chronic, and Repeated Stress." *Free Radical Biology and Medicine* 55 (February): 109–18. <https://doi.org/10.1016/j.freeradbiomed.2012.11.001>.
- Pierpont, Timothy M., Candice B. Limper, and Kristy L. Richards. 2018. "Past, Present, and Future of Rituximab-The World's First Oncology Monoclonal Antibody Therapy." *Frontiers in Oncology*. Frontiers Media S.A. <https://doi.org/10.3389/fonc.2018.00163>.
- Plosker, Greg L., and David P. Figgitt. 2003. "Rituximab: A Review of Its Use in Non-Hodgkin's Lymphoma and Chronic Lymphocytic Leukaemia." *Drugs*. <https://doi.org/10.2165/00003495-200363080-00005>.
- Polyak, Maria J., Haidong Li, Neda Shariat, and Julie P. Deans. 2008. "CD20 Homo-Oligomers Physically Associate with the B Cell Antigen Receptor: Dissociation upon Receptor Engagement and Recruitment of Phosphoproteins and Calmodulin-Binding Proteins." *Journal of Biological Chemistry* 283 (27): 18545–52. <https://doi.org/10.1074/jbc.M800784200>.
- Ponader, Sabine, Shih Shih Chen, Joseph J. Buggy, Kumudha Balakrishnan, Varsha Gandhi, William G. Wierda, Michael J. Keating, Susan O'Brien, Nicholas Chiorazzi, and Jan A. Burger. 2012. "The Bruton Tyrosine Kinase Inhibitor PCI-32765 Thwarts Chronic Lymphocytic Leukemia Cell Survival and Tissue Homing in Vitro and in Vivo." *Blood* 119 (5): 1182–89. <https://doi.org/10.1182/blood-2011-10-386417>.
- Primo, Daniel, Lydia Scarfò, Aliko Xochelli, Mattias Mattsson, Pamela Ranghetti, Ana Belén Espinosa, Alicia Robles, et al. 2018. "A Novel Ex Vivo High-Throughput Assay Reveals Antiproliferative Effects of Idelalisib and Ibrutinib in Chronic Lymphocytic Leukemia." *Oncotarget* 9 (40): 26019–31.

- <https://doi.org/10.18632/oncotarget.25419>.
- Purdue, P. Edward, Sonia M. Castro, Vladimir Protopopov, and Paul B. Lazarow. 1996. "Targeting of Human Catalase to Peroxisomes Is Dependent upon a Novel C-Terminal Peroxisomal Targeting Sequence." *Annals of the New York Academy of Sciences* 804 (4): 775–76. <https://doi.org/10.1111/j.1749-6632.1996.tb18699.x>.
- Quan F., Korneluk R.G., Tropak M.B. and Gravel R.A. 1986. "Nucleic Acids Research Nucleic Acids Research." *Methods* 12 (21): 8235–51. https://doi.org/10.1007/978-3-642-04898-2_214.
- Quan, Xiaoyuan, Seung Oe Lim, and Guhung Jung. 2011. "Reactive Oxygen Species Downregulate Catalase Expression via Methylation of a CpG Island in the Oct-1 Promoter." *FEBS Letters* 585 (21): 3436–41. <https://doi.org/10.1016/j.febslet.2011.09.035>.
- Queirós, Ana C., Renée Beekman, Roser Vilarrasa-Blasi, Martí Duran-Ferrer, Guillem Clot, Angelika Merkel, Emanuele Raineri, et al. 2016. "Decoding the DNA Methylome of Mantle Cell Lymphoma in the Light of the Entire B Cell Lineage." *Cancer Cell* 30 (5): 806–21. <https://doi.org/10.1016/j.ccell.2016.09.014>.
- Quesada, Víctor, Laura Conde, Neus Villamor, Gonzalo R. Ordóñez, Pedro Jares, Laia Bassaganyas, Andrew J. Ramsay, et al. 2012. "Exome Sequencing Identifies Recurrent Mutations of the Splicing Factor SF3B1 Gene in Chronic Lymphocytic Leukemia." *Nature Genetics* 44 (1): 47–52. <https://doi.org/10.1038/ng.1032>.
- Rafikov, Ruslan, Sanjiv Kumar, Saurabh Aggarwal, Yali Hou, Archana Kangath, Daniel Pardo, Jeffrey R. Fineman, and Stephen M. Black. 2014. "Endothelin-1 Stimulates Catalase Activity through the PKC δ -Mediated Phosphorylation of Serine 167." *Free Radical Biology and Medicine* 67 (February): 255–64. <https://doi.org/10.1016/j.freeradbiomed.2013.10.814>.
- Rainis, Tova, Irit Maor, Amos Lanir, Sergay Shnizer, and Alexandra Lavy. 2007. "Enhanced Oxidative Stress and Leucocyte Activation in Neoplastic Tissues of the Colon." *Digestive Diseases and Sciences* 52 (2): 526–30. <https://doi.org/10.1007/s10620-006-9177-2>.
- Rawat, Divya, Saurabh Kumar Chhonker, Rayees Ahmad Naik, and Raj Kumar Koiri. 2020. "Modulation of Antioxidant Enzymes, SIRT1 and NF- κ B by Resveratrol and Nicotinamide in Alcohol-aflatoxin B1-induced Hepatocellular Carcinoma." *Journal of Biochemical and Molecular Toxicology*, September. <https://doi.org/10.1002/jbt.22625>.
- Reth, Michael. 2002. "Hydrogen Peroxide as Second Messenger in Lymphocyte Activation." *Nature Immunology*. *Nat Immunol*. <https://doi.org/10.1038/ni1202-1129>.
- Reth, Michael, and Tilman Brummer. 2004. "Feedback Regulation of Lymphocyte Signalling." *Nature Reviews Immunology*. Nature Publishing Group. <https://doi.org/10.1038/nri1335>.
- Roit, Fabio Da, Patrick J. Engelberts, Ronald P. Taylor, Esther C.W. Breij, Giuseppe Gritti, Alessandro Rambaldi, Martino Introna, Paul W.H.I. Parren, Frank J. Beurskens, and José Golay. 2015. "Ibrutinib Interferes with the Cell-Mediated Anti-Tumor Activities of Therapeutic CD20 Antibodies: Implications for Combination Therapy." *Haematologica* 100 (1): 77–86. <https://doi.org/10.3324/haematol.2014.107011>.
- Rossi, Davide, Alessio Brusca, Valeria Spina, Silvia Rasi, Hossein Khiabani, Monica Messina, Marco Fangazio, et al. 2011. "Mutations of the SF3B1 Splicing Factor in Chronic Lymphocytic Leukemia: Association with Progression and Fludarabine-Resistoriness." *Blood* 118 (26): 6904–8. <https://doi.org/10.1182/blood-2011-08-373159>.
- Rozman, and Montserrat. 1995. "REVIEW ARTICLES CURRENT CONCEPTS

CHRONIC LYMPHOCYTIC LEUKEMIA.”

- Saify, Khyber. 2016. “Genetic Polymorphisms in the Promoter Region of Catalase Gene, Creates New Potential PAX-6 and STAT4 Response Elements.” *Molecular Biology Research Communications* 5 (2): 97–100. <https://doi.org/10.22099/mbr.2016.3662>.
- Saify, Khyber, Iraj Saadat, and Mostafa Saadat. 2016. “Influence of A-21T and C-262T Genetic Polymorphisms at the Promoter Region of the Catalase (CAT) on Gene Expression.” *Environmental Health and Preventive Medicine* 21 (5): 382–86. <https://doi.org/10.1007/s12199-016-0540-4>.
- Sander, C. S., F. Hamm, P. Elsner, and Jens J. Thiele. 2003. “Oxidative Stress in Malignant Melanoma and Non-Melanoma Skin Cancer.” *British Journal of Dermatology* 148 (5): 913–22. <https://doi.org/10.1046/j.1365-2133.2003.05303.x>.
- Sandstrom, Paul A., and Thomas M. Buttke. 1993. “Autocrine Production of Extracellular Catalase Prevents Apoptosis of the Human CEM T-Cell Line in Serum-Free Medium.” *Proceedings of the National Academy of Sciences of the United States of America* 90 (10): 4708–12. <https://doi.org/10.1073/pnas.90.10.4708>.
- Sato, K, K Ito, H Kohara, Y Yamaguchi, K Adachi, and H Endo. 1992. “Negative Regulation of Catalase Gene Expression in Hepatoma Cells.” *Molecular and Cellular Biology* 12 (6): 2525–33. <https://doi.org/10.1128/mcb.12.6.2525>.
- Schriner, Samuel E., Nancy J. Linford, George M. Martin, Piper Treuting, Charles E. Ogburn, Mary Emond, Pinar E. Coskun, et al. 2005. “Medicine: Extension of Murine Life Span by Overexpression of Catalase Targeted to Mitochondria.” *Science* 308 (5730): 1909–11. <https://doi.org/10.1126/science.1106653>.
- Schults, Marten A., Roland K. Chiu, Peter W. Nagle, Lonneke C. Wilms, Jos C. Kleinjans, Frederik J. Van Schooten, and Roger W. Godschalk. 2013. “Genetic Polymorphisms in Catalase and CYP1B1 Determine DNA Adduct Formation by Benzo(a)Pyrene Ex Vivo.” *Mutagenesis* 28 (2): 181–85. <https://doi.org/10.1093/mutage/ges070>.
- Scupoli, Maria Teresa, and Giovanni Pizzolo. 2012. “Signaling Pathways Activated by the B-Cell Receptor in Chronic Lymphocytic Leukemia.” *Expert Review of Hematology*. <https://doi.org/10.1586/ehm.12.21>.
- Seda, Vaclav, and Marek Mraz. 2015. “B-Cell Receptor Signalling and Its Crosstalk with Other Pathways in Normal and Malignant Cells.” *European Journal of Haematology* 94 (3): 193–205. <https://doi.org/10.1111/ejh.12427>.
- Shanafelt, Tait D., Victoria Wang, Neil E. Kay, Curtis A. Hanson, Susan M. O’Brien, Jacqueline C Barrientos, Harry P. Erba, Richard M. Stone, Mark R. Litzow, and Martin S. Tallman. 2018. “A Randomized Phase III Study of Ibrutinib (PCI-32765)-Based Therapy Vs. Standard Fludarabine, Cyclophosphamide, and Rituximab (FCR) Chemoimmunotherapy in Untreated Younger Patients with Chronic Lymphocytic Leukemia (CLL): A Trial of the ECOG-ACRIN Cancer Research Group (E1912).” *Blood* 132 (Supplement 1): LBA-4-LBA-4. <https://doi.org/10.1182/blood-2018-120779>.
- Shingu, Masao, Kazunori Yoshioka, Masashi Nobunaga, and Koji Yoshida. 1985. “Human Vascular Smooth Muscle Cells and Endothelial Cells Lack Catalase Activity and Are Susceptible to Hydrogen Peroxide.” *Inflammation* 9 (3): 309–20. <https://doi.org/10.1007/BF00916279>.
- Sies, Helmut, Carsten Berndt, and Dean P. Jones. 2017. “Oxidative Stress.” *Annual Review of Biochemistry* 86 (June): 715–48. <https://doi.org/10.1146/annurev-biochem-061516-045037>.
- Singh, Dinesh Kumar, Dhiraj Kumar, Zaved Siddiqui, Sandip Kumar Basu, Vikas Kumar, and Kanury V.S. Rao. 2005. “The Strength of Receptor Signaling Is Centrally Controlled through a Cooperative Loop between Ca²⁺ and an Oxidant Signal.” *Cell* 121 (2): 281–93. <https://doi.org/10.1016/j.cell.2005.02.036>.

- Skarzynski, Martin, Carsten U. Niemann, Yuh Shan Lee, Sabrina Martyr, Irina Maric, Dalia Salem, Maryalice Stetler-Stevenson, et al. 2016. "Interactions between Ibrutinib and Anti-CD20 Antibodies: Competing Effects on the Outcome of Combination Therapy." *Clinical Cancer Research* 22 (1): 86–95. <https://doi.org/10.1158/1078-0432.CCR-15-1304>.
- Steinbrecher, Daniela, Billy Michael Chelliah Jebaraj, Christof Schneider, Jennifer Edelmann, Florence Cymbalista, Véronique Leblond, Alain Delmer, et al. 2018. "Telomere Length in Poor-Risk Chronic Lymphocytic Leukemia: Associations with Disease Characteristics and Outcome." *Leukemia and Lymphoma* 59 (7): 1614–23. <https://doi.org/10.1080/10428194.2017.1390236>.
- Stevenson, Freda K., Sergey Krysov, Andrew J. Davies, Andrew J. Steele, and Graham Packham. 2011. "B-Cell Receptor Signaling in Chronic Lymphocytic Leukemia." *Blood* 118 (16): 4313–20. <https://doi.org/10.1182/blood-2011-06-338855>.
- Strati, Paolo, and Tait D. Shanafelt. 2015. "Monoclonal B-Cell Lymphocytosis and Early-Stage Chronic Lymphocytic Leukemia: Diagnosis, Natural History, and Risk Stratification." *Blood*. American Society of Hematology. <https://doi.org/10.1182/blood-2015-02-585059>.
- Sullivan, Lucas B., and Navdeep S. Chandel. 2014. "Mitochondrial Reactive Oxygen Species and Cancer." *Cancer and Metabolism* 2 (1): 1–12. <https://doi.org/10.1186/2049-3002-2-17>.
- Taniguchi, Makoto, Mayumi Hashimoto, Naohiro Hori, and Kenzo Sato. 2005. "CCAAT/Enhancer Binding Protein- β (C/EBP- β), a Pivotal Regulator of the TATA-Less Promoter in the Rat Catalase Gene." *FEBS Letters* 579 (25): 5785–90. <https://doi.org/10.1016/j.febslet.2005.09.068>.
- Tedder, T. F., and S. F. Schlossman. 1988. "Phosphorylation of the B1 (CD20) Molecule by Normal and Malignant Human B Lymphocytes." *Journal of Biological Chemistry* 263 (20): 10009–15.
- Toda, H., T. Takeuchi, N. Hori, and K. Ito. 1997. "Inverted Repeats in the TATA-Less Promoter of the Rat Catalase Gene." *Journal of Biochemistry* 121 (6): 1035–40. <https://doi.org/10.1093/oxfordjournals.jbchem.a021691>.
- Tome, Margaret E., David B.F. Johnson, Lisa M. Rimsza, Robin A. Roberts, Thomas M. Grogan, Thomas P. Miller, Larry W. Oberley, and Margaret M. Briehl. 2005. "A Redox Signature Score Identifies Diffuse Large B-Cell Lymphoma Patients with a Poor Prognosis." *Blood* 106 (10): 3594–3601. <https://doi.org/10.1182/blood-2005-02-0487>.
- Trachootham, Dunyaporn, Yan Zhou, Hui Zhang, Yusuke Demizu, Zhao Chen, Helene Pelicano, Paul J. Chiao, et al. 2006. "Selective Killing of Oncogenically Transformed Cells through a ROS-Mediated Mechanism by β -Phenylethyl Isothiocyanate." *Cancer Cell* 10 (3): 241–52. <https://doi.org/10.1016/j.ccr.2006.08.009>.
- Tsagiopoulou, Maria, Nikos Papakonstantinou, Theodoros Moysiadis, Larry Mansouri, Viktor Ljungström, Martí Duran-Ferrer, Andigoni Malousi, et al. 2019. "DNA Methylation Profiles in Chronic Lymphocytic Leukemia Patients Treated with Chemoimmunotherapy." *Clinical Epigenetics* 11 (1): 177. <https://doi.org/10.1186/s13148-019-0783-1>.
- Tsai, Shih Meng, Szu Hsien Wu, Ming Feng Hou, Yueh Ling Chen, Hsu Ma, and Li Yu Tsai. 2012. "Oxidative Stress-Related Enzyme Gene Polymorphisms and Susceptibility to Breast Cancer in Non-Smoking, Non-Alcohol-Consuming Taiwanese Women: A Case-Control Study." *Annals of Clinical Biochemistry* 49 (2): 152–58. <https://doi.org/10.1258/acb.2011.011098>.
- Tsubata, Takeshi. 2020. "Involvement of Reactive Oxygen Species (ROS) in BCR Signaling as a Second Messenger." In *Advances in Experimental Medicine and*

- Biology*, 1254:37–46. Springer. https://doi.org/10.1007/978-981-15-3532-1_3.
- Vega, Mario I., Sara Huerta-Yepe, Melisa Martinez-Paniagua, Bernardo Martinez-Miguel, Rogelio Hernandez-Pando, Cesar R. González-Bonilla, Paul Chinn, et al. 2009. “Rituximab-Mediated Cell Signaling and Chemo/Immuno-Sensitization of Drug-Resistant B-NHL Is Independent of Its Fc Functions.” *Clinical Cancer Research* 15 (21): 6582–94. <https://doi.org/10.1158/1078-0432.CCR-09-1234>.
- Wahl, Matthew I., Anne Catherine Fluckiger, Roberta M. Kato, Hyunsun Park, Owen N. Witte, and David J. Rawlings. 1997. “Phosphorylation of Two Regulatory Tyrosine Residues in the Activation of Bruton’s Tyrosine Kinase via Alternative Receptors.” *Proceedings of the National Academy of Sciences of the United States of America* 94 (21): 11526–33. <https://doi.org/10.1073/pnas.94.21.11526>.
- Wang, Cheng Di, Yan Sun, Nan Chen, Lin Huang, Jing Wen Huang, Min Zhu, Ting Wang, and Yu Lin Ji. 2016. “The Role of Catalase C262T Gene Polymorphism in the Susceptibility and Survival of Cancers.” *Scientific Reports* 6: 1–8. <https://doi.org/10.1038/srep26973>.
- Wang, Peng, Chao feng Zhu, Ming zhe Ma, Gang Chen, Ming Song, Zhaolei Zeng, Wen hua Lu, et al. 2015. “Micro-RNA-155 Is Induced by K-Ras Oncogenic Signal and Promotes ROS Stress in Pancreatic Cancer.” *Oncotarget* 6 (25): 21148–58. <https://doi.org/10.18632/oncotarget.4125>.
- Wang, Qiong, Wenshu Chen, Lang Bai, Wenjie Chen, Mabel T. Padilla, Amy S. Lin, Shaoqing Shi, Xia Wang, and Yong Lin. 2014. “Receptor-Interacting Protein 1 Increases Chemoresistance by Maintaining Inhibitor of Apoptosis Protein Levels and Reducing Reactive Oxygen Species through a MicroRNA-146a-Mediated Catalase Pathway.” *Journal of Biological Chemistry* 289 (9): 5654–63. <https://doi.org/10.1074/jbc.M113.526152>.
- Wen, Jin Kun, Takashi Osumi, Takashi Hashimoto, and Masana Ogata. 1990. “Molecular Analysis of Human Acatalasemia. Identification of a Splicing Mutation.” *Journal of Molecular Biology* 211 (2): 383–93. [https://doi.org/10.1016/0022-2836\(90\)90359-T](https://doi.org/10.1016/0022-2836(90)90359-T).
- Winternitz, M C, and C R Meloy. 1908. “Occurrence of Catalase in Human Tissues .” *Journal of Experimental Medicine* 10 (6): 759–81. <https://doi.org/doi:10.1084/jem.10.6.759>.
- Woyach, Jennifer A., Amy S. Ruppert, Nyla A. Heerema, Weiqiang Zhao, Allison M. Booth, Wei Ding, Nancy L. Bartlett, et al. 2018. “Ibrutinib Regimens versus Chemoimmunotherapy in Older Patients with Untreated CLL.” *New England Journal of Medicine* 379 (26): 2517–28. <https://doi.org/10.1056/nejmoa1812836>.
- Wu, Wen Sheng. 2006. “The Signaling Mechanism of ROS in Tumor Progression.” *Cancer and Metastasis Reviews*. Cancer Metastasis Rev. <https://doi.org/10.1007/s10555-006-9037-8>.
- Wu, Wen Sheng, Rong Kung Tsai, Chung Hsing Chang, Sindy Wang, Jia Ru Wu, and Yu Xun Chang. 2006. “Reactive Oxygen Species Mediated Sustained Activation of Protein Kinase C α and Extracellular Signal-Regulated Kinase for Migration of Human Hepatoma Cell Hepg2.” *Molecular Cancer Research* 4 (10): 747–58. <https://doi.org/10.1158/1541-7786.MCR-06-0096>.
- Xu, Xiuling, Alexandria Wells, Mabel T. Padilla, Kosuke Kato, Kwang C.hul Kim, and Yong Lin. 2014. “A Signaling Pathway Consisting of MiR-551b, Catalase and MUC1 Contributes to Acquired Apoptosis Resistance and Chemoresistance.” *Carcinogenesis* 35 (11): 2457–66. <https://doi.org/10.1093/carcin/bgu159>.
- YAMADA, MICHIIYUKI, KAZUYA HASHINAKA, JOHJI INAZAWA, and TATSUO ABE†. 1991. “Expression of Catalase and Myeloperoxidase Genes in Hydrogen Peroxide-Resistant HL-60 Cells.” *DNA and Cell Biology* 10 (10): 735–42. <https://doi.org/10.1089/dna.1991.10.735>.
- Yamanashi, Y., Y. Fukui, B. Wongsasant, Y. Kinoshita, Y. Ichimori, K. Toyoshima, and

- T. Yamamoto. 1992. "Activation of Src-like Protein-Tyrosine Kinase Lyn and Its Association with Phosphatidylinositol 3-Kinase upon B-Cell Antigen Receptor-Mediated Signaling." *Proceedings of the National Academy of Sciences of the United States of America* 89 (3): 1118–22. <https://doi.org/10.1073/pnas.89.3.1118>.
- Yan, Hong, and John J. Harding. 1997. "Glycation-Induced Inactivation and Loss of Antigenicity of Catalase and Superoxide Dismutase." *Biochemical Journal* 328 (2): 599–605. <https://doi.org/10.1042/bj3280599>.
- Yang, Qingshan, Prexy Modi, Terry Newcomb, Christophe Quéva, and Varsha Gandhi. 2015. "Idelalisib: First-in-Class PI3K Delta Inhibitor for the Treatment of Chronic Lymphocytic Leukemia, Small Lymphocytic Leukemia, and Follicular Lymphoma." *Clinical Cancer Research* 21 (7): 1537–42. <https://doi.org/10.1158/1078-0432.CCR-14-2034>.
- Yang, Weiwei, Jia Zhang, Haiya Wang, Weili Shen, Pingjin Gao, Manpreet Singh, and Ningyuan Fang. 2011. "Peroxisome Proliferator-Activated Receptor γ Regulates Angiotensin II-Induced Catalase Downregulation in Adventitial Fibroblasts of Rats." *FEBS Letters* 585 (5): 761–66. <https://doi.org/10.1016/j.febslet.2011.01.040>.
- Yosifov, Deyan Y., Christine Wolf, Stephan Stilgenbauer, and Daniel Mertens. 2019. "From Biology to Therapy: The CLL Success Story." *HemaSphere*. Wolters Kluwer Health. <https://doi.org/10.1097/HS9.000000000000175>.
- Young, Ryan M., and Louis M. Staudt. 2013. "Targeting Pathological B Cell Receptor Signalling in Lymphoid Malignancies." *Nature Reviews Drug Discovery*. Nature Publishing Group. <https://doi.org/10.1038/nrd3937>.
- Yu, Duonan, Camila O. Dos Santos, Guowei Zhao, Jing Jiang, Julio D. Amigo, Eugene Khandros, Louis C. Dore, et al. 2010. "MiR-451 Protects against Erythroid Oxidant Stress by Repressing 14-3-3 ζ ." *Genes and Development* 24 (15): 1620–33. <https://doi.org/10.1101/gad.1942110>.
- Zarei, Narjes, Iraj Saadat, and Majid Farvardin-Jahromi. 2015. "The Relationship between NQO1 C609T and CAT C-262T genetic Polymorphisms and the Risk of Age-Related Cataracts." *Molecular Biology Research Communications* 4 (3): 143–49. <https://doi.org/10.22099/mbrc.2015.3116>.
- Zenz, Thorsten, Hartmut Döhner, and Stephan Stilgenbauer. 2007. "Genetics and Risk-Stratified Approach to Therapy in Chronic Lymphocytic Leukemia." *Best Practice and Research: Clinical Haematology*. Best Pract Res Clin Haematol. <https://doi.org/10.1016/j.beha.2007.02.006>.
- Zhang, Honghong, Weiyong Zhao, Dongying Gu, Mulong Du, Weida Gong, Yongfei Tan, Meilin Wang, Juan Wen, Yongning Zhai, and Zhi Xu. 2018. "Association of Antioxidative Enzymes Polymorphisms with Efficacy of Platin and Fluorouracil-Based Adjuvant Therapy in Gastric Cancer." *Cellular Physiology and Biochemistry* 48 (6): 2247–57. <https://doi.org/10.1159/000492642>.
- Zhong, Yimin, Jingming Li, Joshua J. Wang, Chen Chen, Julie-Thu A. Tran, Anisse Saadi, Qiang Yu, et al. 2012. "X-Box Binding Protein 1 Is Essential for the Anti-Oxidant Defense and Cell Survival in the Retinal Pigment Epithelium." Edited by Neeraj Vij. *PLoS ONE* 7 (6): e38616. <https://doi.org/10.1371/journal.pone.0038616>.